# GAS-LIQUID REACTORS: PREDICTIONS OF A MODEL RESPECTING THE PHYSICS OF THE PROCESS

By

Daniel White, Jr.

A DISSERTATION PRESENTED TO THE GRADUATE COUNCIL
OF THE UNIVERSITY OF FLORIDA IN
PARTIAL FULFILLMENT OF THE REQUIREMENTS
FOR THE DEGREE OF DOCTOR OF PHILOSOPHY

UNIVERSITY OF FLORIDA

1982

TABLE OF CONTENTS

LIST OF TABLES

LIST OF FIGURES

KEY TO SYMBOLS

| | |
|---|---|
| A | gaseous reactant |
| a | interfacial surface area per unit volume, $cm^{-1}$ |
| B | liquid reactant |
| $B_R$ | dimensionless heat of reaction |
| $B_S$ | dimensionless heat of solution |
| C | concentration in the liquid phase, $gmole/cm^3$ |
| $C_P$ | heat capacity of the liquid, $cal/gmole \cdot {}^oK$ |
| D | diffusivity, $cm^2/sec$ |
| $D_a$ | Damkohler number |
| $D_{ai}$ | Damkohler number for the interfacial region |
| $D_{a1}$, $D_{a2}$, $D_{a3}$, $D_{a4}$ | value of the Damkohler number such that $\theta$ equals $m_1$, $m_2$, $s_1$ and $s_2$ |
| E | activation energy, cal/gmole |
| $E_R$ | error |
| E* | reaction factor |
| $f_b$ | fraction of gas absorbed into the bulk liquid that reacts |
| $f_i$ | fraction of gas absorbed that reacts near the interface |
| $f_R$ | fraction of gas absorbed that reacts |
| $g(\theta)$ | function of the steady state temperature that equals the Damkohler number |
| H | dimensionless heat transfer coefficient |
| $H_R$ | heat of reaction, $-\Delta H_R$, cal/gmole |
| $H_S$ | heat of solution, $-\Delta H_S$, cal/gmole |
| $H_o$ | Henry's Law coefficient, $atm \cdot cm^3/gmole$ |
| $H_1$ | inverse of the characteristic time for heat transfer, $H = H_1\tau$, $sec^{-1}$ |
| $h_L$, $h_L^o$ | heat transfer coefficient with and without reaction, cm/sec |

| | |
|---|---|
| $k$ | second order rate constant, $cm^3/gmole \cdot sec$ |
| $k_o$ | frequency factor for k, $cm^3/gmole \cdot sec$ |
| $k_1$ | pseudo-first order rate constant, $k_1 = kC_{Bf}$, $sec^{-1}$ |
| $k_{10}$ | frequency factor for $k_1$, $sec^{-1}$ |
| $k_L$, $k_L^o$ | mass transfer coefficient with and without reaction, cm/sec |
| $\mathscr{k}$ | thermal conductivity, $cal/cm \cdot sec \cdot {}^oK$ |
| M | dimensionless group, $k_1 D/(k_L^o)^2$ |
| $m_1$, $m_2$ | dimensionless temperatures where the determinant is zero |
| $P_A$ | partial pressure of gas A, atm |
| $Q_G$ | heat generation function |
| $Q_R$ | heat removal function |
| $Q_1$, $Q_2$ | slope of $Q_R$ and $Q_G$ with respect to $\theta$ |
| q | volumetric flow rate of the liquid, $cm^3/sec$ |
| R | gas constant, $cal/gmole \cdot {}^oK$ |
| $R_a$ | rate of absorption, gmole/sec |
| $R_r$ | relative rate of absorption |
| $r_1$ | inverse of the resistance due to reaction |
| $r_2$ | inverse of the resistance due to mass transfer |
| S | stoichiometric ratio of the concentration of A to that of B at feed conditions |
| $S_c$ | surface area available for cooling, $cm^2$ |
| $s_1$, $s_2$ | dimensionless temperatures where the trace is zero |
| T | temperature, $^oK$ |
| t | time, sec |
| t' | dimensionless time |
| U | overall heat transfer coefficient, $cal/cm^2 \cdot {}^oK \cdot sec$ |
| V | volume of the liquid phase, $cm^3$ |

| | |
|---|---|
| $x$ | dimensionless concentration |
| $x_i$ | dimensionless concentration of A at the interface |
| $z$ | distance from the interface, cm |

GREEK SYMBOLS

| | |
|---|---|
| $\alpha$ | thermal diffusivity, $cm^2/sec$ |
| $\beta$ | dimensionless mass transfer coefficient |
| $\gamma$ | dimensionless activation energy |
| $\delta$ | film thickness, cm |
| $\nu$ | stoichiometric coefficient |
| $\rho$ | liquid density, $gmole/cm^3$ |
| $\eta$ | dimensionless exponent for solubility |
| $\theta$ | dimensionless temperature |
| $\lambda$ | coefficient which defines the location of the reaction front for instantaneous reaction, $cm^2/sec$ |
| $\tau$ | holding time, sec |
| $\tau_i$ | interfacial exposure time, sec |
| $\tau_H$, $\tau_M$, $\tau_R$, $\tau_{Ri}$ | characteristic times for heat transfer, mass transfer, reaction and reaction at the interface, sec |
| $\phi$ | enhancement factor |
| $\phi_I$ | enhancement factor for instantaneous reaction |

SUBSCRIPTS

| | |
|---|---|
| A | gaseous reactant |
| B | liquid-phase reactant |
| b | bulk |
| c | cooling water |
| FK | Frank-Kamenetskii approximation |
| f | feed |
| H | heat transfer |

| | |
|---|---|
| i | interfacial |
| ℓ | bulk liquid |
| M | mass transfer |
| R | reaction |

Abstract of Dissertation Presented to the Graduate Council
of the University of Florida in Partial Fulfillment of the
Requirements for the Degree of Doctor of Philosophy

GAS-LIQUID REACTORS: PREDICTIONS OF A MODEL RESPECTING
THE PHYSICS OF THE PROCESS

By

Daniel White, Jr.

December 1982

Chairman: L. E. Johns
Major Department: Chemical Engineering

The opposing effects of temperature on gas solubility and chemical reaction rate imply oscillations in gas-liquid reactors. In this study a model is proposed for a specific class of gas-liquid reactors and is investigated to establish the basis for such oscillations.

We study the class of gas-liquid continuously fed stirred tank reactors where excess gas is bubbled through the liquid and where the reaction occurs in the liquid phase. The model accounts for the interfacial temperature rise due to fast reaction which can significantly affect enhanced absorption and which has been neglected in previous studies. Six characteristic times scale the individual processes occurring in the reactor and these allow us to identify two controlling regimes of reactor performance and five operating regions. A maximum of five steady states is possible with at most one in each region.

Uniqueness and multiplicity conditions are given for the steady states and their stability is ascertained. These conditions completely specify the parameter space for a reactor with unenhanced absorption.

The predictions of the model agree with the experimental results for the chlorination of decane.

Three multiplicity patterns are found: s-shaped, mushroom and isola. A method for predicting the existence of isolas and mushrooms is given. For a single-phase reactor the roots of a fifth degree polynomial determine precisely where isolas exist. A previously hypothesized result, that isolas and mushrooms are not possible for an adiabatic reactor, is proven. For a two-phase, gas-liquid reactor the conclusions are less sharp but yield the result that these phenomena can not exist for an adiabatic reactor.

Directions in the search for oscillations are given. The operating region of most interest is the mass transfer controlled region and general conditions for the existence of oscillations are discussed. The results herein indicate how the model can be simplified to quantify these oscillations.

# CHAPTER ONE
# INTRODUCTION

If a reactor could control its feed rate, varying it with time, then there would appear to be a physical basis for anticipating and explaining a natural oscillation in the reactor's performance. The elementary fact that reaction rates increase with temperature whereas absorption rates decrease suggests that a two-phase system where dissolved A reacts with B in the liquid phase but where A is fed in the gas phase should exhibit this phenomenon.

In particular, if a gas containing A is bubbled through a liquid containing B then the feed rate of A into the reacting liquid depends on the saturation concentration of A, a strong function of temperature. Thus it is anticipated that if a system cools, the solubility of A increases, resulting in an increase in the rate of absorption, in the concentration of A in the liquid, in the generation of heat via reaction, and hence in the temperature. So cold systems show a tendency to heat up. Conversely, in hot systems the decreased solubility of A reduces the rate of absorption, the rate of reaction and hence the generation of heat, cooling the system. This seems to suggest that oscillations are characteristic of such two-phase systems. However, these oscillations can not be like those found in single-phase reactors which can only originate in the nonlinearity of the reaction rate. Here the primary cause is the interaction of the temperature-dependent solubility and the rate of reaction. The ultimate objective of this study then is to find conditions which will guarantee the existence of such oscillations

and to show that they are relatively commonplace. But before this can be done a model of the system must be constructed and its multiplicity and stability implications investigated. This then is the primary objective of this study.

In a single-phase continuous stirred-tank reactor (CSTR)[1] for a simple but important class of reactions, the model equations are simple and the multiplicity and stability problems are essentially resolved. But in two-phase systems the model equations are more complex and results have been obtained only in simple limiting cases. Most recent investigations have focused on the special case where one reactant enters in the gas phase and another nonvolatile reactant enters in the liquid phase with reaction occurring in the liquid phase only. The models proposed for this system are simplified so that they resemble the single-phase model for which the method of analysis is well established. But this simplification confuses the physics and may alter the interaction of the mass transfer and the reaction processes. And it is just this interaction between gas solubility and reaction that must exist to produce the above scenario for oscillations. So a model must be constructed which is capable of describing the requisite physics for natural oscillations. That is, the opposing effects of temperature on the solubility of the gaseous reactant and on the reaction rate must be adequately described so that the competition between reaction and mass transfer is evident. This requires a temperature-dependent solubility (Henry's law constant) and separate descriptions of the mass transfer and the reaction processes.

[1]The name CSTR identifies an idealization satisfying the following condition: on some scale the contents of the reactor are spatially uniform.

In full generality such a model would be too complex to give useful conditions for multiplicity and stability so a less general case but one that still contains the above physics is necessary. Many of the gas-liquid reactions carried out in a CSTR involve a pure gas (and/or a gas fed in excess) and a liquid reactant, e.g. chlorination, hydrogenation, nitration, oxidation and sulfonation. The gaseous reactant dissolves in the liquid and reacts forming a liquid product. If a gaseous product is formed, it is often so dilute that there is no significant effect on the gas phase. Under these conditions the only influence the gas phase exerts on the reactor is through the pressure dependence of the solubility (partial pressure if not pure but only fed in excess), obviating the gas-phase mass balance. For this reaction scheme it should be possible to analyze the multiplicity, stability and oscillatory behavior of a two-phase CSTR without neglecting the requisite physics for natural oscillations. Thus with this description of the system such phenomena can be sought.

## CHAPTER TWO
## LITERATURE REVIEW

Models for single-phase CSTR's and their multiplicity and stability analysis were developed over the years 1955-1976, culminating in Poore's method of analysis, see Poore (1973). Before this the classical method was graphical. The steady state mass balance was solved and substituted into the energy balance. This was written in the form: rate of generation of heat equals the rate of removal. When these two functions are plotted versus temperature their intersections are the steady states.[1] The heat removal function is a straight line hence the shape of the heat generation function determines the number of possible steady states. For a first order reaction this is

$$\frac{\tau k}{1 + \tau k}$$

where $\tau$ is the holding time and k is the rate constant. This function is s-shaped with respect to temperature and thus the maximum number of steady states is three (Figure 2.1). In addition to providing multiplicity information these graphs give the first of two conditions for stability, the slope condition. This is the determinant condition for the corresponding linearized system and is a sufficient condition for instability and a necessary one for stability:

> If the slope of the heat removal function at a steady state is less than the slope of the heat generation function then the steady

[1]The analysis for a single-phase CSTR is summarized in Appendix A.

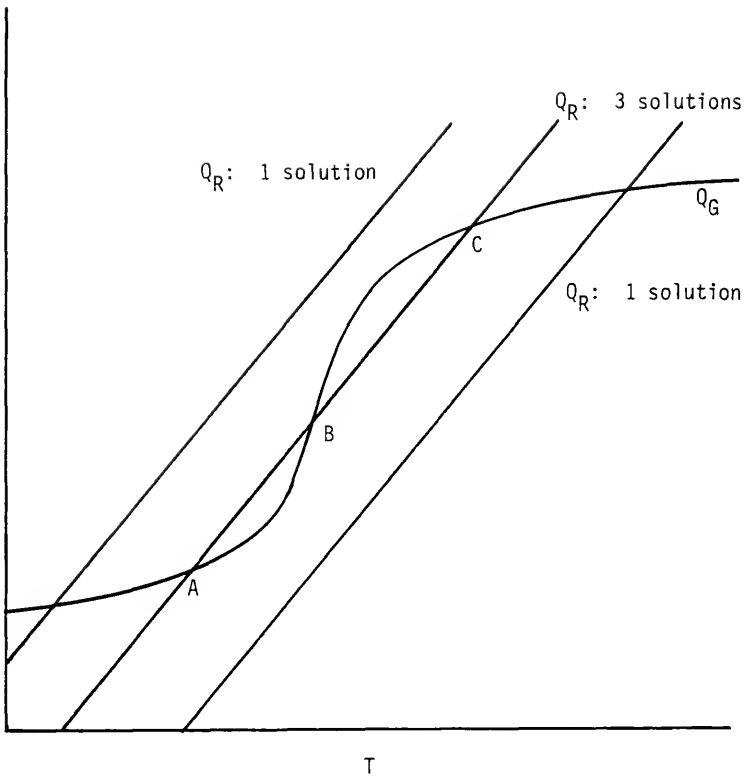


Figure 2.1. Heat generation and heat removal functions versus temperature for a single-phase CSTR.

state is unstable.

For example, in Figure 2.1 the above is true for steady state B; hence it is unstable. That is, if the reactor is operating at B and is perturbed to a slightly higher temperature, then the graph shows that the rate of heat generation is now greater than the rate of removal; thus the temperature continues to rise, ultimately reaching steady state C. Similarly if a perturbation lowers the temperature the steady state shifts to A. For steady states A and C the above does not hold so they may be stable.

This graphical technique gives a necessary, but not sufficient, condition for stability and limited information on regions in phase space of uniqueness and multiplicity. Poore's technique completes the former and generalizes the latter but it is model bound and works only because the single-phase system is so nice. For a CSTR the dynamic equations are ordinary differential equations in only two state variables and hence the linearized system can be characterized by the determinant and the trace of the Jacobian. Also because the system has at most three steady states, the determinant and trace conditions lead to quadratic equations in the temperature which can be solved explicitly to obtain the critical points for uniqueness and stability. From this, regions in phase space for uniqueness and stability can be determined for simple kinetics. Also oscillations in temperature and concentration due to the nonlinearity of the reaction rate constant can be found. If the system were more complex this would be much more difficult, and might be impossible.

In conjunction with the development of the single-phase CSTR model Schmitz and Amundson (1963a-d) proposed a model for a two-phase CSTR. The

model is quite general with reaction possible in both phases and heat and mass transfer between phases. The analysis is only manageable because they assume dilute systems and represent the transport processes in their simplest possible forms. With these simplifications the model becomes very similar to two single-phase reactors with linear coupling. Since the multiplicity and stability analysis was not well developed at the time, only partial answers were possible for these questions.[2] For the limiting cases of physical equilibrium and chemical equilibrium the model takes particularly simple forms: the first is very similar to the single-phase model and the latter is linear; hence only a unique stable steady state exists.

There are two problems with this model. Most gas-liquid reactors are not this complex and the transport processes are not this simple. In the preceding model mass transfer and reaction are treated as independent phenomena but in fact the two interact. In particular, chemical reaction enhances mass transfer by sharpening the concentration gradient at the interface. This enhancement can be significant and needs to be taken into account. Similarly the interfacial temperature may be greater than that in the bulk due to reaction near the interface. This rise needs to be investigated and included because it is the interfacial temperature that determines the solubility of gas.

On the other hand the reactor model is too general, e.g. reaction in both phases, heat and mass transfer resistances in both phases, etc., thus making analysis difficult. Fortunately many systems of industrial

[2]One result which is of interest in our work is that for a system in thermal equilibrium with reaction in one phase only up to three steady states are possible (Henry's law is also independent of temperature).

importance are simpler. Most involve reactions in the liquid phase only with one reactant fed in each phase. Also heat transfer to the gas phase is often negligible due to its low heat capacity and the fact that the most important temperature of the gas is its interfacial temperature which is usually equal to that of the liquid. For example Ding et al. (1974) studied the chlorination of n-decane in an adiabatic CSTR. Pure chlorine was bubbled through liquid decane where it dissolved and reacted. Multiple steady states were observed over a range of holding times. Two stable steady states were found and one unstable state was located via a feedback control scheme.

Hoffman et al. (1975) in an effort to understand Ding et al. (1974) and account for the enhancement of mass transfer via reaction modelled this system using a reaction factor. When a reaction factor is used the rate of mass transfer is defined as

$$E^* \, k_L^\circ \, a \, C_{Ai}$$

where $E^*$ is the reaction factor which accounts for the enhancement and is a function of the rate of reaction near the interface, $k_L^\circ$ is the mass transfer coefficient with no reaction, a is the specific surface area, and $C_{Ai}$ is the interfacial concentration of the gas A in the liquid. Then the reaction factor is found via a theory for the diffusion and reaction processes near the interface.[3]

---

[3]Alternatively one could have used the more common enhancement factor $\phi$ which is the ratio of the mass transfer rate with and without reaction. With this the rate of mass transfer is

$$\phi \, k_L^\circ \, a \, (C_{Ai} - C_{A\ell})$$

where $C_{A\ell}$ is the dissolved gas concentration in the bulk liquid. Thus the reaction factor is smaller than the enhancement factor by

$$E^* = \phi \, (1 - C_{A\ell}/C_{Ai}) \, .$$

The Hoffman model is the basis for all the recent studies of two-phase reactors but it pertains only to the class of well-mixed systems (CSTR) where the reaction

$$A + \nu B \rightarrow \text{Products}$$

occurs in the liquid phase and where the reactant A is fed in the gas and the nonvolatile reactant B in the liquid. For this system it is the most complete description available and includes most of the important phenomena. For this reason it will be reviewed more fully.

The model consists of two overall mass balances, one for each reactant, and an overall energy balance. This differs from previous models in that the balances are not written for each phase and the reaction term is replaced by the reaction factor term $R_A V = E^* k_L^\circ a C_{Ai} V - q C_{A\ell}$ so it is unnecessary to describe the reaction in the bulk. Thus the rate of reaction is the rate of mass transfer (or absorption) to the liquid minus the rate at which unreacted A flows out of the reactor with the liquid. This leaves five unknowns (the concentration of A in the gas, in the liquid, and at the interface, the concentration of B, and the temperature) with only four equations (three overall balances and the Henry's law equilibrium relationship for the interface). Thus another equation is necessary, relating the bulk concentration $C_{A\ell}$ to the other variables. In general such a relationship would be derived from a mass balance on either of the phases, leading to separate terms for mass transfer and reaction, but the liquid-phase mass balance has already been used to define the reaction rate. Hoffman et al. (1975) circumvent the need for another equation via the use of a clever boundary condition which determines $C_{A\ell}$ from the interfacial model. This is unusual because the interfacial model is normally used only to determine

the reaction factor. With the bulk concentration determined from an interfacial model the choice for this model assumes undue importance.

The reaction factor, like a mass transfer coefficient, is found by modelling the interfacial region, calculating the flux at the interface and equating it with the mass transfer rate in the reaction factor form:

$$E^* \, k_L^\circ \, a \, C_{Ai} \, V \quad .$$

Several interfacial models can be used but the results, at least for the enhancement factor (the ratio of the mass transfer coefficients with and without reaction, see previous footnote), are insensitive to the one chosen. Hoffman et al. chose the simplest, the film theory.[4] To determine the reaction factor Hatta's film theory is followed, including corrections to his final result, except that a new boundary condition at the bulk liquid is used. This condition accounts for reaction in the bulk and effectively defines the reaction rate in a mass balance on the liquid phase. Hatta's model is for the steady state diffusion and reaction (pseudo-first order because B is assumed to be in excess) of a gas A through a stagnant liquid film. At the gas-liquid interface, the gas concentration is $C_{Ai}$ whereas at the bulk liquid boundary it is zero.

---

[4]Although the main features of results derived from the film theory are usually correct, e.g. the reaction factor, occasionally this theory gives incorrect parameter dependencies. Thus using this model to determine the bulk concentration $C_{A\ell}$ may be suspect. This result needs to be verified and compared with the other more physically plausible models, e.g. penetration and surface-renewal. Also these models were constructed to estimate the rate of mass transfer at the interface and extrapolating their results to the bulk to obtain a quantitative value seems unjustified. There is some question as to whether the film model is the proper choice since this is a steady state model and the mass transfer process it describes is a dynamic one. A more appropriate choice might have been the time-varying models from the penetration or surface-renewal theories.

But in Hoffman's model this zero boundary condition is replaced by a flux condition. The flux from the film to the bulk is equated with the rate of reaction of A in the bulk plus the loss of A due to the unreacted A flowing out with the liquid:

$$-V\ a\ D\ \frac{dC_A}{dZ} = V\ k\ C_A\ C_B\ (\varepsilon - a\ \delta) + q\ C_A \quad .$$

Here $C_A$ is the concentration at the film-bulk boundary which is assumed equal to the bulk concentration.

Solving the diffusion-reaction equation with this boundary condition yields a reaction factor similar to Hatta's and an expression for $C_{A\ell}$. But Hatta's result was for the liquid reactant B in excess and its concentration equal to the bulk concentration. Historically this was corrected by van Krevelen and Hoftijzer (1948) who estimated the interfacial concentration of B and used this in the film theory equations. Thus the model is still pseudo-first order but with a more accurate estimate of the B concentration. Hoffman et al. (1975) also use this correction to account for the lower value of the B concentration due to reaction. But originally this correction was only valid for $C_{A\ell}$ equal to zero, so an additional correction due to Teramoto et al. (1969) is also used. The resulting equations for $E^*$ and $C_{A\ell}$ must then be solved iteratively with the original reactor equations to determine the steady state.

This technique appears to be somewhat backwards. Here the liquid phase mass balance is placed in the interfacial model in the form of a boundary condition. From this both the reaction factor and the liquid phase concentration of A are calculated. Normally an interfacial model is used just to estimate the enhancement of the mass transfer rate which is then substituted into the mass balance. As shown in Sherwood,

Pigford and Wilke (1975) the interfacial model used for this is not very important since the results are all similar. But in the analysis of Hoffman et al. (1975) not only is the enhancement found but also the liquid concentration. This would appear to make the choice of interfacial model quite important. This technique does have an obvious drawback, confusion. Combining the liquid balance with the interfacial model and using the two corrections discussed in the last paragraph yields a system where the physics have been scrambled. That is because all the reaction has been obscured in the function $E^*$, any structure the system once had is lost. Thus none of the recent authors can describe their results so that it is clear physically which processes are important and when they are important. As an example of some unnecessary confusion and complexity, consider the two corrections used in the film theory. These are not needed together. The van Krevelen-Hoftijzer correction accounts for the lower concentration of the liquid reactant at the interface which is necessary only for fast reactions, whereas the Teramoto correction is used when the gas concentration in the bulk liquid is nonzero which happens only for slow reaction.[5] Thus adding the Teramoto correction to that of van Krevelen-Hoftijzer is an unnecessary complication which, even though it does not create any error, obfuscates the results with extraneous complexities. This can lead to errors in the calculation scheme if not handled properly.

[5]This can be shown via a time scale argument which will be explained in the text. Astarita (1967) also discusses when the bulk concentration goes to zero and finds this to be true for fast reactions. Some conditions are given in the literature for the bulk concentration to go to zero and they are in terms of the Hatta number, see van Dierendonck and Nelemans (1972).

Solving the model equations numerically Hoffman et al. (1975) find up to five steady states with at least two unstable. The slope condition which is a necessary condition for stability and also a sufficient condition for uniqueness can not be used to find regions of guaranteed stability or uniqueness due to the iterative nature of the solution. Thus the utility of the model is reduced because of its inherent complexity. Yet its complexity does not seem necessary or even appropriate considering the interfacial model and corrections which are used.

Sharma et al. (1976) extend this analysis to two consecutive reactions in the liquid phase of a nonadiabatic CSTR and find up to seven steady states. They are also able to fit their model to the data of Ding et al. (1974) and predict the ignition and extinction points quite closely. A parametric study revealed the existence of an isola. An isola is a multiplicity pattern where a shift from the low temperature to the high temperature steady state can not occur by increasing or decreasing the independent parameter, e.g. the residence time.

Raghuram and Shah (1977) simplify Hoffman's model in order to obtain explicit formulae for uniqueness and multiplicity. The most important assumption is that the liquid reactant B is in excess and the concentration of B in the film is the same as that in the bulk. Thus in Hoffman's film theory the van Krevelen-Hoftijzer and the Teramoto corrections are not necessary, and analytical expressions for the reaction factor and the concentration of the gas in the bulk liquid can be written explicitly. This obviates Hoffman's iteration thereby allowing conditions for uniqueness and multiplicity to be deduced. In addition they assume that the volumetric flow rates of the gas in and out of the reactor are the same, whereas Hoffman et al. (1975) correct the flow

rates for the gas that is transferred to the liquid. This is true if the reactant gas is dilute in the gas phase, or if very little gas is transferred, or if the gas flow rate is very large and in excess. Raghuram and Shah (1977) also analyze the case of instantaneous reaction where the reaction factor is very simple and the concentration of gas in the bulk is zero.

An observation on the expression of Henry's law used by Raghuram and Shah (1977) seems pertinent. Henry's law is a proportionality between the partial pressure of a gas and its mole fraction in the liquid:

$$P_A = H(T)\ X_A$$

where H(T), the Henry's law constant, can be represented via

$$H(T) = H_o\ e^{-H_S/RT} .$$

They write it in terms of the molar concentration in both phases

$$C_{Ag} = H'(T)\ C_{Ai}$$

and presume

$$H'(T) = H'_o\ e^{-H_S/RT} .$$

But if $C_{Ag} = P_A/RT$ and $C_{Ai} = \rho\ X_A$ then

$$H'(T) = H(T)/\rho RT .$$

It appears that Raghuram and Shah have missed a factor of 1/T.

The result of this simplified model is a seemingly explicit inequality (slope condition) for uniqueness and stability. This inequality is a sufficient condition for uniqueness and a necessary condition for stability. Unfortunately the inequality is not fully explicit requiring a solution of the steady state equations for its evaluation. This makes it very difficult to determine regions of uniqueness, multiplicity, and stability in parameter space. But for a

specific system (Ding et al., 1974) where the values of the parameters are taken from Hoffman et al. (1975) they are able to show numerically regions of one, three or five steady states. A result more conservative than the slope condition but explicit is also deduced from the inequality and is a sufficient condition for uniqueness. This condition is that the activation energy of the reaction be less than twice the heat of solution (where the heat of solution is the exponent in Henry's law). It is a very weak condition in that it is almost never true except for very slow reactions.

More explicit results are found for two special cases, fast reaction and instantaneous reaction. For both, the reaction occurs near the interface and the bulk concentration of the gas is zero. The corresponding reaction factors are simple. For fast reaction Raghuram and Shah (1977) find up to three steady states whereas for instantaneous reaction the steady state is always unique. They conclude that "the possibility of five steady states is a direct consequence of the liquid phase concentration of the gaseous reactant being nonzero." Again the formulation of their model, like Hoffman's, confuses the physics so an interpretation of the results becomes difficult. Accounting for the finite value of the bulk concentration in the fast reaction model can not give five steady states, in fact we will show that the bulk concentration is vanishingly small here. The reason only three are possible is that the fast reaction model holds only in the region where the reaction is fast. Thus any solutions in the regions of slow reaction or physical absorption without reaction are lost. That is, simplifying a general model to a specific region can only give useful results pertinent to that region and can not be expected to give results pertaining

to the solution of the general model outside this region. Thus if any solutions are found outside the assumed region they are probably meaningless. This will be shown in the text. Raghuram et al. (1979) extend this analysis to a nonadiabatic CSTR and to a cascade of n CSTRs. They obtain five steady states but only for an extremely narrow range of parameters, thus concluding that five steady states are probably not physically observable for a gas-liquid reactor.

Huang and Varma (1981a) use a simplified version of Raghuram and Shah's (1977) model for fast reaction to determine explcit necessary and sufficient conditions for uniqueness and multiplicity, and for stability. They also predict the direction and stability of limit cycles. Their model is the same as Raghuram and Shah's except that they assume that the concentration of B is constant at the feed composition and their reactor is nonadiabatic. The fast reaction assumption implies that the reaction factor has the simple form

$$E^* = \phi = \sqrt{k_1 D}\,/k_L^\circ$$

and that the bulk liquid concentration of the gas is zero hence no iteration is necessary. The model then consists of two equations, one for the gas concentration and one for the temperature. But due to the form of the reaction factor and Henry's law these equations are equivalent to those for a single-phase CSTR. In establishing the equivalence it is necessary only to identify the apparent activation energy with one half the activation energy minus the heat of solution:

$$E_{App} = \tfrac{1}{2} E - H_S \quad .$$

Thus the entire theory of single-phase reactors (Uppal et al., 1974 and 1976) can be applied to this problem although Huang and Varma (1981a) do not avail themselves of this.

Sufficient conditions for uniqueness are obtained in terms of the parameters, free of the steady state temperature. Thus these conditions can be used without solving the steady state equations and as such are a great simplification over the results of Raghuram and Shah (1977). Also, simplifying the sufficient condition for uniqueness gives a similar condition to that of Raghuram and Shah (1977):

$$E < 2H_S + 8RT_f \qquad \text{Huang and Varma (1981a)} \qquad (2.1)$$

$$E < 2H_S \qquad \text{Raghuram and Shah (1977).} \qquad (2.2)$$

The two models give the same maximum number of steady states, three as expected. Comparing a prediction of Huang and Varma's (1981a) model with the data of Ding et al. (1974) shows a reasonable prediction of the ignition and extinction points and a qualitative prediction of the multiplicity pattern, even though the reaction of Ding et al. was not fast. But it should be noted that not all the parameters necessary for this model were found or reported by Ding et al. so there is some discrepancy between the values used by Huang and Varma (1981a) and those used by the previous authors. Apparently some of these parameters have been used to fit the authors' model to the data of Ding et al. (1974). Finally Huang and Varma (1981a) find conditions implying the existence of limit cycles but the corresponding values of the parameters necessary are unrealistic, vis-a-vis a gas-liquid reactor.

Both Raghuram and Shah's (1977) and Huang and Varma's (1981a) models are fast reaction models and make sense only when the reaction is fast. That is, if the model predicts a solution outside the fast reaction region the solution is meaningless. Limiting cases are instructive here. If the rate constant $k_1$ goes to zero the reaction factor $E^*$ goes to zero and the mass transfer from the gas to the liquid vanishes. But

of course there are nonreactive conditions under which the amount absorbed can be quite large. So any solution found that is in the slow reaction region is incorrect or at the least is suspect. Conversely, in the opposite limit of instantaneous reaction ($k_1 \to \infty$), the reaction factor overpredicts the rate of mass transfer, viz.,

$$\lim_{k_1 \to \infty} E^* \to \infty \quad .$$

But in reality the reaction factor is bounded, viz.,

$$E^* \leq 1 + C_{B\ell} / \nu C_{Ai}$$

where $C_{B\ell}$ is the bulk concentration of the liquid phase reactant and $\nu$ is the stoichiometric coefficient. Again any result here is meaningless. Finally it will be shown in the text that of the three steady states found from this model, two are outside its region of applicability and the one remaining solution, which is the only real steady state for a gas-liquid reactor, is the middle unstable steady state. Hence the multiplicity and stability results of this model do not apply to any real system.

Huang and Varma (1981b) remove the requirement of fast reaction allowing all reaction regimes, the concomitant price being a return to the complex model of Hoffman et al. (1975) and numerical solutions. The film theory used is identical to that of Hoffman et al. but the overall balances for the reactor differ as they did in the previous paper. Predicted results for the experiment of Ding et al. (1974) using values of the parameters as given by Sharma et al. (1976) show reasonable agreement with the data for short residence times and for the prediction of the extinction point. The numerical results also show the existence of an isola, a multiplicity pattern where no ignition point from the low

temperature steady state exists and two extinction points exist for the high temperature branch. For the adiabatic case an isola with five steady states was found to be possible. But even a small heat loss reduced the system to three steady states. Explicit conditions for uniqueness and stability are not possible due to the complexity of the model. As in the previous papers little insight into the interaction of the mass transfer and reaction processes is obtained.

All the models incorporating the reaction factor suffer from confusion due to their combination of mass transfer and reaction into one complex function $E^*$. This complexity essentially eliminates the possibility of a multiplicity analysis. Also the results from the interfacial model are extrapolated to deduce results in the bulk liquid, whereas originally these models were hypothesized to estimate the mass transfer coefficient only. This has not been justified and at the least makes one uncomfortable. Thus if an understanding of a gas-liquid reactor is to be found, the model should handle the reaction and mass transfer processes separately except where the mass transfer process is influenced by interfacial reaction. Here an interfacial model should be used only to determine the factors describing this interaction.

None of the previous studies in this area is based upon a model that captures the full effect of the temperature interaction between gas solubility and liquid phase reaction. Schmitz and Amundson (1963a-d) neglect the effect of temperature on the distribution coefficient (Henry's law constant). Hoffman et al. (1975) and the studies based on this work assume the temperature is everywhere uniform even though all the reaction may take place in the neighborhood of the interface, cf. the fast reaction studies. Whenever mass transfer is enhanced, i.e.

whenever appreciable reaction takes place in the interfacial region, the interfacial temperature will be greater than the bulk temperature. Because heats of reaction and solution can be large, this effect could be significant. And it is just the highly exothermic systems that would be of interest when searching for unusual phenomena such as oscillations, where the surface temperature rise is especially likely to be important. Because temperature sensitivity seems to be required for natural oscillations and this sensitivity appears in the gas solubility which is determined by the interfacial temperature, the overlooked phenomenon of an interfacial temperature rise would seem to be of importance.

Interfacial temperature rises in gas absorption with and without reaction have been observed. Recently Verma and Delancy (1975) found temperature rises in the nonreacting systems ammonia-water and propane-decane. They predicted this increase to be as large as 18°C. In reacting systems larger values have been observed. Beenackers (1978) estimated from flux measurements a rise up to 50°C. Mann and Clegg (1975) and Mann and Moyes (1977) indirectly measured temperature rises up to 53°C for chlorination and 58°C for sulfonation using a laminar jet technique. Temperature increases of this magnitude will significantly affect reaction rates and solubilities, hence they should be accounted for in absorption-reaction systems.

Recent theoretical analyses have been able to predict large temperature rises similar to those observed experimentally. Shah (1972) constructs numerical "solutions" to the partial differential equations from the penetration theory model for mass and energy diffusion with reaction and shows that large temperature rises are possible. Clegg

and Mann (1969) obtain an expression for the rise but it is quite complicated even after some strong restrictions are made. The analysis is similar to the early work of Danckwerts (1951), who noted that since the thermal diffusivity is much greater than the mass diffusivity, the distance over which the thermal gradient exists is much greater than that over which the concentration gradient exists. Thus the mass transfer and reaction process appears to take place at a constant temperature, whereas in the heat transfer process, the heat of reaction appears as an interfacial flux. But Danckwerts assumed the interfacial concentration of the gas, the solubility, to be constant, i.e. independent of temperature. Clegg and Mann (1969) correct this but approximate the solubility with a linear relationship. This restricts their results to a small region about the initial temperature. Also they use a temperature independent rate constant. This weakens their results because as solubility decreases with temperature, resulting in a lower prediction for the temperature rise, the reaction rate increases thereby enhancing the rise. But even with the latter assumption, the predictions demonstrate the possibility of a large interfacial temperature rise for the chlorination of toluene.

Mann and Moyes (1977) derive a relatively simple transcendental equation for the interfacial temperature using the film theory. As above they assume the thermal diffusivity to be greater than the molecular diffusivity and hence the film thickness for mass transfer to be much less than the film thickness for heat transfer. The mass transfer problem can then be solved at a constant temperature, that of the interface. The temperature rise is obtained via an overall energy balance over the heat transfer film. The rate of energy transport to

the bulk can be equated to the heat of solution times the mass flux at the interface plus the heat of reaction times the excess flux into the film, i.e. the difference between the mass flux in and out of the film. From this it is possible to obtain for a general reaction a transcendental equation for the interfacial temperature, but Mann and Moyes did so only for the two limiting cases: no reaction and fast reaction. If a linear solubility relationship is used, the no reaction case gives an explicit expression for the interfacial temperature. This is not possible for the fast reaction limit unless the rate constant is independent of temperature. The general expression that can be obtained from this technique, see Appendix B, is applicable over the range of no reaction to fast reaction. However, it is not applicable when the reaction is not first order, i.e. when the liquid reactant is not in excess, and when the reaction becomes instantaneous. But the correction is straightforward and involves only correcting the enhancement factor for these cases. This technique presents the same problem that is encountered whenever the film theory is used. Even though the result seems reasonable the physical basis for the calculation is suspect, especially in this particular case. The existence of a stagnant film is difficult to believe in a turbulent system but it is even more improbable for two films of different thicknesses to exist. The technique used by Mann and Moyes assumes a different film thickness for mass and heat transfer, with the latter being much greater than the former.[6] This does not agree with the film theory view that a stagnant film separates the

[6]Note: if the film thicknesses are the same the temperature rise is less than the above by factor of $\sqrt{\alpha / D}$ or about ten!

gas from the bulk liquid. Here the bulk liquid is characterized by a uniform concentration and temperature whereas in the above analysis the mass transfer film does not contact liquid with the bulk temperature. It will be shown that this inconsistency can be avoided by using the surface-renewal theory and the result can be generalized for all reaction rates up to instantaneous.

With this background a model for gas-liquid reactors is constructed which contains the processes necessary for understanding the natural oscillations expected. It contains separate terms for the chemical reaction and the mass transfer processes. The role of the reaction in enhancing the mass transfer coefficient is deduced via the surface-renewal theory. The enhancement factor is then approximated piecewise by very simple explicit expressions of reasonable accuracy in the slow, fast and instantaneous reaction regimes. Simultaneously the reaction-induced surface temperature rise is deduced via the surface-renewal theory. These are used together with a temperature dependent form of Henry's law to represent the gas solubility.

# CHAPTER THREE
# MODEL FOR ABSORPTION AND REACTION IN A GAS-LIQUID CSTR

A simple method for contacting a gaseous reactant with a liquid reactant is to bubble the gas through the agitated liquid. In general each component of each phase may transfer to the other phase and react. The resulting system may exhibit multiple reactions in each phase and mass and energy transport between them. The concentrations and temperature of each phase and their dependence on the reactor parameters must be taken into account. In this generality the complexity of the process precludes all but the most superficial results.

For a large class of important reactions, viz., for chlorinations, hydrogenations, oxidations, etc., the reaction takes place in the liquid phase only. Here a pure gas A is bubbled through a nonvolatile liquid containing a reactant B into which the gas absorbs and reacts, via $A + \nu B \rightarrow$ Products. The gas is often supplied in excess, obviating a mass balance for this phase and implying that the only way the gas phase can affect the two-phase reactor is through the pressure dependence of the solubility. For this type of reaction the physical phenomena imply a reactor model that strikes a reasonable balance between the possibilities of in-depth analysis and physically interesting predictions.

We investigate this simple class of two-phase, continuous stirred-tank reactors. The assumptions that define this class are:

A1. The gas flow rate is greatly in excess of that required for absorption so that the interfacial area, a, is constant in space and time.

A2. The partial pressure of gas A, $P_A$, is constant in space and time.

A3. The reactant A enters the reactor only in the gas phase.

A4. The liquid-phase solvent, the reactant B and the products are nonvolatile.

A5. The reaction occurs only in the liquid phase.

A6. Thermal equilibrium exists between the two phases and the thermal capacity of the gas phase is vanishingly small.

A7. Physical equilibrium exists at the interface between the phases and can be described by a temperature dependent Henry's law constant:

$$P_A = H(T)\, C_{Ai}(T) \tag{3.1}$$

$$H(T) = H_o\, e^{-H_S/RT} \quad .$$

A8. Mass transfer is controlled by the liquid phase.

A9. The volume of the interfacial "film"[1] is much less than that of the bulk liquid.

The first five assumptions obviate balances on the gas phase. Now the system is like a single-phase (liquid) reactor with separate feeds for each reactant, component A via absorption and component B in the liquid feed. Therefore the feed rate of A is controlled by the reactor temperature and this is an essential part of the natural oscillation scheme proposed. Assumptions six and seven describe the temperature dependence of the solubility. The interfacial concentration of A is a decreasing function of temperature and an increasing function of the partial pressure of gas A. This pressure dependence is the only influence the gas phase will have on the gas-liquid reactor. The last

[1]By film we do not mean to suggest the film theory of intraphase mass transfer. Here film refers to regions where concentration variations are significant; bulk refers to regions where they are not.

assumption makes it unnecessary to distinguish between the bulk liquid volume and the total liquid volume because in most systems this difference is vanishingly small.

The model consists of two parts, the overall mass and energy balances describing the performance of the system and the interfacial mass and energy balances describing the absorption process. The second establishes the feed rate of A in the first. The overall mass balances for A and B in the bulk liquid are

$$V \frac{dC_A}{dt} = - q C_A - V k C_B C_A + V \phi k_L^\circ a(C_{Ai} - C_A)(1 - f_i) \qquad (3.2)$$

$$V \frac{dC_B}{dt} = q(C_{Bf} - C_B) - \nu V k C_B C_A - \nu V \phi k_L^\circ a(C_{Ai} - C_A)f_i. \qquad (3.3)$$

The similarity to the single-phase reactor equations is evident, see Appendix A. The only difference in the first balance is that the feed rate of A is the rate of mass transfer to the bulk liquid. This is the product of the overall rate of mass transfer times the fraction that does not react in the interfacial region, $(1 - f_i)$. The feed rate is a function of temperature hence the conditions inside the reactor control the feed as described in the introduction. That is, if a system becomes cold the solubility of A, $C_{Ai}$, increases resulting in a larger feed rate or rate of absorption, $V \phi k_L^\circ a (C_{Ai} - C_A)$, which increases the concentration of A in the liquid, the generation of heat via reaction and hence the temperature. So cold systems show a tendency to heat up. Conversely in hot systems the decreased solubility of A reduces the rate of absorption hence the rate of reaction, the generation of heat and the temperature. We note that this description holds when there is no enhancement of mass transfer, i.e. when $\phi = 1$ and $f_i = 0$.

Otherwise, inasmuch as $\phi$ and $f_i$ increase with temperature, the rate of absorption and heat generation may not follow the above, depending on the interaction of the solubility and the interfacial reaction. Consequently we anticipate that oscillations will be found even when there is not enhancement. The balance on B is also similar to the corresponding balance for the single-phase reactor except that there are two reaction terms, one for reaction in the bulk and the other for reaction near the interface. The reaction near the interface is the product of the rate of mass transfer of A and the fraction of A absorbed that reacts, $f_i$.

The energy balance is also very similar to that of the single-phase reactor, viz.,

$$V \rho C_p \frac{dT}{dt} = q \rho C_p(T_f - T) - U S_c(T - T_c) + H_S V \phi k_L^\circ a(C_{Ai} - C_A) + H_R [V k C_B C_A + V \phi k_L^\circ a(C_{Ai} - C_A)f_i] \quad . \qquad (3.4)$$

The only difference is that the source term is more complex. Here there are three sources, the heat of solution, $H_S$, the heat of reaction, $H_R$, in the bulk and the heat of reaction in the interfacial region.[2] The generation terms also follow the scenario for oscillations, being large for high mass transfer rates corresponding to high interfacial gas concentrations and low temperatures and vice versa.

Before this system of equations becomes a complete representation of the reactor performance a model for the interfacial processes is needed so that the enhancement factor, $\phi$, the fraction that reacts in

[2]The heat of solution, $H_S$, is normally positive and the heat of reaction, $H_R$, is positive for exothermic reactions.

the interfacial region, $f_i$, and the interfacial temperature, $T_i$, can be estimated. Several physical descriptions of the contacting of a gas and liquid are available. The most common models are from the film, penetration and surface-renewal theories. But because all the models contain an unknown constant which sets the mass transfer coefficient, $k_L^\circ$, and because our purpose is not so much to get the right numbers for a specific system but to get a general picture of how the performance of the mass transfer process changes from system to system over a wide range of systems, $k_L^\circ$ is to be viewed as a free parameter, defining the contacting. Thus what we seek from these theories is a way of predicting the enhancement of $k_L^\circ$ via reaction. Sherwood, Pigford and Wilke (1975) say that these standard models are interchangeable for this purpose. So we will adopt the model that is most physically plausible for this system and yields the quantities sought most easily.

The film theory, which is a steady state description of the mass transfer process, is less appealing physically than the others because the mass transfer process between a system of rising bubbles and an agitated liquid is a dynamic one. For a rising gas bubble the simplest physical picture suggests the penetration model insofar as the liquid elements attach themselves at the leading edge of the bubble, flow around the surface and detach at the trailing edge, thereby contacting the gas for the length of time necessary for the bubble to pass. But for a system of variously sized bubbles and for a well-mixed liquid this contact time might be random, suggesting the surface-renewal theory which averages the penetration theory results over a distribution of contact times. We adopt this model for these reasons and because certain quantities of interest can most easily be found.

At the gas-liquid interface the concentration of A is established by the condition that the liquid phase be in equilibrium with the gas phase whose state we are free to set. The A that dissolves reacts with B while diffusing away from the interface; the B that reacts is replaced by diffusion from the bulk, thus obtaining

$$\frac{\partial C_A}{\partial t} = D_A \frac{\partial^2 C_A}{\partial z^2} - k\, C_B\, C_A \tag{3.5}$$

$$\frac{\partial C_B}{\partial t} = D_B \frac{\partial^2 C_B}{\partial z^2} - \nu\, k\, C_B\, C_A \quad . \tag{3.6}$$

Because the absorption and the reaction processes generate heat, a temperature gradient or at least a temperature rise can be expected. This is not considered in the standard models mentioned but can be handled in a similar fashion. The heat of absorption is released at the interface whereas the heat of reaction is generated in the liquid phase bordering the interface. Whence an energy balance on this region gives

$$\rho\, C_p \frac{\partial T}{\partial t} = \cancel{k} \frac{\partial^2 T}{\partial z^2} + H_R\, k\, C_B\, C_A \quad . \tag{3.7}$$

We can not write the solution to Equations 3.5-3.7, as simple as they are. However, because the thermal diffusivity, $\alpha = \cancel{k}/\rho\, C_p$, is much greater than the molecular diffusivity, D, (this is almost always true for a gas-liquid system) we may construct a useful approximation to the solution. This condition, $\alpha >> D$, implies that the characteristic distance over which the temperature variation is significant is much greater than the corresponding distance for the concentration variation. Thus we may assume that the absorption-reaction process takes place at a uniform temperature and that the heat generation in the energy balance can be taken to be released at the interface. This allows us to investigate Eqs. 3.5 and 3.6 independently of the energy

balance equation, Eq. 3.7, and we may do this assuming a uniform temperature $T_i$. This temperature is not necessarily the bulk temperature T and must be set so that Eqs. 3.5-3.7 are compatible. We therefore add the assumption:

A10. The thermal diffusivity $\alpha$ is much greater than the molecular diffusivity D; therefore the absorption-reaction process takes place isothermally at the interfacial temperature $T_i$.

The interfacial equations, Eqs. 3.5 and 3.6, remain dependent on the reactor equations through the initial and the boundary conditions:

$$\begin{array}{lll} \text{at } t = 0 & C_A = C_{A\ell} & C_B = C_{B\ell} \\ \text{at } z = 0 \text{ (interface)} & C_A = C_{Ai}(T_i) & dC_B/dz = 0 \\ \text{as } z \to \infty & C_A = C_{A\ell} & C_B = C_{B\ell} \end{array} \qquad (3.8)$$

where the subscript $\ell$ denotes the value in the bulk liquid. What makes it possible for us to get the information that we seek is that the physics of gas-liquid reactions enables us to handle the problem for reactant B via a useful approximation (to be discussed) and to uncouple the interfacial and bulk equations for reactant A. The latter follows on comparing the time scales of the several processes necessary in gas-liquid absorption and reaction. In particular, we can show that whenever mass transfer is enhanced by reaction the bulk liquid concentration of A is vanishingly small, i.e. whenever $\phi$ is other than one and $f_i$ is other than zero their correct values are found by assuming that the bulk concentration of A is zero, $C_{A\ell} = 0$. This means either that $\phi = 1$ and $f_i = 0$ (and the interfacial equation for A becomes very simple) or that we can investigate the interfacial equation for A independently of the overall reactor equations. Thus the equations are independent of the bulk. This will now be shown.

To each process in the reactor we associate a characteristic time. This is a measure of the relative speed of the process. A long time signifies a slow process, whereas a short time signifies a fast one. These times can be used to scale the processes. Six characteristic times are apparent (Table 3.1); four originate in the reactor model and two in the absorption model. In the reactor equations, Eqs. 3.2-3.4, we identify a holding time $\tau$ which characterizes the feed rate of B, a mass transfer time $\tau_M$ which characterizes the feed rate of A, a reaction time $\tau_R$ and a heat transfer time $\tau_H$. In the absorption model we find an average interfacial exposure or contact time $\tau_i$ and an interfacial reaction time $\tau_{Ri}$. The interfacial reaction time differs from the bulk reaction time because the temperature and composition of the bulk and interface may differ.

Mass transfer is enhanced via reaction near the interface. This is significant if the interfacial reaction rate is fast compared to the exposure time of the liquid to the gas, that is, if the interfacial reaction time is less than or equal to the interfacial exposure time, viz., if[3]

$$\tau_i \gtrsim \tau_{Ri} \quad .$$

Suppose we have enhanced absorption and consider the corresponding conditions in the bulk liquid. The bulk reaction time is always greater than or equal to the interfacial reaction time because the bulk temperature is always less than or equal to the interfacial temperature.

---

[3]In the following we are speaking qualitatively. Hence the symbol $\sim$ will denote an approximate equality or an order of magnitude relationship between two quantities.

TABLE 3.1
CHARACTERISTIC TIMES

| | |
|---|---|
| **Reactor** | |
| Holding Time | $\tau = V / q$ |
| Reaction Time | $\tau_R = 1 / k\, C_B$ |
| Mass Transfer Time | $\tau_M = 1 / k_L^o\, a$ |
| Heat Transfer Time | $\tau_H = \rho\, C_p\, V / U\, S_c$ |
| **Absorption Process** | |
| Exposure Time | $\tau_i = D / (k_L^o)^2$ |
| Reaction Time | $\tau_{Ri} = 1 / k(T_i)\, C_B$ |

At the first sign of enhancement the two temperatures are nearly the same (because little reaction has occurred at the interface) and we have

$$\tau_i \sim \tau_{Ri} \sim \tau_R \quad .$$

It is the nature of gas-liquid systems that the mass transfer time is much greater than the interfacial exposure time, see Astarita (1967), viz.,

$$\tau_M >> \tau_i$$

whence, at the onset of enhancement

$$\tau_M >> \tau_R \quad .$$

It follows that the reaction rate in the bulk is very fast as compared with the feed rate of A (mass transfer rate) and hence that mass transfer is the controlling process when enhancement begins. This implies that the bulk concentration of A must be vanishingly small and that we may take the initial and boundary conditions appropriate to the absorption model to be

$$\begin{aligned} &\text{at } t = 0 && C_A = 0 \\ &\text{at } z = 0 && C_A = C_{Ai}(T_i) \\ &\text{as } z \to \infty && C_A = 0 \end{aligned} \tag{3.9}$$

thereby uncoupling the interfacial and bulk problems. This continues to hold throughout the enhanced mass transfer region because

$$\tau_M >> \tau_i \sim \tau_R \text{ (onset)} > \tau_R \text{ (enhanced)} \quad .$$

We can construct the solution of the absorption model equations, Eqs. 3.5, 3.6 and 3.9, in two limiting cases: reactant B in excess and instantaneous reaction. The first is almost always true for a practical gas-liquid reaction. That is, the concentration of the liquid phase reactant is usually much greater than the concentration of the dissolved

gaseous reactant. Thus to a reasonable approximation the concentration of B is constant throughout the reactor (albeit not necessarily at the feed value). The interfacial model is then reduced to a single diffusion equation with pseudo-first order reaction. Solving this linear equation for an exposure time t and averaging the result over all the elements of liquid at the interface assuming a random distribution of exposure times

$$\frac{1}{\tau_i} e^{-t/\tau_i}$$

obtains the mass transfer coefficient, $k_L$, and enhancement factor, $\phi$, see Appendix C:

$$\phi = k_L/k_L^\circ = \sqrt{1 + \tau_i/\tau_{Ri}} \tag{3.10}$$

where $k_L^\circ$ is the mass transfer coefficient without reaction. The fraction of A that reacts near the interface in the process of absorption is the ratio of the rate of reaction to the rate of absorption, viz.,

$$f_i = \frac{(1/\tau_i) \int_0^\infty e^{-t/\tau_i} \left[ \int_0^\infty k\, C_B\, C_A\, dz\, (Va) \right] dt}{V\, \phi\, k_L^\circ\, a\, C_{Ai}} .$$

Using results in Appendix C obtains

$$f_i = \frac{\tau_i / \tau_{Ri}}{1 + \tau_i/\tau_{Ri}} . \tag{3.11}$$

This is the same as the fraction that reacts in a single-phase CSTR with holding time $\tau_i$ and reaction time $\tau_{Ri}$, see Appendix A.

The time scale argument given previously now can be understood better. When the ratio $\tau_i/\tau_{Ri}$ is much less than one, practically no reaction and hence no enhancement occurs, i.e. $\phi \sim 1$, $f_i \sim 0$. Only when the ratio is of the order of one does the enhancement become important.

It follows that if the bulk concentration of A becomes significant so that the above boundary conditions, Eq. 3.9, become inappropriate, the above result nonetheless exhibits the correct limit.

The second limiting case which admits simple results is that in which the interfacial reaction becomes instantaneous. This means that the reactants A and B can not coexist together in the liquid, that is they react immediately upon contact. Thus when an element of liquid first contacts the gas all of the liquid reactant B at the interface is instantly consumed. As the absorption of A progresses a reaction plane moves into the liquid. At this plane and only there the reaction takes place and the concentrations of A and B vanish, see Figure 3.1. This uncouples the diffusion and reaction equations for A and B by removing the reaction. To the left of the plane, A diffuses from the interface to the reaction plane; to the right B diffuses from the bulk to the plane. Solving the two diffusion equations and equating the fluxes at the reaction plane, adjusted for the stoichiometry, gives the concentration profiles and the position of the reaction plane, see Appendix C. Averaging the flux at the interface over all exposure times obtains the enhancement factor, viz.,

$$\phi = \phi_I \equiv 1 + \frac{C_{B\ell}}{\nu C_{Ai}} \quad . \tag{3.12}$$

This is the upper bound for the enhancement factor. On comparing this with the previous expression for $\phi$ we can estimate the condition for the onset of instantaneous reaction, viz.,[4]

[4]This is an estimate because in the first expression $C_B = C_{B\ell}$ everywhere and in the second $C_B$ vanishes throughout part of the interfacial region. Evidently there is a transition region and its description is the aim of the van Krevelen-Hoftijzer approximation.

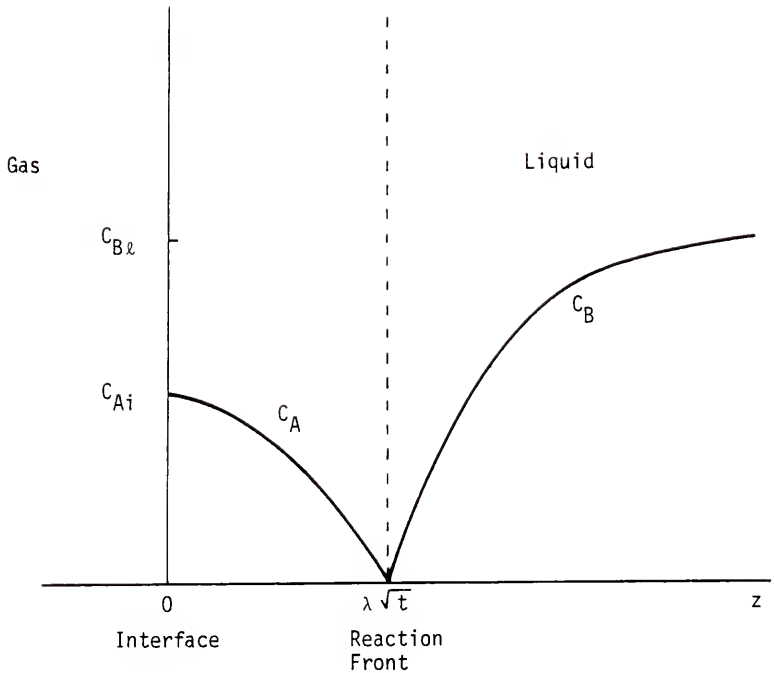


Figure 3.1. Concentration profiles near the interface for instantaneous reaction.

$$1 + \tau_i / \tau_{Ri} > 1 + C_{B\ell} / \nu C_{Ai} \ .$$

That is, whenever the noninstantaneous enhancement factor exceeds the instantaneous value then the latter must be used. Whenever enhancement is significant, $\tau_i/\tau_{Ri}$ is much greater than one and because $C_{B\ell}/\nu C_{Ai}$ is almost always much greater than one, a simpler form of the above condition is possible, viz.,

$$\frac{\tau_i}{\tau_{Ri}} > \left(\frac{C_{B\ell}}{\nu C_{Ai}}\right)^2 \ . \tag{3.13}$$

All of this is consistent with the intuitive idea that the fraction that reacts for instantaneous reaction must be approximately one.

There appears to be three limiting cases for the enhancement factor corresponding to slow, fast and instantaneous interfacial reaction:

$$\begin{aligned} \phi &= 1 && \text{slow} \\ \phi &= \sqrt{1 + \tau_i/\tau_{Ri}} && \text{fast} \\ \phi &= 1 + C_{B\ell}/\nu C_{Ai} && \text{instantaneous.} \end{aligned} \tag{3.14}$$

This can be seen in Figure 3.2 where the enhancement factor is plotted against the rate constant (similar to a plot against temperature). Now that the enhancement factor is known for the limiting cases we must establish what happens in the transition region between fast and instantaneous reaction. The fast reaction expression, because it is based on B in excess, breaks down when the concentration of B becomes small near the interface. But the reaction does not become instantaneous until B goes to zero there. So in the transition region the variation in the concentration of B must be considered. This can be done using the van Krevelen-Hoftijzer approximation, see Sherwood, Pigford and Wilke (1975), which corrects for the variation in the concentration of B by making an estimate of its interfacial value and using that in place of

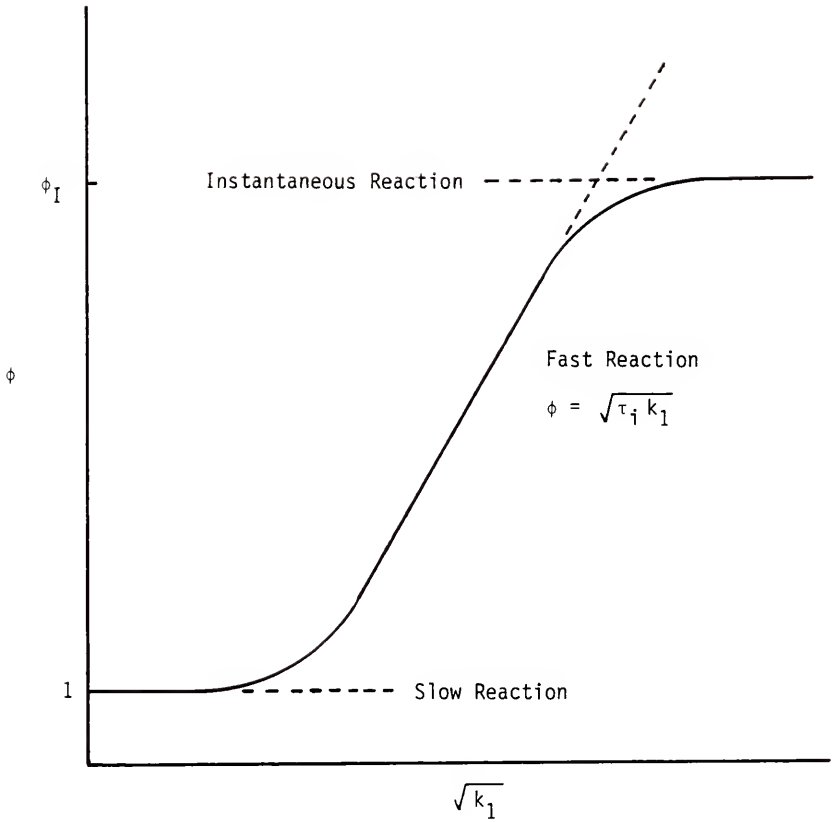


Figure 3.2. Enhancement factor versus $\sqrt{k_1}$ .

the bulk concentration in the excess B result. The interfacial concentration of B is estimated by equating the rate of diffusion of B toward the interface, stoichiometrically corrected, to the excess rate of absorption of A, i.e. the fraction that reacts. This concentration can be used in place of $C_{B\ell}$ in the original calculation of the enhancement factor to obtain

$$\phi = \sqrt{1 + \frac{\tau_i}{\tau_{Ri}} \left( \frac{\phi_I - \phi}{\phi_I - 1} \right)} \tag{3.15}$$

where $\phi_I$ is the instantaneous enhancement factor, Eq. 3.12.

This result is shown in Sherwood, Pigford and Wilke (1975, p 328) to correctly bridge the limiting conditions of excess B and instantaneous reaction. But this result is more complicated than the previous ones and using it makes the analyses to follow quite difficult. How much error would be introduced by replacing this intermediate regime result by an extrapolation of its limits? The transition region is small as illustrated in Figure 2.3 and the enhancement factor does not differ greatly from the extrapolation of its limits. This suggests that without the loss of any important phenomena, we can represent the transition region by this approximation. Thus in keeping with the desire for a simple model, the enhancement factor will be approximated by extrapolating these two limiting cases to their intersection in the transition region.

The results of the interfacial model are:

$$\text{for } \frac{\tau_i}{\tau_{Ri}} < \left( \frac{C_{B\ell}}{\nu C_{Ai}} \right)^2 \qquad \text{then} \quad \phi = \sqrt{1 + \tau_i/\tau_{Ri}}$$

$$f_i = \frac{\tau_i/\tau_{Ri}}{1 + \tau_i/\tau_{Ri}}$$

$$\text{and for } \frac{\tau_i}{\tau_{Ri}} > \left( \frac{C_{B\ell}}{\nu C_{Ai}} \right)^2 \qquad \text{then } \phi_I = 1 + C_{B\ell}/\nu C_{Ai}$$

$$f_i = 1 \,. \qquad (3.16)$$

Both the enhancement factor and the fraction that reacts are S-shaped functions of temperature. In fact $f_i$ is the same function that determines the multiplicity in a single-phase CSTR if $\tau_i$ is the holding time. The function $f_i$ varies from zero to one. The enhancement factor ranges from one to $\phi_I$ where $\phi_I$ depends on temperature through the gas solubility, i.e. $C_{Ai}$. Both functions increase monotonically with temperature. But the temperature they depend on is the interfacial temperature which has yet to be determined.

Just as reaction near the interface increases the concentration gradient, and hence the mass transfer, it increases the local temperature through the heat of reaction. The interfacial temperature can also rise due to the release of the heat of solution of the gas upon absorption. We can construct the solution of the energy balance equation, Eq. 3.7, in two special cases: that of no reaction where the temperature rise is due solely to the heat of solution and that of instantaneous reaction where the heat of solution is vanishingly small. The temperature rise due to gas absorption without reaction will be found first.

For no reaction the concentration and temperature near the interface are described by the diffusion equations:

$$\frac{\partial C_A}{\partial t} = D \frac{\partial^2 C_A}{\partial z^2}$$

$$\frac{\partial T}{\partial t} = \alpha \frac{\partial^2 T}{\partial z^2}$$

with the initial and boundary conditions:

| | | |
|---|---|---|
| at $t = 0$ | $C_A = 0$ | $T = T_\ell$ |
| at $z = 0$ | $C_A = C_{Ai}(T_i)$ | $T = T_i$ |
| as $z \to \infty$ | $C_A = 0$ | $T = T_\ell$ . |

The relationship between $C_{Ai}$ and $T_i$ is given by Henry's law, viz.,

$$C_{Ai} = \frac{P_A}{H(T_i)} = \frac{P_A}{H_o} \, e^{H_S/RT_i}$$

where $P_A$ is the gas partial pressure and $H(T_i)$ is the Henry's law coefficient which depends on the heat of solution $H_S$. The solution of these equations is given in Appendix D. The interfacial temperature $T_i$ can be found by equating the heat released on absorption to the flux of energy into the liquid at the interface:

$$- D \frac{\partial C_A}{\partial z}\bigg|_{z=0} H_S = -k \frac{\partial T}{\partial z}\bigg|_{z=0} .$$

Solving obtains an implicit equation for the temperature rise:

$$T_i - T_\ell = \frac{H_S}{\rho C_p} \sqrt{\frac{D}{\alpha}} \; C_{Ai}(T_i) . \qquad (3.17)$$

Since $H_S$ and the ratio $D/\alpha$ are usually small the temperature rise due to the heat of solution will usually be small. Using parameters as reported for the chlorination of decane studied by Ding et al. (1974), yields a temperature rise of three degrees Celsius.

When the reaction is instantaneous, all the reaction takes place at a plane which moves into the liquid. The solution of the mass balance equation is known and so therefore is the motion of the reaction plane, see Appendix C. For the energy balance equation the heat generation is

confined to the reaction plane and is known. The problem then is simply to find the temperature field that disposes of this heat. If the gas-liquid interface is assumed to be an adiabatic surface, which is a reasonable approximation, then on the interfacial side of the reaction plane the energy balance equation is satisfied if the temperature is a constant, $T_i$. That is, the heat generated at the moving reaction front heats the liquid behind it to a constant temperature. On the bulk side of the front the heat of reaction is conducted from the moving plane at a temperature $T_i$ to a reservoir at infinity at temperature $T_\ell$. The corresponding temperature profile is known, see Appendix D. The interfacial temperature $T_i$ can be obtained by equating the heat generated by reaction at the front to the heat conducted away from the front:

$$- H_R D \frac{\partial C_A}{\partial z} = - k \frac{\partial T}{\partial z} \qquad \text{at } z = \lambda\sqrt{t} \quad .$$

The result is complicated but if the thermal diffusivity is much greater than the molecular diffusivity, $\alpha >> D$, and $C_{B\ell}/(\nu C_{Ai}) >> 1$ (which are both true for most gas-liquid systems) it can be simplified to, see Appendix D,

$$T_i - T_\ell = \frac{H_R}{\rho C_p} \sqrt{\frac{D}{\alpha}}\, \phi_I\, C_{Ai} \quad . \tag{3.18}$$

This equation is still implicit in $T_i$ because the instantaneous enhancement factor and the solubility are functions of $T_i$. We expect the temperature rise for instantaneous reaction to be much larger than that for absorption not only because heats of reaction are usually larger than those of solution but also because the enhancement factor can be much greater than one, that is, the rate of absorption is much greater with reaction.

Both temperature rise results have the same form (i.e. the product of the heat released and the rate of absorption) which suggests that the instantaneous reaction result can be corrected for the effect of the heat of solution by replacing the heat of reaction with the sum of the heat of reaction and the heat of absorption. Using the data of Ding et al. (1974), this prediction yields a temperature rise of 92 degrees Celsius. Even though this is an upper limit, any rise of this order of magnitude must be important.

In the intermediate regime where the reaction near the interface is fast enough to be important but not instantaneous, we can not construct the solution to the problem. Nonetheless we may deduce a reasonable approximation as follows. Because $\alpha >> D$, the mass transfer process appears to take place at a constant temperature $T_i$ with known result. This implies a known release of energy due to absorption and reaction. All that remains then is to find the temperature field which accommodates this heat generation. In particular, the interfacial temperature is maintained by the heats of solution and reaction which appear to be released at the interface. That is, because the heat transfer process takes place over a much greater distance than the mass transfer process, the generation of heat via absorption and reaction appears as a surface source for heat transfer rather than a bulk source. On this basis the temperature profile can be found from the diffusion equation with constant interfacial and bulk temperatures, viz.,

$$\frac{\partial T}{\partial t} = \alpha \frac{\partial^2 T}{\partial z^2}$$

at $t = 0$ $\quad T = T_\ell$

at $z = 0$ $\quad T = T_i$ $\quad$ and $\quad$ as $z \to \infty$ $\quad T = T_\ell$ .

Then the interfacial temperature is obtained by an energy balance at the interface. The heat generated by absorption and reaction is equated to the energy flux at the interface where both have been averaged for the surface-renewal theory, see Appendix D, viz.,

$$(H_S + H_R f_i)\left(- D \frac{\partial C_A}{\partial z}\bigg|_0\right) = -k \frac{\partial T}{\partial z}\bigg|_0 \quad .$$

The resulting temperature rise is

$$T_i - T_\ell = \left(\frac{H_S}{\rho C_p} + \frac{H_R}{\rho C_p} f_i\right) \sqrt{\frac{D}{\alpha}} \; \phi \; C_{Ai} \quad . \tag{3.19}$$

This result is similar in form to the two previous limiting results. In each the temperature rise is the product of three terms: the rate of absorption, the heat released, and the inverse of the heat transfer coefficient. The heat released for each mole of gas absorbed is the sum of the heat of solution and the product of the heat of reaction and the fraction that reacts. The rate of absorption is $\phi \; k_L^\circ \; C_{Ai}$. The heat transfer coefficient is $\sqrt{\alpha/D} \; \rho \; C_p \; k_L^\circ$ where $\sqrt{\alpha/D}$ has to do with converting a mass transfer coefficient into a heat transfer coefficient. Eq. 3.19 also has the proper limits:

$$\lim_{k \to 0} (T_i - T_\ell) = \frac{H_S}{\rho C_p} \sqrt{\frac{D}{\alpha}} \; C_{Ai}$$

$$\lim_{k \to \infty} (T_i - T_\ell) = \left(\frac{H_S + H_R}{\rho C_p}\right) \sqrt{\frac{D}{\alpha}} \; \phi_I \; C_{Ai} \quad .$$

The first is the result for absorption without reaction. The second is the result for instantaneous reaction, where $f_i = 1$ and $\phi = \phi_I$, with the effect of the heat of solution added. Thus the general result for the interfacial temperature rise, Eq. 3.19, seems to be reasonable, it is

easily interpreted physically and gives the proper limits for slow and fast reaction.

This result also agrees with what one might estimate from the instantaneous reaction temperature rise by equating the ratios of the reaction rates and the temperature rises for instantaneous and non-instantaneous reaction. That is the ratio of the temperature rise for noninstantaneous reaction to that for instantaneous should be equal to the corresponding ratio of the interfacial reaction rates. The reaction rates are the mass transfer rates times the fraction that reacts. Thus we have

$$\frac{(T_i - T_\ell)}{(T_i - T_\ell)_{Inst.}} = \frac{f_i \phi k_L^\circ C_{Ai}}{\phi_I k_L^\circ C_{Ai_I}} \quad .$$

The instantaneous rise is known, i.e. Eq. 3.18, so

$$(T_i - T_\ell) = \frac{H_R}{\rho C_p} \sqrt{\frac{D}{\alpha}} \; f_i \phi C_{Ai} \quad .$$

This is the result obtained above if the heat of solution is neglected. Thus the predicted temperature rise agrees with physical intuition.

The mass and energy balances for the reactor complemented by the interfacial results for the enhancement factor, the fraction absorbed that reacts, and the temperature rise, constitute a complete description of the reactor dynamics. The use of the averaged interfacial results in a dynamic reactor model is justified because the characteristic time for variations near the interface is much less than that for the reactor. In Table 3.2 these equations are shown in their dimensionless form. But as previously seen, a better understanding of the physics of the processes may be obtained by writing the equations in

terms of the time scales, Table 3.3. This will become more evident when the steady state results are examined.

The scenario for oscillations, outlined originally, can be made more precise. In the temperature equation, the generation terms, containing the heats of solution and reaction, operate to decrease the temperature at high temperatures and increase it at low ones. At high temperatures the solubility $x_i$ is small hence the heat generated via absorption, $B_S\ (\tau\ /\ \tau_M)\ \phi\ (x_i - x_A)$, and interfacial reaction, $B_R\ (\tau\ /\ \tau_M)\ \phi\ f_i\ (x_i - x_A)$, can be small. Also the bulk concentration of A, $x_A$, must be small for small $x_i$, whence the bulk reaction term, $B_R\ (\tau\ /\ \tau_R)\ x_A$, must be small. Thus as the heat generation decreases and the heat removal increases for high temperatures, we anticipate $dT/dt < 0$. Conversely, for decreasing temperatures the rate of absorption increases hence the rate of reaction may also increase because $x_A$ is large. Thus we anticipate that for low temperatures, $dT/dt > 0$. But we observe that the effect of the enhancement factor and of the fraction that reacts on absorption is contrary to the above, viz., increasing temperature increases absorption and interfacial reaction, hence the generation of heat. So it may be that oscillations do not appear in systems with enhanced mass transfer and that the most likely regime for oscillations is the one that precedes enhancement. This discussion is premature because before the dynamics can be adequately understood, the steady state behavior must be known. The steady state results will be investigated first to provide a basis for dynamic studies.

TABLE 3.2
DIMENSIONLESS EQUATIONS

$$\frac{dx_A}{dt'} = -\left(1 + D_a\, x_B\, e^{\gamma\theta/(1+\theta)}\right) x_A + \phi\,\beta\,(1 - f_i)\left[\, e^{-n\theta_i/(1+\theta_i)} - x_A \,\right]$$

$$\frac{dx_B}{dt'} = (1 - x_B) - S\left[\, D_a\, x_A\, x_B\, e^{\gamma\theta/(1+\theta)} + \phi\,\beta\, f_i\, (e^{-n\theta_i/(1+\theta_i)} - x_A) \,\right]$$

$$\frac{d\theta}{dt'} = -(1 + H)\,\theta + H\,\theta_c + B_R\, D_a\, x_A\, x_B\, e^{\gamma\theta/(1+\theta)}$$

$$+ \left[\, B_S + B_R\, f_i \,\right] \phi\,\beta\, (e^{-n\theta_i/(1+\theta_i)} - x_A)$$

$$\theta_i = \theta + \left[\, B_S + B_R\, f_i \,\right] \sqrt{D/\alpha}\;\; \phi\, e^{-n\theta_i/(1+\theta_i)}$$

if $S^2\, D_{ai}\, e^{(\gamma-2n)\theta_i/(1+\theta_i)} < x_B$

then $\phi = \sqrt{1 + D_{ai}\, x_B\, e^{\gamma\theta_i/(1+\theta_i)}}$

$$f_i = \frac{D_{ai}\, x_B\, e^{\gamma\theta_i/(1+\theta_i)}}{1 + D_{ai}\, x_B\, e^{\gamma\theta_i/(1+\theta_i)}}$$

or if $S^2\, D_{ai}\, e^{(\gamma-2n)\theta_i/(1+\theta_i)} > x_B$

then $\phi = 1 + (x_B/S)\, e^{n\theta_i/(1+\theta_i)}$

$f_i = 1$

TABLE 3.2--continued

where

$x_A = C_A / C_{Aif}$ $\qquad C_{Aif} = (P_A / H_o)\, e^{\eta}$

$x_B = C_B / C_{Bf}$ $\qquad \eta = H_S / (R\, T_f)$

$\theta = (T - T_f) / T_f$ $\qquad \theta_i = (T_i - T_f) / T_f$

$\theta_c = (T_c - T_f) / T_f$

$t' = t / \tau$ $\qquad \gamma = E / (R\, T_f)$

$D_a = \tau\, k_o\, C_{Bf}\, e^{-\gamma}$ $\qquad D_{ai} = \tau_i\, k_o\, C_{Bf}\, e^{-\gamma}$

$\beta = \tau\, k_L^{\circ}\, a$ $\qquad H = (U\, S_c) / (\rho\, C_p\, q)$

$B_S = (H_S\, C_{Aif}) / (\rho\, C_p\, T_f)$ $\qquad B_R = (H_R\, C_{Aif}) / (\rho\, C_p\, T_f)$

$S = (\nu\, C_{Aif}) / C_{Bf}$

TABLE 3.3
EQUATIONS IN TERMS OF TIME SCALES

$$\frac{dx_A}{dt'} = -(1 + \tau / \tau_R)\, x_A + \phi\, (\tau / \tau_M)\, (x_i - x_A)\, (1 - f_i)$$

$$\frac{dx_B}{dt'} = (1 - x_B) - S\, (\tau / \tau_R)\, x_A - S\, \phi\, (\tau / \tau_M)\, (x_i - x_A)\, f_i$$

$$\frac{d\theta}{dt'} = -(1 + \tau / \tau_H)\, \theta + (\tau / \tau_H)\, \theta_c + B_S\, (\tau / \tau_M)\, \phi\, (x_i - x_A) + B_R \left[ (\tau / \tau_R)\, x_A + \phi\, (\tau / \tau_M)\, (x_i - x_A)\, f_i \right]$$

$$\theta_i = \theta + \left[ B_S + B_R\, f_i \right] \sqrt{D/\alpha}\ \phi\, x_i$$

if $\dfrac{\tau_i}{\tau_{Ri}} < \left( \dfrac{x_B}{S\, x_i} \right)^2$ then $\phi = \sqrt{1 + \tau_i / \tau_{Ri}}$

$$f_i = \frac{\tau_i / \tau_{Ri}}{1 + \tau_i / \tau_{Ri}}$$

if $\dfrac{\tau_i}{\tau_{Ri}} > \left( \dfrac{x_B}{S\, x_i} \right)^2$ then $\phi = 1 + x_B / (S\, x_i)$

$$f_i = 1$$

$$\frac{\tau}{\tau_R} = D_a\, x_B\, e^{\gamma\theta/(1+\theta)} \qquad \frac{\tau_i}{\tau_{Ri}} = D_{ai}\, x_B\, e^{\gamma\theta_i/(1+\theta_i)}$$

$$x_i = e^{-n\theta_i/(1+\theta_i)}$$

TABLE 3.3--continued

where

$x_i = C_{Ai} / C_{Aif}$

$\tau = V / q$ (sec)

$\tau_i = D / (k_L^\circ)^2$ (sec)

$\tau_R = 1 / (k\ C_B)$ (sec)

$\tau_{Ri} = 1 / (k(T_i)C_B)$ (sec)

$\tau_M = 1 / (k_L^\circ\ a)$ (sec)

$\tau_H = \tau/H = (\rho\ C_p\ V)/(U\ S_c)$ (sec)

$k = k_o\ e^{-E/(R\ T)}$ ($cm^3$/gmole·sec)

# CHAPTER FOUR
# STEADY STATE RESULTS

The steady state equations are obtained by setting the time derivatives of the concentrations and temperature to zero in the model. In terms of the time scales, see Table 3.3, these are

$$
\begin{aligned}
0 &= -(1 + \tau/\tau_R)\, x_A + (\tau/\tau_M)\, \phi\, (x_i - x_A)\, (1 - f_i) \\
0 &= (1 - x_B) - S\, (\tau/\tau_R)\, x_A - S\, (\tau/\tau_M)\, \phi\, (x_i - x_A)\, f_i \\
0 &= -(1 + \tau/\tau_H)\, \theta + (\tau/\tau_H)\, \theta_c + B_S\, (\tau/\tau_M)\, \phi\, (x_i - x_A) \\
&\quad + B_R \{ (\tau/\tau_R)\, x_A + (\tau/\tau_M)\, \phi\, (x_i - x_A)\, f_i \} .
\end{aligned}
\tag{4.1}
$$

The concentration of B and the temperature also appear implicitly; $x_B$ appears in $\tau_R$, $\phi$ and $f_i$ whereas $\theta$ appears in $\tau_R$ and in $\phi$, $f_i$ and $x_i$ through their $\theta_i$ dependence, see Table 3.3. Only the concentration of A can be found explicitly, viz.,

$$
x_A = \frac{\phi \frac{\tau}{\tau_M} x_i\, (1 - f_i)}{\{ 1 + \frac{\tau}{\tau_R} + \phi \frac{\tau}{\tau_M} (1 - f_i) \}} . \tag{4.2}
$$

Eliminating the concentration of A using Eq. 4.2 obtains two implicit equations for $x_B$ and $\theta$, viz.,

$$
x_B = 1 - S \frac{\phi \frac{\tau}{\tau_M} x_i\, (1 + \frac{\tau}{\tau_R})}{\{ 1 + \frac{\tau}{\tau_R} + \phi \frac{\tau}{\tau_M} (1 - f_i) \}} \left( \frac{\frac{\tau}{\tau_R} + f_i}{1 + \frac{\tau}{\tau_R}} \right) \tag{4.3}
$$

and

$$(1 + \tau/\tau_H)\ \theta - (\tau/\tau_H)\ \theta_c = \frac{\phi \frac{\tau}{\tau_M} x_i \left(1 + \frac{\tau}{\tau_R}\right)}{\left\{ 1 + \frac{\tau}{\tau_R} + \phi \frac{\tau}{\tau_M} (1 - f_i) \right\}} \cdot$$

$$\left\{ B_S + B_R \left( \frac{\frac{\tau}{\tau_R} + f_i}{1 + \frac{\tau}{\tau_R}} \right) \right\} \quad . \qquad (4.4)$$

Although complicated, these balances can be easily interpreted. The amount of A absorbed in time $\tau$ is

$$\phi \frac{\tau}{\tau_M} (x_i - x_A) = \frac{\phi \frac{\tau}{\tau_M} x_i \left(1 + \frac{\tau}{\tau_R}\right)}{\left\{ 1 + \frac{\tau}{\tau_R} + \phi \frac{\tau}{\tau_M} (1 - f_i) \right\}} \qquad (4.5)$$

and the total fraction of absorbed A that reacts is[1]

$$f_R = \left( \frac{\tau/\tau_R + f_i}{1 + \tau/\tau_R} \right) . \qquad (4.6)$$

Equation 4.3 then says that the concentration of B is its initial concentration minus the product of the amount of A absorbed, the fraction

---

[1]Because $f_R$ is the ratio of the rate of reaction in the bulk and in the interfacial region to the rate of absorption, viz.,

$$f_R = \frac{f_b\ V\ \phi\ k_L^\circ\ a\ (C_{Ai} - C_A)\ (1 - f_i) + f_i\ V\ \phi\ k_L^\circ\ a\ (C_{Ai} - C_A)}{V\ \phi\ k_L^\circ\ a\ (C_{Ai} - C_A)}$$

$$= f_b\ (1 - f_i) + f_i \ ,$$

and $f_b$ is the fraction of A absorbed into the bulk that reacts in the bulk

$$f_b = \frac{V\ k\ C_B\ C_A}{V\ \phi\ k_L^\circ\ a\ (C_{Ai} - C_A)\ (1 - f_i)} = \frac{\tau/\tau_R}{1 + \tau/\tau_R} \ ,$$

we obtain

$$f_R = \frac{\tau/\tau_R + f_i}{1 + \tau/\tau_R} \ .$$

that reacts and the stoichiometric constant S. The energy balance, Eq. 4.4, is written in the classical form: the heat removed from the reactor in time $\tau$ equals the heat generated. The heat removed is the sum of the energy lost to the effluent and to the cooling medium, viz.,

$$\theta + (\tau/\tau_H)\ (\theta - \theta_c)$$

and is linear in temperature. The heat generated is the product of the amount of A absorbed and the total heat released via absorption and reaction per mole absorbed. The latter is the sum of the heat of solution and the product of the heat of reaction times the fraction that reacts. Inasmuch as the heat removal function is a straight line with respect to $\theta$, identical to that for the single-phase reactor, it is the shape of the heat generation function with respect to $\theta$ which determines the steady state multiplicity, as will be seen (see also Appendix A where the same is true for the single-phase CSTR).

Classically the steady states are found by plotting the left and right sides of the energy balance, Eq. 4.4, versus the temperature. But Eq. 4.4 is complicated, so before doing this we seek a better understanding of the system and of the interaction between the physical processes by considering a special case: an isothermal reactor with the concentration of reactant B equal to its feed value (therefore the reaction is pseudo-first order), see Sherwood, Pigford and Wilke (1975). By varying the rate constant for this system, we can consider an ensemble of cases without the complicated temperature equation and determine how the reactor is affected. Inasmuch as the greatest temperature dependence is through the rate constant, the results should give us an indication of how the system will respond to variations in the temperature.

Because the heat generation is proportional to the rate of absorption, one should expect that a knowledge of this function will greatly help in the understanding of the heat generation function and hence the multiplicity of solutions to the steady state reactor equations. The rate of absorption of A is

$$R_a = \phi\,(V/\tau_M)\,(C_{Ai} - C_A) = \frac{\phi\,\frac{\tau}{\tau_M}\,(qC_{Ai})\,(1 + \tau/\tau_R)}{\{\,1 + \frac{\tau}{\tau_R} + \phi\,\frac{\tau}{\tau_M}\,(1 - f_i)\,\}} \quad . \tag{4.7}$$

The effect of the solubility can be removed by introducing a relative rate of absorption, viz.,

$$R_r = R_a / (qC_{Ai}) = \frac{\phi\,\frac{\tau}{\tau_M}\,(1 + \tau/\tau_R)}{\{\,1 + \frac{\tau}{\tau_R} + \phi\,\frac{\tau}{\tau_M}\,(1 - f_i)\,\}} \tag{4.8}$$

where $qC_{Ai}$ is the rate of absorption if the liquid is in equilibrium with the gas. Observing that $1/R_r$ can be written as a sum of resistances gives

$$1/R_r = 1/r_1 + 1/r_2$$

$$\text{where} \quad r_1 = \frac{(1 + \tau/\tau_R)}{(1 - f_i)} = (1 + \tau/\tau_R)\,(1 + \tau_i/\tau_{Ri}) \tag{4.9}$$

$$\text{and} \quad r_2 = \phi\,(\tau/\tau_M) \quad . \tag{4.10}$$

Here we have scaled the system by $\tau$ which is a measure of the flow rate or, more specifically, a measure of the rate of flow of dissolved A out of the reactor. Thus the overall resistance to absorption is the sum of the resistance to the removal of A from the reactor , $1/r_1$, and the resistance to the mass transfer of A into the reacting liquid, $1/r_2$, cf. Figure 4.1. The removal of A is accomplished in two ways, via flow and via reaction, where reaction consists of two parts: bulk reaction

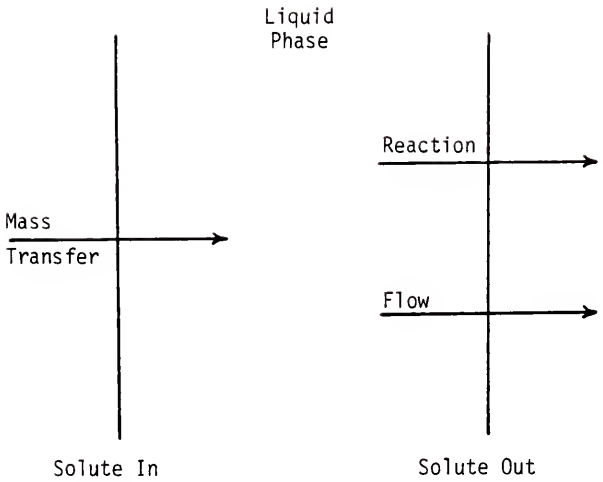


Figure 4.1. Series and parallel resistances for absorption and reaction.

and interfacial reaction. Because $\tau >> \tau_i$ always and $\tau_R \simeq \tau_{Ri}$ at the onset of enhanced mass transfer, initially for low temperatures or small rate constants $r_1$ will go as $(1 + \tau/\tau_R)$. The resistance to mass transfer depends on the mass transfer coefficient and the specific surface area, $r_2 = \tau\phi k_L^\circ a$. This is a constant until the temperature or the rate constant is large enough so that the mass transfer becomes enhanced.

The only temperature dependence in these resistances is in the rate constant $k_1$ which appears in $\tau_R$, $\tau_{Ri}$ and $\phi$. If $r_1$ and $r_2$ are plotted versus the rate constant $k_1$ then insight into the behavior of the rate of absorption as a function of temperature can be gained because the relative rate of absorption will approximately equal the lesser of $r_1$ and $r_2$. For small values of $k_1$, $r_1$ is approximately one, cf. Figure 4.2. Only when $\tau/\tau_R \simeq 1$ does it begin to increase and when $\tau/\tau_R >> 1$, it goes as $\tau/\tau_R = \tau k_1$. This continues until enhancement begins, $\tau_i/\tau_{Ri} \simeq 1$, and thereafter $r_1$ increases even faster, eventually going to the limit

$$r_1 = \frac{\tau}{\tau_R}\frac{\tau_i}{\tau_{Ri}} = \tau\ \tau_i\ k_1(\theta)\ k_1(\theta_i)\ .$$

For the mass transfer process $r_2$ is $\tau\phi k_L^\circ a$ and has no $k_1$ dependence (or temperature dependence) except through the enhancement factor, viz.,

$$\phi = \sqrt{1 + \tau_i/\tau_{Ri}} = \sqrt{1 + \tau_i\ k_1(\theta_i)}\ .$$

So $r_2$ is a constant, $\tau k_L^\circ a$, with $k_1$ until $\tau_i/\tau_{Ri} \simeq 1$, cf. Figure 4.2; then $r_2$ goes as $\tau k_L^\circ a \sqrt{\tau_i k_1}$ until $\phi$ reaches its maximum for instantaneous reaction viz.,

$$\phi_I = 1 + \frac{x_B}{S x_i}$$

when

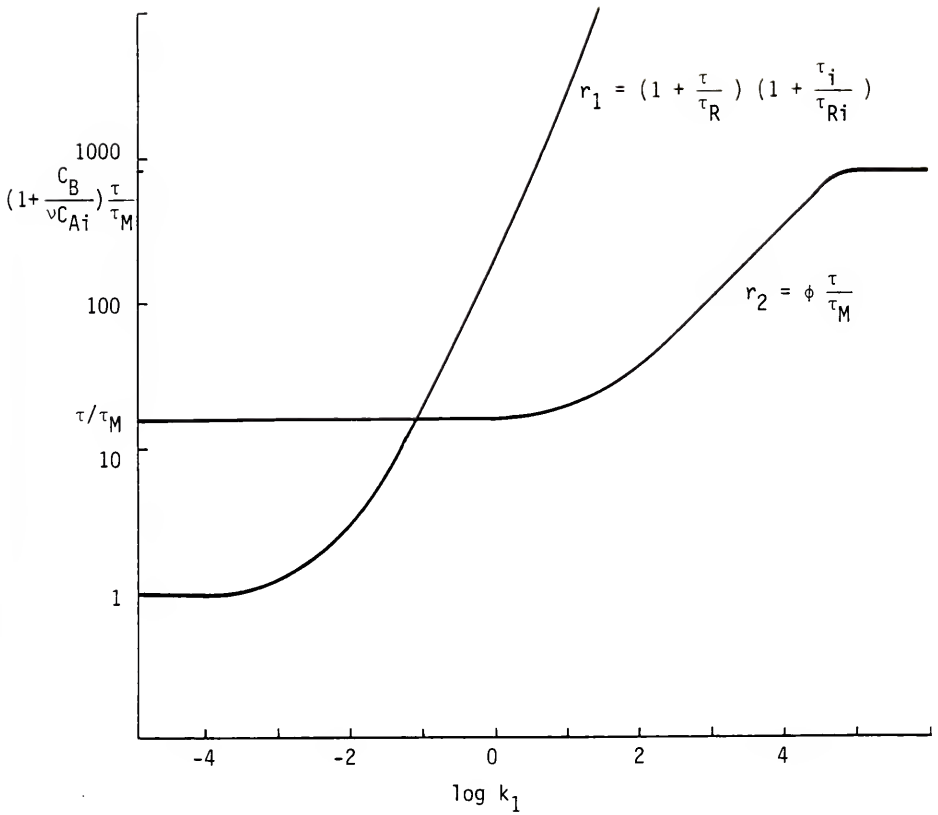


$\tau$ = 200 sec $\qquad$ $\tau_i$ = 0.0375 sec

$\tau_M$ = 12.5 sec $\qquad$ $\frac{C_B}{\nu C_{Ai}}$ = 50

Figure 4.2. $r_1$ and $r_2$ versus rate constant.

$$\frac{\tau_i}{\tau_{Ri}} = \left( \frac{x_B}{Sx_i} \right)^2 .$$

Figure 4.2 shows $r_1$ and $r_2$ and Figure 4.3 shows the relative rate of absorption $R_r$ versus the rate constant.

Figure 4.2 is drawn for a fixed value of $\tau$. Because $\tau$ is ordinarily an order of magnitude greater than $\tau_M$, for small $k_1$ mass transport easily supplies what flow can dispatch. Thus $r_1$ and $r_2$ stand in the small $k_1$ or low temperature relation shown in Figure 4.2 where it is fair to say that flow controls, viz.,

$$C_A \simeq C_{Ai} .$$

When the rate constant increases we have the following:

i) bulk reaction increases, opening a parallel pathway for the removal of the solute which reduces the resistance, $1/r_1$, without limit and ii) interfacial reaction increases which reduces the mass transfer resistance, $1/r_2$, but it opens no new pathway and its influence is limited. This sets the general shapes of the curves in Figure 4.2. The details follow.

Reaction can affect absorption in two ways, through the overall concentration difference and the mass transfer coefficient, i.e. the local concentration gradient. Reaction in the bulk liquid increases the overall concentration difference from the interface to the bulk thereby increasing the rate of absorption. Exceptionally fast reaction steepens the local gradient at the interface, increasing the value of the mass transfer coefficient as reflected by the enhancement factor. In Figure 4.2 $r_1$ illustrates how reaction increases the overall difference and hence the rate of absorption. For slow reaction (small $k_1$) we have $R_r = r_1 = 1$, hence $R_a$ is $(qC_{Ai})$. That is, mass transfer easily

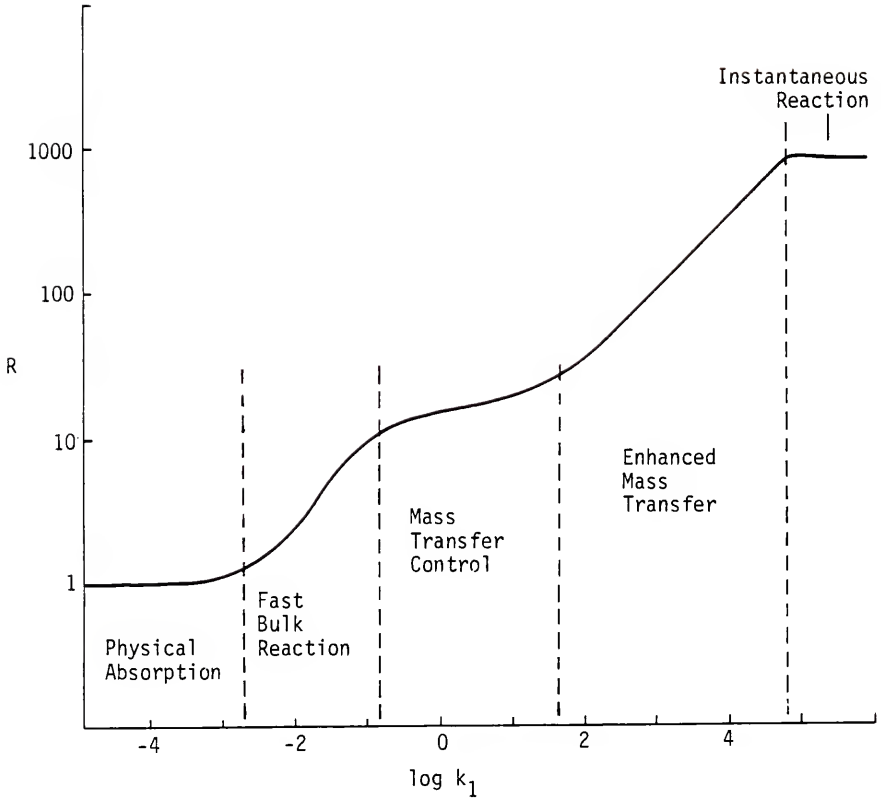


Figure 4.3. Relative rate of absorption versus rate constant.

supplies all that flow can remove whence the rate of absorption equals the rate of A flowing out of the reactor at the equilibrium concentration. This condition persists until $1/\tau_R$ increases to the order of $1/\tau$. Thereafter the loss of A via bulk reaction becomes significant and the rate of absorption increases due to the larger concentration difference, viz.,

$$r_1 \simeq \tau/\tau_R = \tau k_1 ,$$

so that $r_1$ becomes proportional to $k_1$. Thus $r_1$ increases rapidly, driving $C_A$ to zero and turning control over to $r_2$. Of course, $r_1$ increases even more rapidly when $1/\tau_{Ri}$ increases to the order of $1/\tau_i$, but as shown in Chapter Three, this occurs only after $r_1$ is already so large vis-a-vis $r_2$ that it is no longer of interest, i.e. after absorption becomes mass transfer controlled. In Chapter Three we concluded that when enhancement begins, $\tau_i/\tau_{Ri} = 1$ and $\tau_R = \tau_{Ri}$ (i.e. the interfacial temperature equals the bulk temperature because before the onset of enhancement there can be no significant reaction near the interface). Because $\tau_M >> \tau_i$ this implies $\tau_M >> \tau_R$ and $\tau/\tau_M << \tau/\tau_R$. Thus $r_2 << r_1$ when enhancement begins and $r_2$ will be controlling $R_r$. Therefore the rate of absorption has two important subregions when it is under $r_1$ control, one for slow bulk reaction and the other for fast bulk reaction. The first is the physical absorption region where $C_A \simeq C_{Ai}$ and is defined by

$$\tau/\tau_R << 1 \quad \text{or} \quad \tau k_1 << 1 .$$

The second is the fast bulk reaction region, defined by

$$1 << \tau/\tau_R << \tau/\tau_M$$

or

$$1 << \tau k_1 << \tau k_L^o a \ .$$

The critical point separating these two subregions of $r_1$ control is defined by

$$\tau/\tau_R = 1 \ .$$

We say that control of absorption shifts from the $r_1$ or flow-bulk-reaction regime to the $r_2$ or mass transfer regime when

$$\tau/\tau_M = \tau/\tau_R \quad \text{or} \quad \tau_R = \tau_M \ .$$

Here $R_r = r_2$ and hence $R_r$ is a constant with respect to $k_1$ because the reaction in the bulk has gone essentially to completion. It remains constant until enhancement begins and the mass transfer coefficient increases. This unenhanced mass transfer controlled subregion is the second plateau in $R_r$, cf. Figure 4.3. Here the relative rate of absorption is $\tau/\tau_M$ and the region is bounded by $\tau_R = \tau_M$ and $\tau_i/\tau_{Ri} = 1$, i.e. $\tau_M \geq \tau_R \geq \tau_i$ where $\tau_R = \tau_{Ri}$ here. So this subregion of the mass transfer controlled regime lies between the fast bulk reaction subregion of the flow-bulk-reaction controlled regime and the enhanced mass transfer subregion of the mass transfer controlled regime. For larger values of the rate constant the reaction near the interface becomes significant, enhancing the mass transfer coefficient. Hence the enhancement factor becomes greater than one, increasing $r_2$ and $R_r$. This region of enhanced mass transfer is defined by

$$1 << \frac{\tau_i}{\tau_{Ri}} << \left( \frac{x_B}{Sx_i} \right)^2$$

where $\tau_{Ri}$ is now the variable and the relative rate of absorption is approximately

$$R_r = r_2 = (\tau/\tau_M) \sqrt{\tau_i/\tau_{Ri}} = (\tau/\tau_M) \sqrt{\tau_i \ k_1(\theta_i)} \ .$$

In this region the rate increases as the square root of $k_1$ as seen in Figures 4.2 and 4.3. The enhancement factor $\phi$ has a maximum $\phi_I$, the instantaneous enhancement factor, which establishes the upper bound for $R_r$ and establishes the final subregion. Here we have

$$R_r = r_2 = \frac{\tau}{\tau_M} \phi_I = \frac{\tau}{\tau_M} \left( 1 + \frac{x_B}{Sx_i} \right)$$

which holds for

$$\frac{\tau_i}{\tau_{Ri}} >> \left( \frac{x_B}{Sx_i} \right)^2 .$$

This is the third plateau in the figures.

The rate of absorption graph can now be divided into five operating regions: physical absorption, fast bulk reaction, mass transfer controlled, enhanced mass transfer, and instantaneous reaction, cf. Figure 4.3 and Table 4.1. In the second and fourth regions, fast bulk reaction and enhanced mass transfer, the reaction increases the rate of absorption and $R_r$ is an increasing function of $k_1$, proportional to $k_1$ and $\sqrt{k_1}$ respectively. Otherwise $R_r$ is independent of $k_1$. In the first region, physical absorption, the reaction is vanishingly small and the rate of absorption is controlled by the gas solubility. In the third region, mass transfer control, the reaction is so fast that it has essentially gone to completion in the bulk, resulting in the maximum overall concentration gradient. In the fifth region, instantaneous reaction, the interfacial reaction is instantaneous, resulting in the maximum mass transfer coefficient. The rate of absorption for each region and an order of magnitude estimate for the critical points are shown in Tables 4.1 and 4.2, both in terms of the time scales and the reactor parameters.

TABLE 4.1
OPERATING REGIONS

| | Region | Rate of Absorption | Bounds (Time Scales) |
|---|---|---|---|
| 1. | Physical Absorption | $(qC_{Ai})$ | $\tau/\tau_R \ll 1$ |
| 2. | Fast Bulk Reaction | $\tau k_1(qC_{Ai})$ | $1 \ll \tau/\tau_R \ll \tau/\tau_M$ |
| 3. | Mass Transfer Control | $\tau k_L^o a(qC_{Ai})$ | $\frac{1}{\tau_M} \ll \frac{1}{\tau_R} = \frac{1}{\tau_{Ri}} \ll \frac{1}{\tau_i}$ |
| 4. | Enhanced Mass Transfer | $\tau k_L^o a(qC_{Ai}) \sqrt{\tau_i k_1(\theta_i)}$ | $1 \ll \frac{\tau_i}{\tau_{Ri}} \ll \left(\frac{x_B}{Sx_i}\right)^2$ |
| 5. | Instantaneous Reaction | $\tau k_L^o a(qC_{Ai})(1 + \frac{x_B}{Sx_i})$ | $\left(\frac{x_B}{Sx_i}\right)^2 \ll \frac{\tau_i}{\tau_{Ri}}$ |

TABLE 4.2
CRITICAL POINTS SEPARATING OPERATING REGIONS

| Transition Region | Order of Magnitude (Time Scales) | Order of Magnitude (Parameters) |
|---|---|---|
| 1 - 2 | $\tau/\tau_R = 1$ | $\tau k_1 = 1$ |
| 2 - 3 | $\tau/\tau_R = \tau/\tau_M$ | $k_1 = k_L^o a$ |
| 3 - 4 | $\tau_i/\tau_{Ri} = 1$ | $D k_1(\theta_i) = (k_L^o)^2$ |
| 4 - 5 | $\frac{\tau_i}{\tau_{Ri}} = \left(\frac{x_B}{Sx_i}\right)^2$ | $D k_1(\theta_i) = \left(\frac{x_B}{Sx_i}\right)^2 (k_L^o)^2$ |

Using this picture we can anticipate the structure of the results. Because the rate of heat generation is proportional to the rate of absorption, Eq. 4.4 may have as many as five solutions. This is evident in Figure 4.3, where the relative rate of absorption is composed of two s-shaped curves, suggesting that it may intersect the straight line for the rate of heat removal as many as five times, once in each operating region. Of course Figure 4.3 shows only the relative rate of absorption which needs to be multiplied by $(qC_{Ai})$ and to be corrected for varying $C_B$.

If the reactor is not isothermal, the relative rate of absorption behaves with temperature almost exactly as it does with the rate constant $k_1$. The only difference will be in the area of enhanced mass transfer. Here the rates may increase because of a higher interfacial temperature which increases $k_1$ and hence $\phi$. Also $\phi_I$ increases because of its dependence on the temperature through $C_{Ai}$. More importantly the actual rate of absorption is the product of the relative rate and $qC_{Ai}$. Inasmuch as the solubility decreases with temperature, the plateau regions seen in Figure 4.3 will not be constant with temperature but will decrease. The two regions affected by reaction will still increase with temperature as long as the products $k_1C_{Ai}$ and $\sqrt{k_1}\ C_{Ai}$ increase with temperature. But if the solubility decreases fast enough then the rate of absorption will decrease with temperature everywhere. This implies that only one intersection with the heat removal line is possible and hence only one steady state is possible, which leads us to anticipate an uniqueness condition, viz. that $(k_1C_{Ai})$ decreases with temperature. Because

$$k_1C_{Ai} = k_{10}\frac{P_A}{H_o}\exp\left\{\frac{-(E - H_S)}{RT}\right\}$$

this condition is

$$E \leq H_S \tag{4.11}$$

that is, if the activation energy is less than the heat of solution then only one steady state solution exists. This is similar to but stronger than Huang and Varma's (1981a) and Raghuram and Shah's (1977) results, Eqs. 2.1 and 2.2. If the solubility is not so rapidly decreasing then it will not significantly affect the shape of the rate of absorption function. Hence five steady state solutions should be possible.

The final assumption used in the above is that the concentration of the liquid reactant B is constant, i.e. $C_B = C_{Bf}$. If this is not true, the major effect is on $\tau_R$ which now depends not only on the rate constant but also on $C_B$, viz.,

$$1/\tau_R = k_1 = kC_B \ .$$

As seen in Table 4.2 this changes the critical temperatures separating the regions. In general because $C_B$ should decrease with increasing temperature, this should shift all the critical points toward higher temperatures except the critical point for instantaneous reaction which should shift to lower temperatures due to the $C_B$ dependence of $\phi_I$. The effect of $C_B$ on the control regions is seen in Table 4.1. Of the three regions independent of the rate constant, only that for instantaneous reaction has any $C_B$ dependence and this is through $\phi_I$. The two remaining regions which depend on reaction, the fast bulk reaction and the enhanced mass transfer regions, will not increase as rapidly with the temperature as they did with the rate constant $k_1$ because the rates of absorption in these regions are proportional to $k_1 = kC_B$ and $\sqrt{k_1} = \sqrt{kC_B}$ and here $C_B$ decreases as temperature increases.

The heat generation function (the right-hand side of Eq. 4.4) is the product of the rate of absorption, now well understood, and the heat released. But the heat released also depends on temperature through the total fraction of absorbed A that reacts, viz.,

$$f_R = \left( \frac{\tau/\tau_R + f_i}{1 + \tau/\tau_R} \right) .$$

Now $f_i$ is the fraction that reacts near the interface and is essentially zero until enhancement begins. But it has been shown previously that when enhancement begins, $\tau/\tau_R >> 1$. That is, bulk reaction is already fast. Therefore $f_R$ goes as the s-shaped function

$$\left( \frac{\tau/\tau_R}{1 + \tau/\tau_R} \right)$$

and is essentially one when enhancement begins. In the physical absorption region $f_R$ is approximately zero hence the heat generation function is a constant multiple of the rate of absorption there. In passing through the fast bulk reaction region $f_R$ is an s-shaped function going from zero to one. Thus in this region the heat generation curve looks like the rate of absorption curve except that the rate of increase is greater due to $f_R$, so the curves should qualitatively be the same. For the mass transfer controlled regime, viz. the last three subregions, $f_R$ equals one so the rate of heat generation is another, higher, constant multiple of the rate of absorption. In summary, the heat generation function has the same critical points as the rate of absorption, see Table 4.2, and is directly proportional to the rate of absorption in all regions except the transition to the fast bulk reaction region, see Table 4.3. Thus the time scale picture for the absorption process can also be applied to the reactor itself.

TABLE 4.3
HEAT GENERATION FUNCTION IN EACH OPERATING REGION

| | Region | Heat Generation Function (right side of Eq. 4.4) |
|---|---|---|
| 1. | Physical Absorption | $B_S\, x_i$ |
| 2. | Fast Bulk Reaction | $(B_S + B_R)\, \frac{\tau}{\tau_R}\, x_i$ |
| 3. | Mass Transfer Controlled | $(B_S + B_R)\, \frac{\tau}{\tau_M}\, x_i$ |
| 4. | Enhanced Mass Transfer | $(B_S + B_R)\, \frac{\tau}{\tau_M} \sqrt{\frac{\tau_i}{\tau_{Ri}}}\, x_i$ |
| 5. | Instantaneous Reaction | $(B_S + B_R)\, \frac{\tau}{\tau_M} \left(x_i + \frac{x_B}{S}\right)$ |

Plotting the heat generation function, i.e. the right side of Eq. 4.4, versus temperature gives a graph similar to Figure 4.3. For the system studied by Ding et al. (1974)[2] where the parameters are given in Table 4.4, this function is graphed in Figure 4.4. The heat generation curve (labelled $Q_G$) has two s-shaped regions like the rate of absorption and one can identify the five regions described. The heat removal function (labelled $Q_R$), i.e. the left side of Eq. 4.4, is a straight line of slope $(1 + \tau/\tau_H)$ and intercept $(-(\tau/\tau_H)\theta_C)$. Although Ding et al. found a maximum of three steady states for the conditions in Table 4.4, it is evident from the figure that $\tau_H$ can be chosen such that $Q_R$ intersects $Q_G$ five times. Thus a maximum of five steady state solutions is possible. Each of these steady state solutions lies in a different region, that is, only one steady state is possible in each region.

The first stability condition can also be seen in this figure. This is the slope condition which says that if the slope of the heat generation function is greater than the slope of the heat removal function at a steady state solution then that solution is unstable. Thus for multiple solutions every other one must be unstable. Moreover if multiple solutions exist then any one in either the fast bulk reaction or enhanced mass transfer regions must be unstable.

At this point we can draw an important conclusion about approximate models. If we assume that a reactor operates in a specific region, we

---

[2]The values of the parameters for this system have variously been reported by several investigators (Hoffman et al. (1975), Sharma et al. (1976), Raghuram and Shah (1977), and Huang and Varma (1981a)) with no two in complete agreement. The values used here are the most commonly quoted ones from the above collection.

TABLE 4.4
PARAMETERS FOR THE CHLORINATION OF DECANE
AS STUDIED BY DING ET AL. (1974)

$k_o$ = 2.10 X $10^{17}$ $cm^3$/gmole·sec

E = 30000. cal/gmole

$H_R$ = 25000. cal/gmole

$\nu$ = 1

$\rho$ = $C_{Bf}$ = 5.10 X $10^{-3}$ gmole/$cm^3$

$C_P$ = 85. cal/gmole·°K

$k$ = 3.35 X $10^{-4}$ cal/cm·sec·°K

D = 6. X $10^{-5}$ $cm^2$/sec

V = 400. $cm^3$

$T_f$ = 297°K

$T_c$ = 298°K

$US_c$ = 0.03 cal/°K·sec

$P_A$ = 1 atm

$H_o$ = 1.12 X $10^7$ atm·$cm^3$/gmole

$H_S$ = 4500. cal/gmole

$k_L^o$ = 0.04 cm/sec

a = 3.0 $cm^{-1}$

Dimensionless Parameters:

$D_a$ = 9.28 X $10^{-8}$ $\tau$

$D_{ai}$ = 3.48 X $10^{-9}$

$B_R$ = 3.57 X $10^{-2}$

$B_S$ = 6.43 X $10^{-3}$

$\beta$ = 0.12 $\tau$

$\gamma$ = 50.8

S = 3.61 X $10^{-2}$

$\eta$ = 7.63

$H_1$ = 1.73 X $10^{-4}$ $\tau$

$\theta_c$ = 3.37 X $10^{-3}$

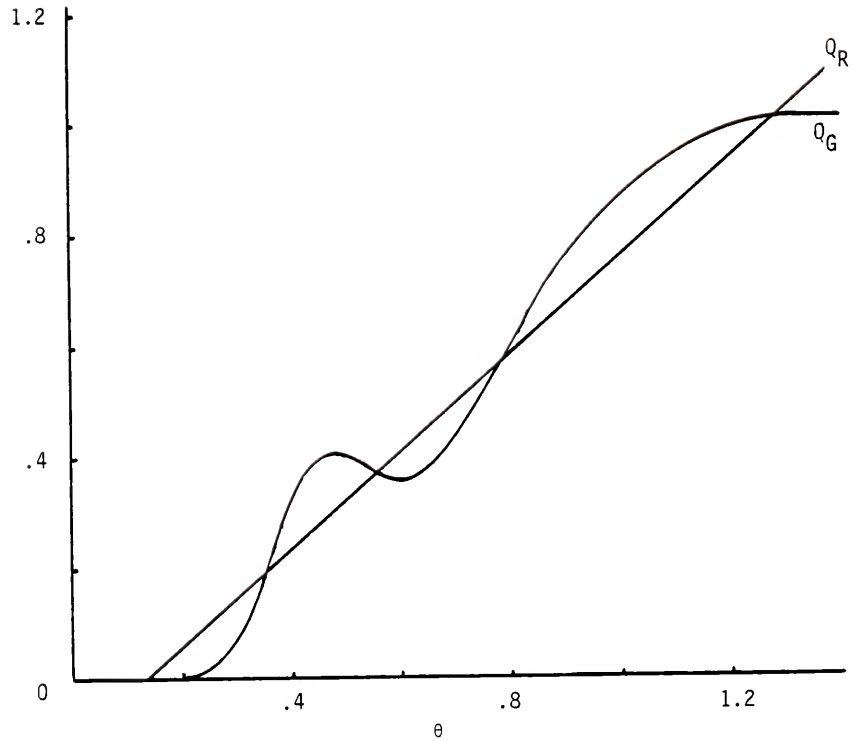


Figure 4.4. Heat generation and heat removal functions versus temperature.

$Q_G$ for system studied by Ding et al. (1974).

$Q_R$ chosen to give five steady states.

can not use the corresponding balance equations to find the number of steady state solutions. The full equations predict at most one solution in each region. Thus if the approximate equations predict more than one solution then all but one are surely meaningless. For example Huang and Varma (1981a) propose an enhanced mass transfer model where $\phi = \sqrt{\tau_i/\tau_{Ri}} = \sqrt{\tau_i k_1(\theta_i)}$ always. From this they determine that three steady state solutions are possible and they deduce conditions for uniqueness and stability. But we know that at most one solution may exist in this region. The two meaningless solutions arise from the slow and fast reaction limits of this enhanced mass transfer model, cf. Figure 4.5:

$$\lim_{k_1 \to 0} \phi \to 0$$

$$\lim_{k_1 \to \infty} \phi \to \infty \ .$$

But these limits for the enhancement factor should be

$$1 \leq \phi \leq \phi_I = \left( 1 + \frac{x_B}{S x_i} \right) .$$

As seen in the figure, the resulting steady state solutions are not the slow reaction and instantaneous reaction solutions. Also the only meaningful solution that is found is unstable (i.e. the slope condition is not satisfied in this region if multiple solutions exist). So the stability conditions are meaningless as are the uniqueness conditions.

Thus models which are restricted to one region have limited capabilities. These pertain to answering questions only about the one steady state found there, for example, the stability of this state could be examined. But uniqueness and multiplicity questions can not be answered. If this information is desired and an approximate model must be used to do the calculations then the approximate model must be

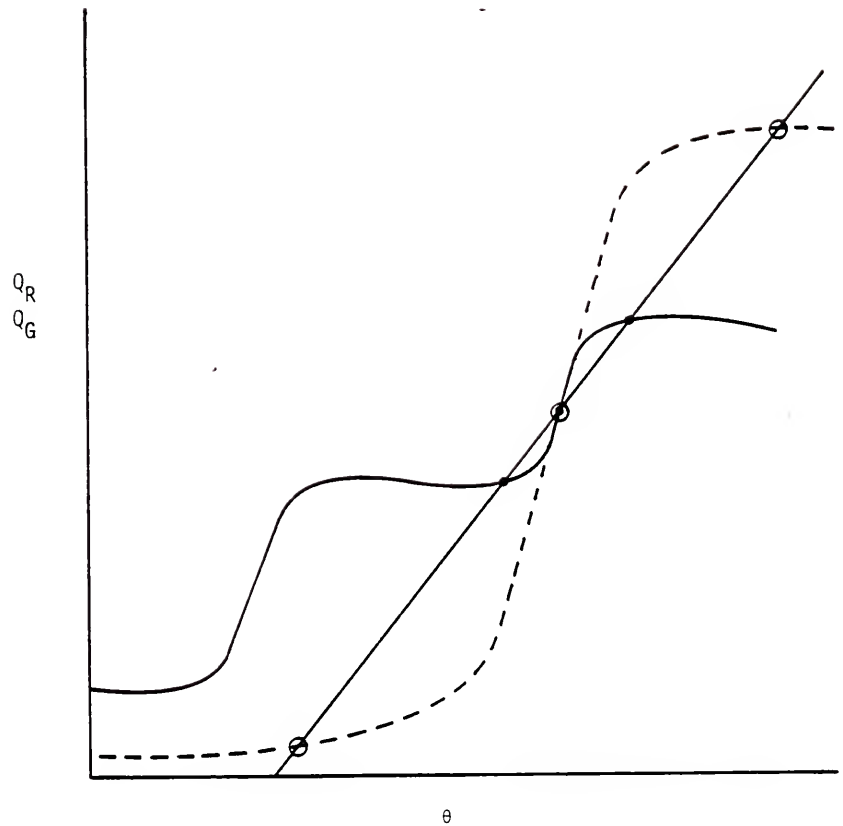


Figure 4.5. Comparison of enhanced mass transfer region model and full model.

- - - - Approximate Model

O Approximate Solutions

general enough to faithfully represent at least one of the two s-shaped regions for the heat generation function. That is, for multiplicity the existence of at least one of the s-shaped regions is necessary. Because two such regions exist in the full model it could be divided into two simpler ones of limited but overlapping validity. From our description of the process, one would consist of the physical absorption, fast bulk reaction and mass transfer control operating regions. Thus the approximations here would be that $\phi = 1$ and $f_i = 0$ everywhere. This unenhanced mass transfer submodel would correspond to the first s-shaped region of the heat generation function. The second approximate model would consist of the mass transfer control, enhanced mass transfer and instantaneous reaction operating regions. This enhanced mass transfer submodel would be for $\tau/\tau_R >> \tau/\tau_M$ and $f_R = 1$ and would correspond to the second s-shaped region of the heat generation function. The uniqueness and multiplicity conditions obtained from each will apply only when the model conditions hold. But it may be possible to combine the results of the simplified models to get conditions which apply everywhere. This will be investigated when we look for uniqueness conditions.

The effect of the parameters on the steady state behavior of the reactor is most easily understood by examining their effect on the heat removal and heat generation functions via graphs like Figure 4.4. Examining the critical points, see Table 4.2, and the values of functions on the operating regions, see Table 4.3, for their parameter dependence will show how these functions change. The results in these tables depend implicitly on the concentration of B. But inasmuch as this concentration should be relatively constant for a gas-liquid reactor, we should be able to determine the important parametric effects

assuming $C_B$ to be constant (except for very large holding times, $\tau$, where most of the B may be consumed). The heat removal function is linear in temperature with slope $(1 + \tau/\tau_H)$ and intercept $-(\tau/\tau_H)\theta_c$. Increasing the holding time increases the slope but only significantly when the ratio $\tau/\tau_H$ is greater than one. Thus for small holding times relative to the heat transfer time, the slope of the heat removal function is independent of this parameter. But at large values of $\tau$ the slope becomes proportional to $\tau$. So the slope of the heat removal function tends to increase with $\tau$, starting from a region of independence. This is the most important variation in this function. We also note that it only varies with the three parameters: $\tau$, $\tau_H$ and $\theta_c$.

For the heat generation function we need to consider both the variation in the magnitude of the function in the various control regions, see Table 4.3, and the variation in the critical temperatures separating these regions, see Table 4.2. The dependence of the heat generation curve on the holding time, the reaction parameters $k_{10}$ and E, and the mass transfer parameters $k_L^o$ and a, is shown in Figures 4.6-4.10. In summary we can see that increasing $\tau$ stretches the first s-shaped region and compresses the second s-shaped region. In the limit of large $\tau$ the second s will ultimately disappear due to the exhaustion of the reactant B in the mass transfer controlled region; hence there can be no enhancement, cf. Figure 4.4. The influence of the reaction parameters, cf. Figures 4.7 and 4.8, is through the critical temperatures separating each region, see Table 4.2. These parameters do not affect the height of the plateau regions which are set by the solubility and the mass transfer parameters, see Table 4.3. Thus increasing the Arrhenius frequency factor $k_{10}$ or decreasing the activation energy E

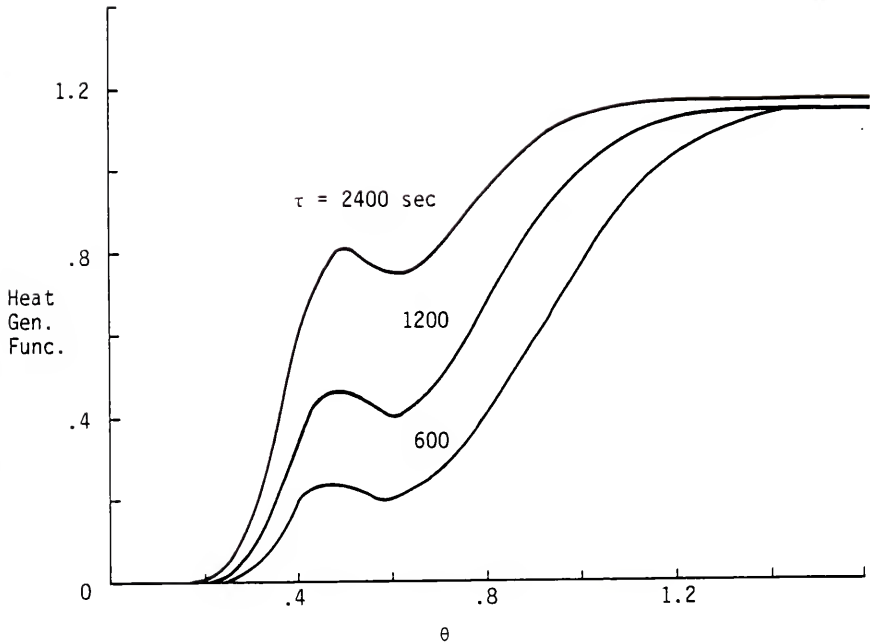


Figure 4.6. Effect of $\tau$ on the heat generation function.

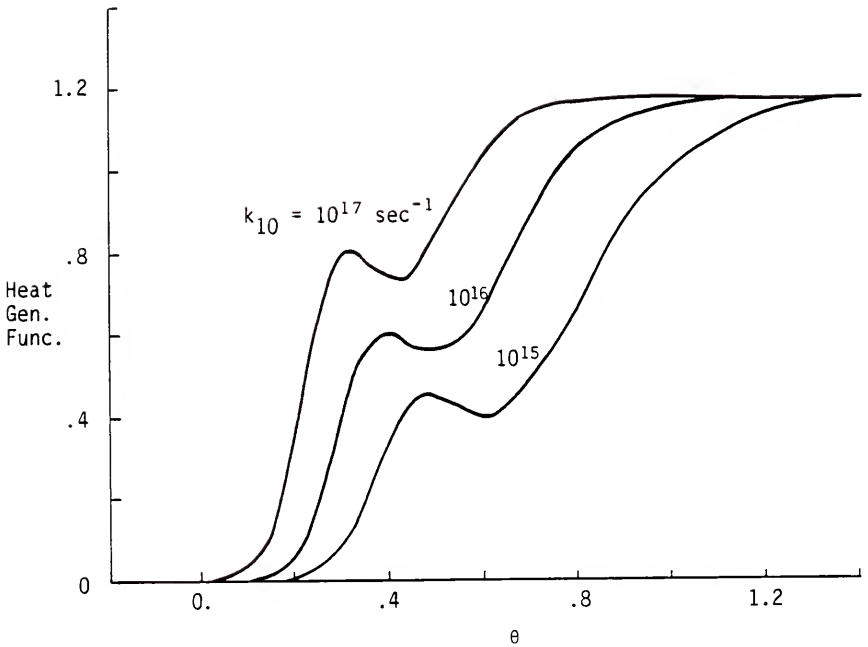


Figure 4.7. Effect of $k_{10}$ on the heat generation function.

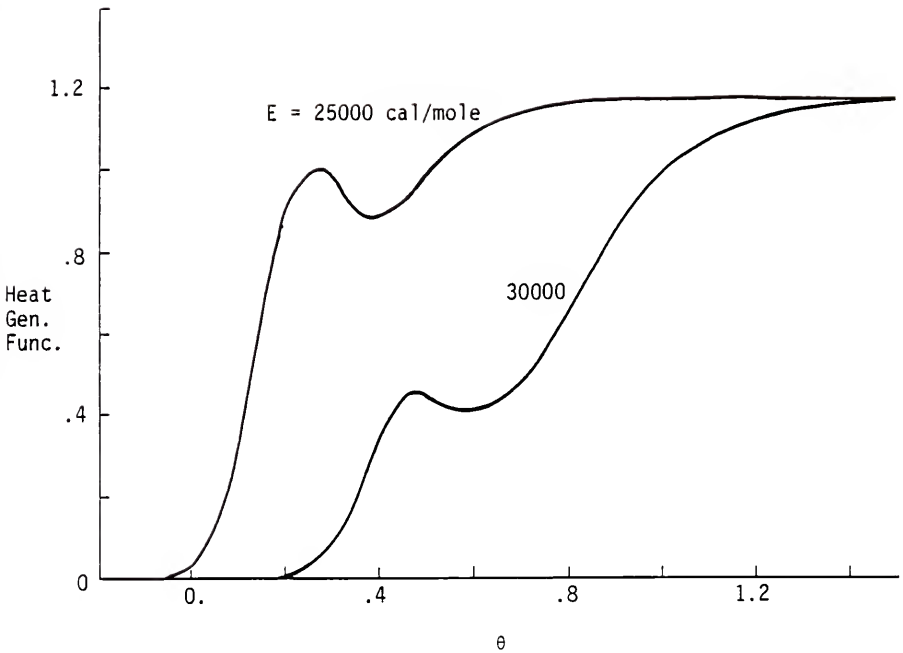


Figure 4.8. Effect of E on the heat generation function.

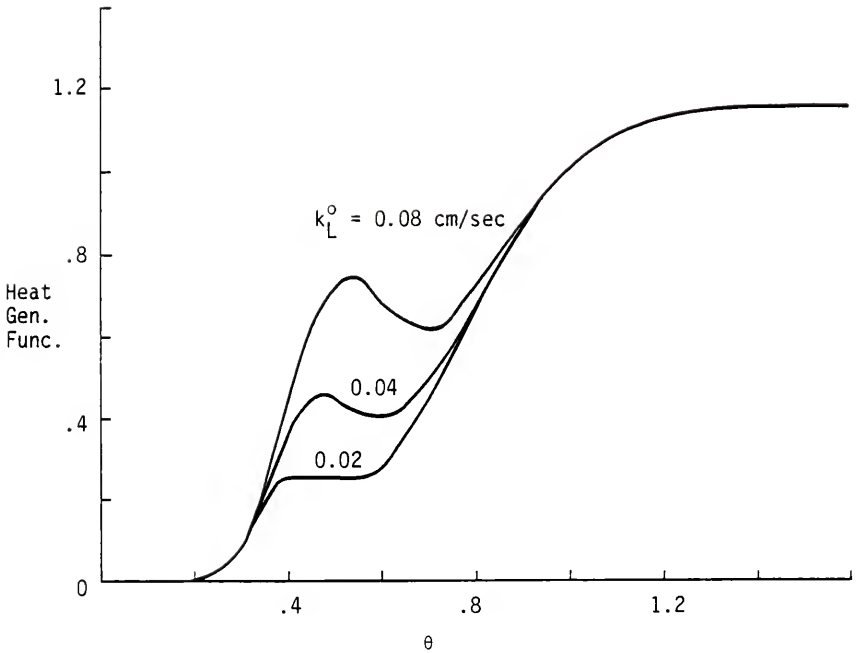


Figure 4.9. Effect of $k_L^o$ on the heat generation function.

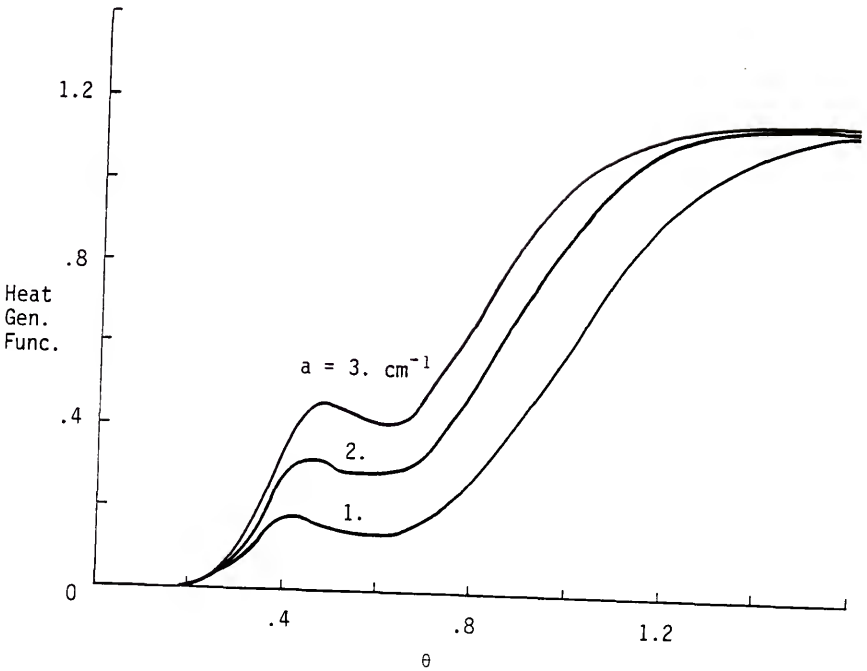


Figure 4.10. Effect of a on the heat generation function.

shifts all the critical temperatures to the left while the plateaus remain the same, except for the larger solubility due to the lower temperatures. The only effect of the heat of reaction, $B_R$, is to increase the heat generated in all the regimes but the first, physical absorption, see Table 4.3. It has no effect on the critical temperatures. The behavior of the mass transfer parameters, $k_L^o$ and a, is interesting because only their product affects the first s-shaped region whereas they individually influence the second. These parameters have no effect on the first critical temperature or on the first two operating regions, cf. Figures 4.9 and 4.10, and they appear as a product through $\tau_M$ when determining the second critical temperature and the height of the mass transfer control region, see Tables 4.2 and 4.3. For the second s-shaped region of the heat generation function, the critical temperature for the onset of enhanced mass transfer depends only on $k_L^o$ and the magnitude of the heat generation function in the enhanced mass transfer region depends only on a. This is due to the fact that the interfacial exposure time depends on $k_L^o$ and not on a, viz., $\tau_i = D/(k_L^o)^2$. Therefore two systems which are identical except for $k_L^o$ and a but have the same product, $k_L^o a$, will behave exactly the same until enhancement begins, which will be at a lower temperature for the system with the smaller value of $k_L^o$.

Inasmuch as the heat removal line and the heat generation curve are complicated functions of the parameters and because their intersections determine the steady state temperatures, we expect the dependence of the solutions on the parameters to be unusual. Using the data of Ding et al. (1974) as reported in Table 4.4 we can solve Eqs. 4.3 and 4.4 numerically for various values of the holding time. The results are

shown in Figure 4.11 where we see that at most three steady states exist and that this system exhibits an isola. The steady state temperatures found experimentally by Ding et al. are also shown and our model predictions agree closely with these.[3] Ding et al. did not run their experiment at large enough holding times to find the end of the multiplicity region so we do not know if the experiments confirm the isola.

Unusual multiplicity patterns such as an isola are also found in a single-phase CSTR. In Appendix A we review the types of patterns possible for this reactor and how they are formed. For a single-phase CSTR the heat generation function has one s-shaped region and hence a maximum of three steady states is possible. This function leads to three basic types of multiplicity with respect to holding time, cf. Figure A.2. The first is called s-shaped multiplicity and here the locus of steady states turns back on itself over an interval in $\tau$. Thus three steady states exist for this interval. This multiplicity pattern is characterized by one ignition point and one extinction point where an ignition point is the point on the locus where a change in $\tau$ in one direction causes a jump up to a higher temperature steady state and an extinction point is where a change in $\tau$ causes a jump down to a lower temperature steady state. In some instances the locus can turn back on itself a second time, cf. Figure A.2b, giving two intervals of multiplicity. This pattern is called a mushroom and is characterized by two ignition and two extinction points. If these two intervals intersect

[3]Our predictions agree most closely with the experimental results if we replace the value of the specific surface area, a=3, given in Table 4.4 with a=2 $cm^{-1}$. Both of these values have been reported in the literature for this experiment. The predictions shown in Figure 4.11 are actually based on this latter value.

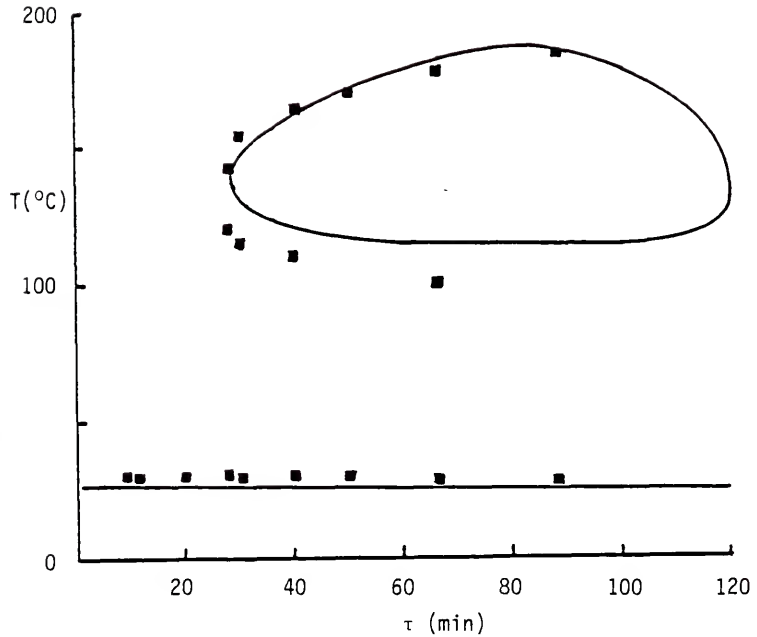


Figure 4.11. T versus τ for the data of Ding et al. (1974).

then an isola is formed, cf. Figure A.2c. Here two extinction points exist but no ignition points exist, thus it is not possible to observe the high temperature steady states when starting from the low temperature branch and varying $\tau$. More will be said about these patterns in Appendix H.

Inasmuch as the heat generation function for the gas-liquid CSTR exhibits two s-shaped regions, we expect all of the above multiplicity patterns and possibly some combinations of these. We do, in fact, observe all of the three basic types of multiplicity and some combinations. This will be discussed next. Later and in Appendix I we will show that certain combinations of multiplicity patterns are not possible.

If we vary the frequency factor, $k_{10}$, and repeat the above calculations for solving Eqs. 4.3 and 4.4 using all the values of the other parameters as given in Table 4.4, we find several interesting multiplicity patterns. Increasing $k_{10}$ by a factor of ten produces an isola with an s-shaped region and hence an interval with five steady states, cf. Figure 4.12. This is the maximum number we anticipated from the graphs of the heat removal and the heat generation functions. If $k_{10}$ is increased further, a mushroom is formed with an s-shaped region and five steady states, cf. Figure 4.13. This mushroom has two ignition and two extinction points, and two "jump" points which are indeterminant. That is, the jump points which bound the region of five steady states could be either ignition or extinction points. The same is true for the previous isola. If $k_{10}$ is increased further, the mushroom disappears and we get double s-shaped multiplicity with five steady states, cf. Figure 4.14. The multiplicity regions can be summarized by plotting the location of the ignition and extinction points on a graph of $k_{10}$ versus $\tau$ in

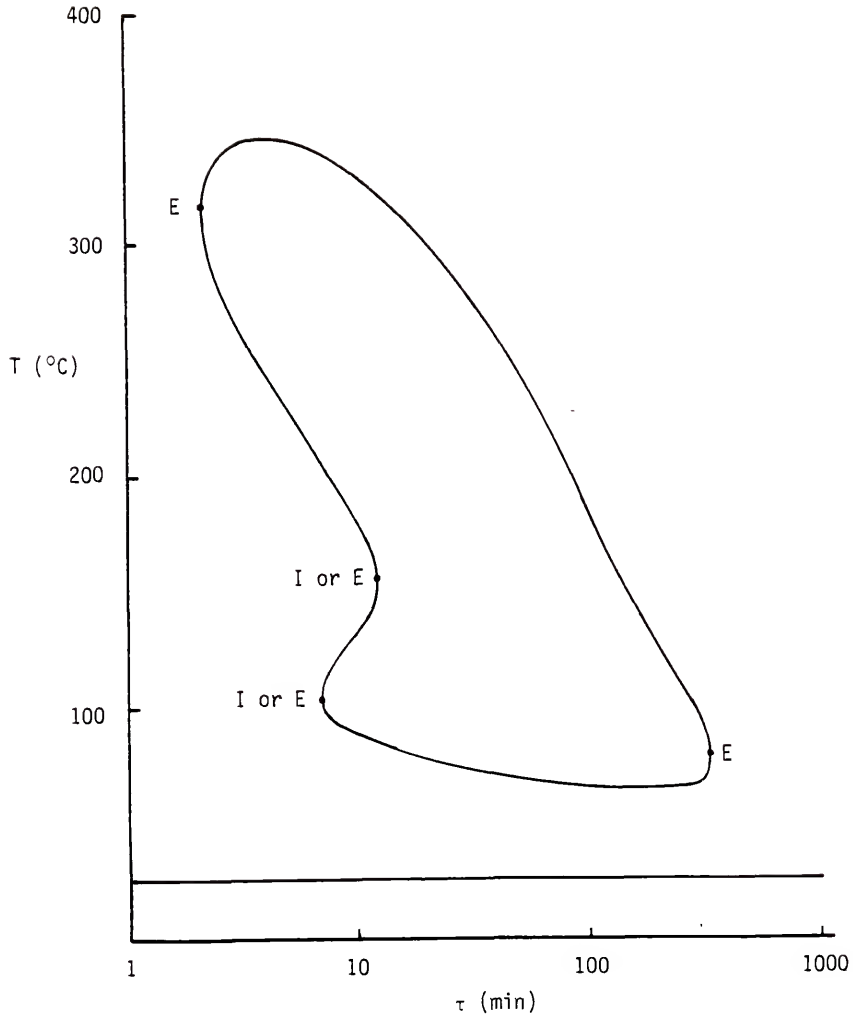


Figure 4.12. T versus τ: isola behavior.

$k_{10} = 10^{17}$ sec$^{-1}$

I = Ignition Point, E = Extinction Point

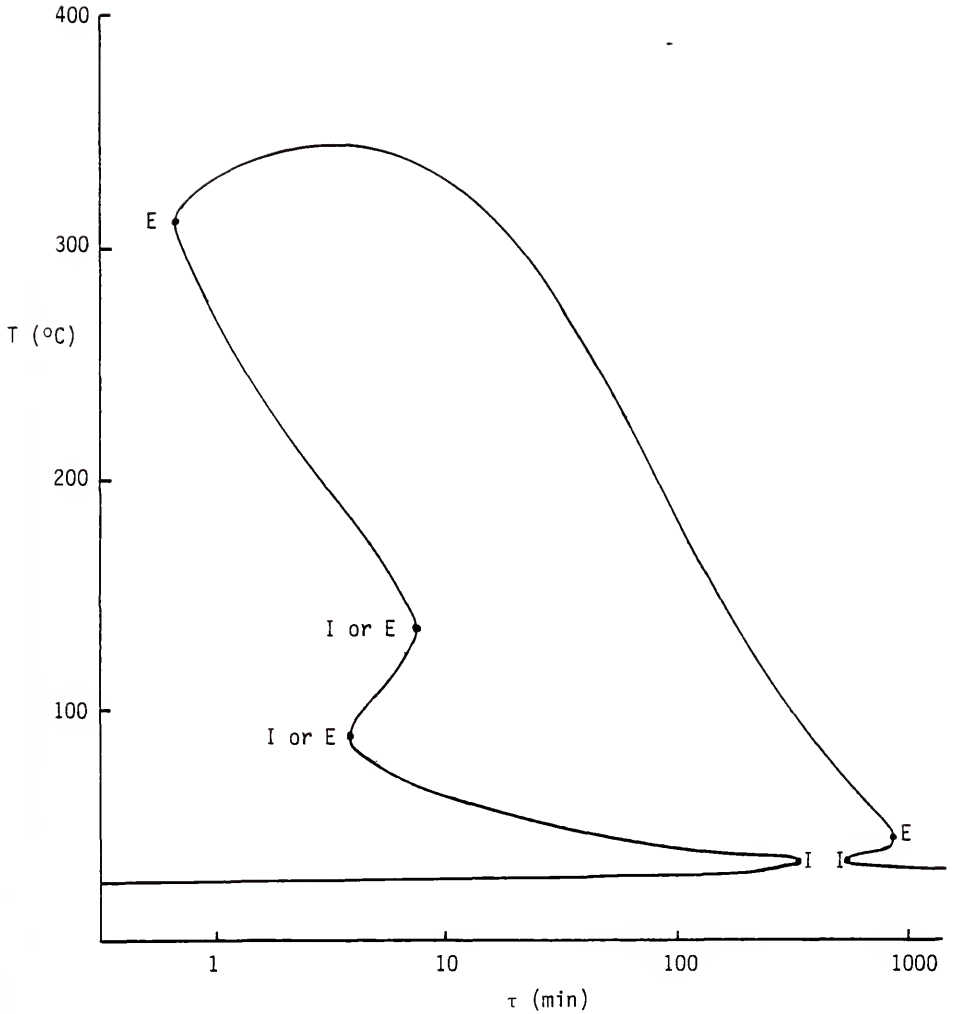


Figure 4.13. T versus τ: mushroom behavior.

$k_{10} = 6. \times 10^{17}$ sec$^{-1}$

I = Ignition Point, E = Extinction Point

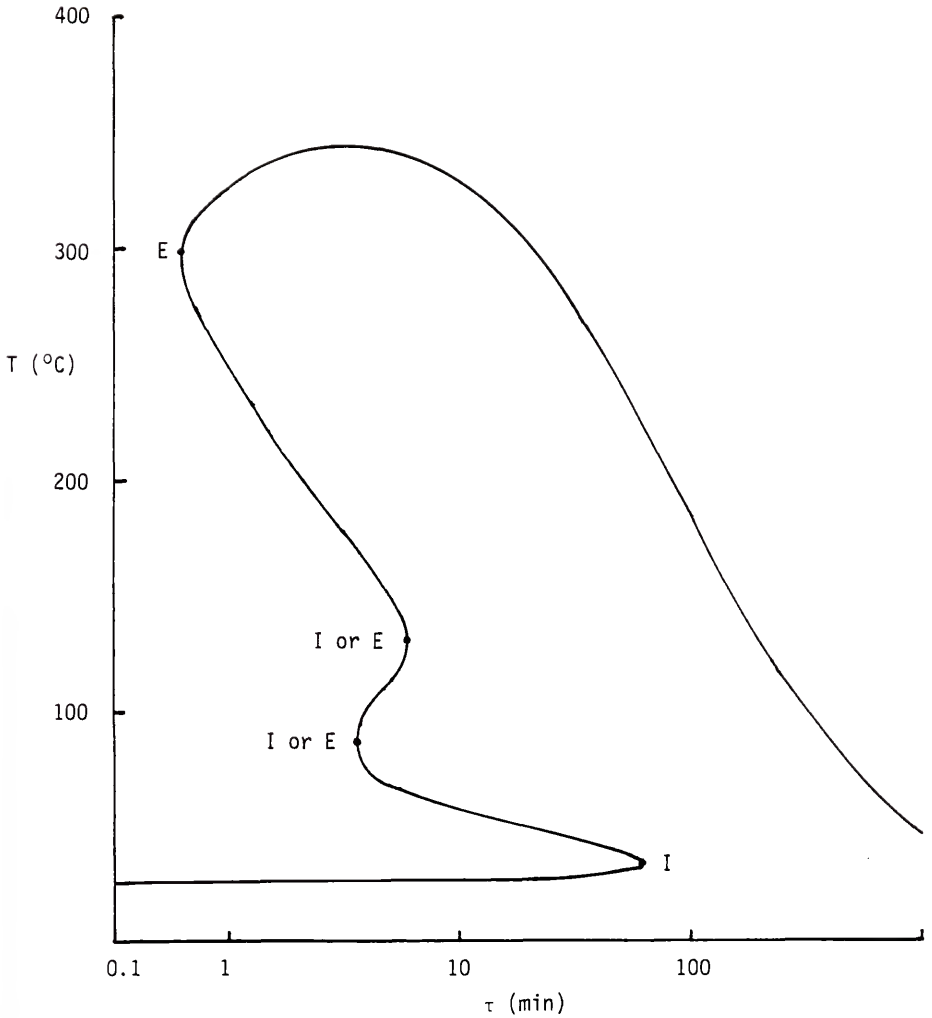


Figure 4.14. T versus τ: s-shaped multiplicity.

$k_{10} = 10^{18}$ $sec^{-1}$

I = Ignition Point, E = Extinction Point

Figure 4.15. The locus of ignition points and the locus of extinction points enclose the region of multiplicity. Outside this region the steady states are unique; inside there are regions of three and five steady states. The loci of the indeterminant jump points divide this multiplicity region into regions of three and five steady states, as shown. This figure also gives the type of multiplicity. For a given value of $k_{10}$ the number of ignition and extinction points determines the type; one of each implies s-shaped (region a) and two of each imply a mushroom (region b), whereas two extinction points imply an isola (region c). From this figure we can find the critical values of $k_{10}$ and $\tau$, above which and below which we have uniqueness. For $k_{10}$ these are $10^{20}$ $sec^{-1}$ and $3 \times 10^{15}$ $sec^{-1}$; and for $\tau$ these are 0.2 min and 800 min.

Any number of figures similar to Figure 4.15 can be generated but they only apply to a subset of the parameters with specific values, viz. all the parameters except $k_{10}$ and $\tau$ are taken from Table 4.4. We would like conditions that would answer the pertinent questions that the last figure did for all values of the parameters without having to solve the full equations, Eqs. 4.3 and 4.4. For example conditions guaranteeing uniqueness and three and five steady states would be very useful. Also we would like conditions under which mushrooms and isolas exist. We will find such conditions next, beginning with the uniqueness problem.

The simplest uniqueness condition is that derived from the slope condition: if the slope of the heat removal function with respect to $\theta$ is always greater than the slope of the heat generation function then only one steady state exists. This is true because, as the graph of these functions illustrates, cf. Figure 4.4, the slope condition must

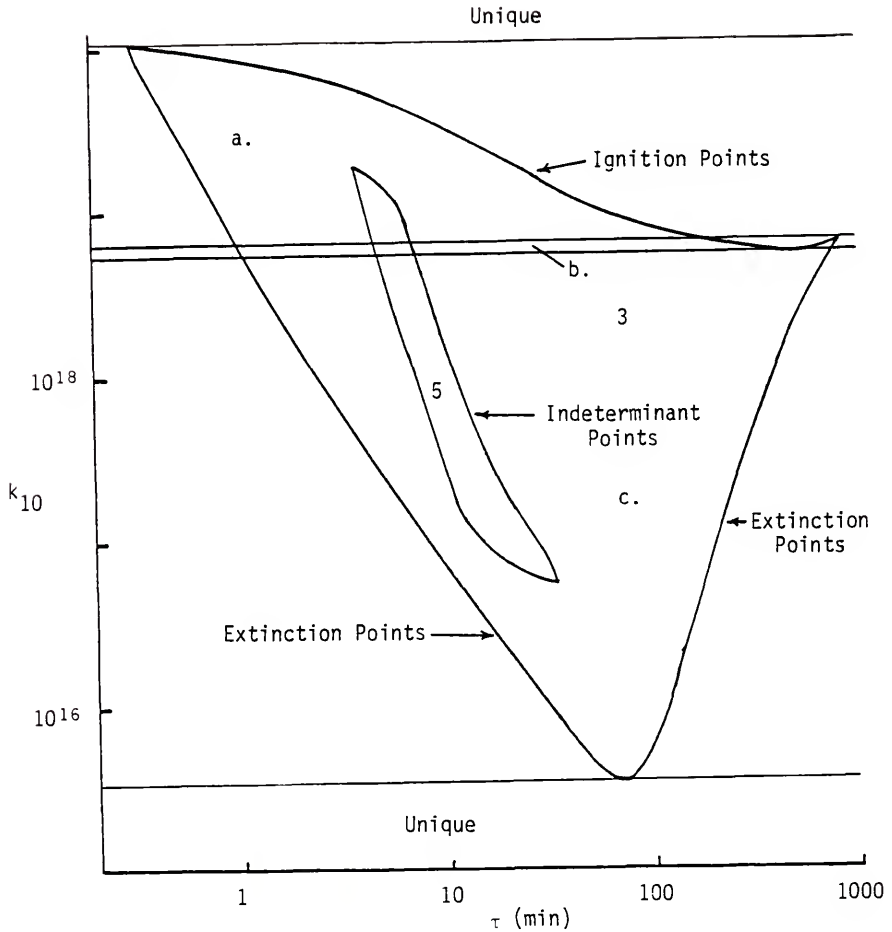


Figure 4.15. $k_{10}$ versus τ: multiplicity regions and type.
a. s-shaped, b. mushroom, c. isola

hold for every other steady state when multiple solutions exist; so if it never holds then there can not be multiple solutions. The slope of the heat removal function (the left side of Eq. 4.4) with respect to temperature is $(1 + H)$ where $H \equiv \tau/\tau_H$. The slope of the heat generation function (the right side of Eq. 4.4) is much more complicated, but we can use our understanding of the reactor to simplify this. In three operating regions this slope is negative, cf. Figure 4.4, so the above condition holds everywhere in these regions. Thus we need only consider the fast bulk reaction region and the enhanced mass transfer region where the slope of the heat generation function may be positive. Using the simplified expressions for the heat generation function in these regions, as given in Table 4.3, we can calculate the slopes, cf. Appendix E. These slopes depend on the steady state temperature so the resulting uniqueness condition requires the solution of the steady state equations. But if we use the steady state equation, Eq. 4.4, and the bounds on the steady state temperature given in Appendix E, this temperature dependence can be removed (of course with the cost of weakening the result). This gives two inequalities in the reactor parameters; the first guarantees uniqueness for the first s-shaped region and the second inequality guarantees uniqueness for the second s-shaped region, viz.,

$$(1 + H) > \frac{(\gamma - n)\,(B_S + B_R)\,\beta}{\left\{ 1 + \left( \frac{H}{1 + H} \right) \theta_c + \frac{B_S\,\beta\,e^{-n}}{(1 + H)} \right\}^2} \tag{4.12}$$

and

$$(1 + H) > \beta \sqrt{\frac{\alpha}{D}}\ \frac{W_3}{1 - W_3} \tag{4.13}$$

where

$$W_3 = \sqrt{\frac{D}{\alpha}}\ \frac{1}{2S}\ \frac{(\gamma - 2\eta)\ (B_S + B_R)}{\{\ 1 + (\ \frac{H}{1+H}\ )\ \theta_c + \frac{B_S\ \beta\ e^{-\eta}}{(1+H)}\ \}^2} \quad . \tag{4.14}$$

The first condition, Eq. 4.12, divides parameter space into two regions: uniqueness and possible multiplicity with a maximum of three steady states; and this applies to the physical absorption, fast bulk reaction and mass transfer controlled regions, i.e. a gas-liquid reactor without enhanced mass transfer. The latter condition, Eq. 4.13, divides the space similarly and is applicable to the mass transfer controlled, enhanced mass transfer and instantaneous reaction regions, i.e. a mass transfer controlled reactor with enhancement. Together these results divide the space into three regions: an uniqueness region, a region of up to three steady states and a region of up to five steady states. The uniqueness region for the gas-liquid reactor is the intersection of the foregoing uniqueness regions, i.e. where Eqs. 4.12 and 4.13 hold. The intersection of the possible multiplicity regions for each condition gives the region where five steady states are possible, i.e. where Eqs. 4.12 and 4.13 do not hold. A maximum of three steady states is possible for the remaining regions, i.e. Eq. 4.12 and not Eq. 4.13, and Eq. 4.13 and not Eq. 4.12. If we could visualize a nine-dimensional parameter space we could show these regions graphically. Figure E.1 illustrates this in two dimensions for simplified versions of Eqs. 4.12 and 4.13.

Equations 4.12 and 4.13 yield very simple conditions on $\eta$ and $\gamma$: $\eta \geq \gamma$ and $2\eta \geq \gamma$. Thus uniqueness is guaranteed for the gas-liquid reactor if $\eta \geq \gamma$, i.e. $H_S \geq E$, which is the result anticipated earlier, Eq. 4.11. This also allows us to interpret the result of Raghuram and

Shah (1977). Their model is applicable to the enhanced mass transfer region and so their result, Eq. 2.2, is the same as the simplification of Eq. 4.13, $2H_S \geq E$, which also holds for the enhanced mass transfer region. Therefore their result is not strong enough to guarantee uniqueness for a reactor that can exhibit a solution in each region.

For a single-phase reactor a stronger uniqueness condition than that derived from the slope condition can be found via an idea of Poore, see Poore (1973) and Uppal et al. (1974 and 1976). However in our two-phase CSTR we can not write the steady state equation in the form Poore (1973) writes his if we try to do the problem in its full generality. But we can apply his idea to the first s-shaped region of the heat generation function, i.e. the first three operating regions of our model. Here we know that the maximum number of steady states is three, a result that we will rediscover, which is the result for a single-phase CSTR that allows Poore to obtain explicit results from this analysis. For the first s-shaped region, i.e. for an unenhanced gas-liquid reactor, $\phi$ equals one, $f_i$ equals zero and $\theta_i$ equals $\theta$. We also assume that the concentration of B is a constant at its feed value and that the heat of solution is negligible compared to the heat of reaction; this greatly simplifies the algebra. The first assumption limits us to moderate values of $\tau$ but the second assumption is true for most systems. One final approximation is helpful both here and in Poore's investigation of the single-phase reactor, which simplifies the temperature dependence of the rate constant and the solubility, viz.,

$$e^{\sigma\theta/(1+\theta)} \simeq e^{\sigma\theta} \quad . \tag{4.15}$$

This is the Frank-Kamenetskii approximation which is often used in reacting systems and which is accurate whenever $\theta$ is small as compared

to one. But this underestimates its usefulness because in reactor analysis the approximation is usually made on functions of the rate constant, e.g. $\tau k/(1 + \tau k)$, and here the approximation is more accurate, cf. Appendix G. The steady state equation, Eq. 4.4, then becomes, in dimensionless parameters,

$$(1 + H)\ \theta - H\ \theta_c = \frac{D_a\ B_R\ \beta\ e^{(\gamma - n)\theta}}{\{\ 1 + \beta + D_a\ e^{\gamma\theta}\ \}} . \tag{4.16}$$

The basis of Poore's (1973) idea is that if the steady state equation can be rewritten such that one parameter equals a function of the state variable $\theta$ and the other parameters, where these parameters are held fixed, then the variation of this function over its admissible domain in $\theta$ determines the multiplicity of the reactor with respect to that one parameter. For example if the function is strictly monotone over its domain in $\theta$ then for any value of the one parameter, and hence this value of the function, only one steady state exists, cf. Figure 4.16a. Otherwise if the function is not monotone, then for some range of values of the one parameter (and values of the function), multiple solutions exist, cf. Figure 4.16b. Therefore if we can determine conditions under which this function is monotone, these will also be uniqueness conditions. Conditions under which the function is not monotone and the range over which it is not, give multiplicity conditions.

The details of this analysis are given in Appendix F; we summarize the results here. We can rewrite Eq. 4.16 as

$$D_a = g(\theta;\ H,\ \theta_c,\ B_R,\ \beta,\ \gamma,\ n) . \tag{4.17}$$

Thus over the admissible domain in $\theta$, cf. Eq. F.5, $g(\theta)$ varies from zero to infinity which is the possible range of $D_a$. $g(\theta)$ is monotonically

increasing if and only if g has no turning points in the admissible domain in $\theta$, i.e. if

$$dg/d\theta \neq 0$$

anywhere in this domain, cf. Figure 4.16. Thus whenever the turning points of g are nonreal numbers then the reactor has an unique steady state. This yields uniqueness conditions for the unenhanced gas-liquid reactor which are given by the inequalities F.7 and F.10. Graphically we show that at most two turning points exist for g, see Appendix F, therefore a maximum of three steady state solutions exists for Eq. 4.16. If we call these turning points $m_1$ and $m_2$ and calculate them from Eq. F.6, we can define

$$D_{a1} = g(\theta = m_1) \tag{4.18}$$

and

$$D_{a2} = g(\theta = m_2) \tag{4.19}$$

which then allows us to divide the remaining regions of parameter space into areas of uniqueness and of multiplicity. Thus we have the result:

1. if $m_1$ and $m_2$ are nonreal, Eq. F.10,
   then the reactor has an unique steady state;
2. if $m_1$ and $m_2$ are real and
   a. if $D_a < D_{a1}(H, \theta_c, B_R, \beta, \gamma, n)$
      or $D_a > D_{a2}(H, \theta_c, B_R, \beta, \gamma, n)$
      then the reactor has an unique steady state,
   b. if $D_a = D_{a1}$ or $D_a = D_{a2}$
      then two steady states exist,
   c. if $D_{a1} < D_a < D_{a2}$
      then three steady states exist.

The results are most easily understood by examining Figure 4.16. These

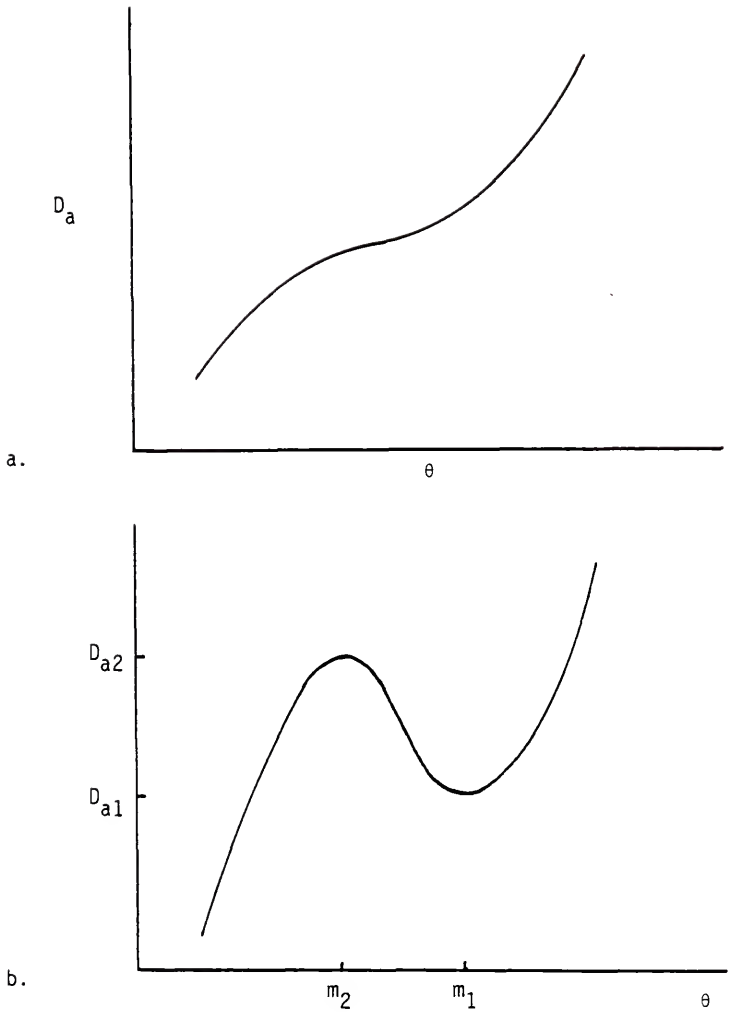


Figure 4.16. $D_a = g(\theta)$ versus $\theta$.

a. Uniqueness b. Multiplicity

conditions are complicated but it is easier to use them than it is to solve the steady state equations for all the different values of the parameters. Also for $\theta_c = 0$, i.e. $T_c = T_f$, the uniqueness condition, Eq. F.10, can be approximated by Eq. F.19, viz. if

$$\eta/\gamma \geq 1 - \sqrt{\frac{1}{2} + \frac{2(1 + H)}{\gamma B_R \beta}} \tag{4.20}$$

then uniqueness is guaranteed. This leads to two additional simple uniqueness conditions, viz.,

$$\gamma B_R \beta \leq 4(1 + H) \tag{4.21}$$

and

$$\eta/\gamma \geq 0.293 \ . \tag{4.22}$$

These conditions are summarized in Table F.1. We conclude with the caveat that these results are for an unenhanced reactor with B in excess.

Inasmuch as these results assume unenhanced absorption and are thereby limited to the first s-shaped region of the heat generation curve, they can not be compared directly with the results shown in Figure 4.15, which are based on the solution of the full equations. But the multiplicity range found via Poore's technique for this special case should be a subset of the multiplicity range found via direct solution of Eqs. 4.3 and 4.4 for the general case. We can check this. For $\tau$ = 10 min we can find $m_1$ and $m_2$ via Eq. F.14, whence $D_{a1}$ and $D_{a2}$ from Eq. F.3. From the definition of the Damkohler number we find the frequency factor for the pseudo-first order rate constant, $k_{10}$, and these are the upper and lower bounds for the multiplicity region, viz.,

$$6.4 \times 10^{17} \leq k_{10} \leq 5.1 \times 10^{18} \text{ sec}^{-1} \ .$$

From Figure 4.13 we can see this is a subset of the range ($7 \times 10^{16}$, $3 \times 10^{19}$ $\text{sec}^{-1}$). If we repeat the calculation for $\tau$ = 1 min, the result

is $(4.3 \times 10^{19}, 6.0 \times 10^{19})$ which again is a subset of the range $(8 \times 10^{18}, 9 \times 10^{19})$. Thus the results of Poore's analysis for an unenhanced reactor give a subset of the multiplicity region for the general reactor.

If we attempt Poore's (1973) analysis on the second s-shaped region, i.e. the enhanced mass transfer controlling regime, we immediately encounter two problems. First we can not write the energy balance for these regions, Eq. F.19, in the form $D_a = g(\theta)$ because of the complicated dependence of $\phi$ on $D_a$. In fact when the reaction becomes instantaneous, $\phi$ and hence the energy balance have no dependence on $D_a$ at all. If we attempt to use a different parameter than $D_a$, we are thwarted because the bounds on $\theta$ depend on all of the other parameters, cf. Eq. F.4. This means that $g(\theta)$ is implicit in all the other parameters. Even if we could overcome this, we must differentiate the function g, but g depends on $\phi$ which is only piecewise differentiable in our model. Thus this technique gives no information in these regions.

In addition to the transition from unique to multiple solutions we must also investigate the transition from the more common s-shaped multiplicity to the unusual multiplicity patterns, e.g. mushrooms and isolas. Little has been written about this problem for a single-phase reactor, let alone a gas-liquid reactor, so we will address the problem for a single-phase reactor first, hoping that we can apply the same technique to the two-phase reactor. The multiplicity patterns observed in a single-phase CSTR as a function of holding time are shown in Figure H.1. There are three basic types: s-shaped, mushroom and isola. Each has its own distinguishing characteristics which should be useful in deducing criteria for its existence. For example each can be distinguished by its corresponding number of ignition and extinction points.

An s-shaped multiplicity has one of each, mushrooms have two of each, and isolas have two extinction points but no ignition points. These patterns have other distinguishing characteristics. The slope of $\theta$ versus $\tau$ has one zero for an s-shaped pattern or a mushroom and two or three zeros for an isola. This slope becomes infinite twice for an s-shape or an isola and four times for a mushroom which is an observation closely related to the number of ignition and extinction points. We can use such observations to identify the regions in parameter space where each behavior pattern is exhibited.

Because an isola can be distinguished by the number of zeros of the slope of $\theta$ versus $\tau$ we will investigate the function $d\theta/d\tau$, see Appendix H. The steady state equations for a single-phase CSTR can be reduced to a single equation in $\theta$ which we write as, cf. Eq. H.2,

$$\psi(\theta,\tau;\ \text{parameters}) = 0 \ . \tag{4.23}$$

It can then be shown that the zeros of $d\theta/d\tau$ are the zeros of $\partial\psi/\partial\tau$, viz., Eq. H.6,

$$\frac{\partial\psi}{\partial\tau}\,(\theta,\tau;\ \text{parameters}) = 0 \ . \tag{4.24}$$

Thus the number of solutions for these two equations determines the multiplicity pattern; one solution implies an s-shape or a mushroom and three imply an isola. The transition from one to three solutions and from three to one solution signals the birth and the death of the isola, cf. Figure H.1d and H.1e.

Examining these equations yields an immediate conclusion: isolas are not possible in an adiabatic reactor, i.e. for $H = 0$. This result agrees with past experimental and numerical observations, cf. Hlavacek et al. (1970), and we believe this is the first time it has been proven. For $H > 0$ we use one of the above equations to eliminate $\tau$ in the other

and obtain an equation in $\theta$ and the parameters which, if the left and right sides are plotted versus $\theta$, allows us to deduce conditions for an isola. Three intersections of the left and right sides imply an isola; one implies an s-shape or a mushroom. But when two solutions exist this signals the birth or death of the isola. This occurs when the left and right sides are tangent at an intersection point, which leads to an equation for the critical temperatures for the birth and death of an isola and to an equation for the critical values of the parameters. What we have achieved is a simple method for determining the region in phase space for an isola. For any assigned values of the parameters $\theta_c$, $\gamma$ and B, we must solve a fifth degree polynomial equation, Eq. H.21, for the two critical temperatures in the admissible range and from this calculate the two critical values of $(H_1/k_f)$ via Eq. H.22. Then if and only if $(H_1/k_f)$ lies between these, an isola exists. Thus finding the region of isola behavior is reduced to finding the zeros of a fifth degree polynomial. We test this technique using an example problem given in Hlavacek and Van Rompay (1981) and find precisely the same critical values of the heat transfer coefficient reported there, see Appendix H, but at considerably less expense. Hlavacek and Van Rompay must solve three simultaneous nonlinear equations whereas we require only the zeros of a fifth degree polynomial.

The technique simplifies considerably if $\theta_c = 0$. Here the polynomial reduces to third degree and we can deduce a necessary condition for the existence of an isola. That is, if an isola exists then

$$B\gamma \geq 27/4 \ . \tag{4.25}$$

A necessary condition in terms of the heat transfer coefficient and the reaction rate constant at feed conditions can also be found, viz., if

an isola exists then

$$H_1/k_f > 1/4\, e^3 = 5.02 \ . \qquad (4.26)$$

Thus the region of isola behavior can be identified by investigating the number of zeros of $d\theta/d\tau$ and a simple technique has been found for establishing the critical values of the heat transfer coefficient which bound this region. Similarly regions of mushroom behavior can be found by investigating the number of times $d\theta/d\tau$ becomes infinite, cf. Figure H.1. But the only simple result found is that mushrooms can not exist for an adiabatic reactor.

This technique can also be applied to the gas-liquid reactor. But even when reactant B is assumed to be in excess and its concentration taken to be a constant, the results are too complicated for any result except that isolas and mushrooms can not exist for an adiabatic reactor, see Appendix I. Further simplification yields the conclusion that isolas and mushrooms can not exist for unenhanced absorption with B in excess and the heat of solution negligibly small. This is somewhat surprising because the single-phase CSTR exhibits such patterns with just one s-shaped region in the heat generation curve, whereas the simplified two-phase model has one s-shaped region but does not. This paradox can be explained by comparing the effects of $\tau$ on the two different s-shaped regions, see Appendix I, and this suggests that these multiplicity patterns are possible in the two-phase reactor only when the concentration of B is other than $C_{Bf}$. Under such conditions all three state variables are important. Thus the technique can not be easily applied and hence is not as useful for the gas-liquid CSTR as for the single-phase CSTR.

An observation that might prove helpful in the future is this. In the single-phase reactor analysis we found that the critical values of

the parameters for the birth and death of an isola are such that the slope, $d\theta/d\tau$, has a double root, see Appendix H. This gives an additional condition, unused there, which might help identify the critical values, viz., that $d\theta/d\tau$ and $d^2\theta/d\tau^2$ vanish simultaneously.

We summarize the steady state results. The gas-liquid reactor operates in five different regions which have been identified and labelled as: physical absorption, fast bulk reaction, mass transfer controlled, enhanced mass transfer, and instantaneous reaction, see Table 4.2. A maximum of five steady states exists with at most one in each operating region. If multiple steady states occur then the states in the fast bulk reaction and enhanced mass transfer regions are unstable by the slope condition. The model predicts three multiplicity types: s-shape, mushroom, and isola, cf. Figures 4.12-4.14. For the experimental reactor of Ding et al. (1974) it predicts an isola with a maximum of three steady states. The steady state temperatures calculated agree with those found in the above in both magnitude and number but from the data, the existence of an isola is indeterminant, cf. Figure 4.11. Uniqueness conditions for the reactor are found from the slope condition, Eqs. 4.12 and 4.13, and via Poore's analysis. The latter conditions apply only to the operating regions in the first s-shaped region of the heat generation curve, i.e. for a reactor without enhanced mass transfer, but they completely specify the entire parameter space, see Appendix F. A technique for determining the regions of isola and mushroom behavior has been found that is very useful for single-phase CSTR's, but less so for two-phase reactors. However, it does show that these patterns are not possible in an adiabatic reactor and that the concentration of B must vary for their existence.

Finally, we now understand that the multiplicity is caused by two different mechanisms: the interaction of absorption and bulk reaction and the interaction of absorption and interfacial reaction (enhancement). That is, the bulk and the interfacial reaction are important in separate temperature ranges because the physical time scales that cue their performance are widely different. We might be able to put this idea to use by dividing the model into two parts and treating each separately. Each produces one s-shaped curve for the heat generation function and the analysis techniques shown here are pertinent to such systems. Also each separate model can be simplified further. In the unenhanced absorption model, which covers the first s-shaped region, reactant B is in sufficient excess that $C_B = C_{Bf}$ is a good approximation. This reduces the model to a mass balance on A and an energy balance. In the enhanced absorption model $C_B$ is not constant but $C_A$ is zero in the bulk. Thus the model reduces to a mass balance on B and an energy balance. Thus it should be possible to reduce the three-state variable process to a sequence of two two-state variable processes.

# CHAPTER FIVE
# STABILITY OF THE STEADY STATES

We investigate the local asymptotic stability of the steady state solutions of the model exhibited in Chapter Four. To do this we use the first method of Liapunov and construct a linear approximation to the dynamic equations in the neighborhood of each steady state. It would be useful to be able to do this in some generality because every point in the state space is a candidate for a steady state in view of the large number of parameters that define a given problem. But the model for $\phi$ is only piecewise differentiable and this implies a piecewise investigation. Thus we assume first that absorption is not enhanced, i.e. that $\phi = 1$, $f_i = 0$, and $\theta_i = \theta$, whence the results we deduce are pertinent to the first s-shaped piece of the heat generation function and to its corresponding steady state solutions, of which three are possible. Of the two remaining solutions, if they are realized, we already know that the slope condition implies that the solution in the enhanced mass transfer region must be unstable and hence only the solution in the instantaneous reaction region needs to be investigated. We observe that all of the physics explained in the introduction is retained in this unenhanced regime of the model.

In the unenhanced mass transfer regime it is not unreasonable to take $C_B$ to be constant at its feed value and to investigate the dynamics of the concentration of A and the temperature. With little loss of generality we also assume that the heat of solution is negligible, i.e. that $H_S << H_R$, and that the cooling water temperature is equal to the

feed temperature, i.e. that $\theta_c = 0$. These greatly simplify the algebra. The dynamic equations describing the reactor are then the simplified versions of the equations in Table 3.2 and are given in Appendix J, viz. Eqs. J.1 and J.2.

Liapunov's First Theorem guarantees that, unless the critical point (steady state) is a center, the nature of a dynamic system in the neighborhood of a critical point is that of its corresponding linear system. Thus we need only consider a linear approximation to Eqs. J.1 and J.2. Whence the necessary and sufficient conditions for stability are that the eigenvalues of the Jacobian matrix evaluated at the steady state have negative real parts. For two state variables this yields two conditions: the determinant must be positive, Eq. J.7, and the trace must be negative, Eq. J.8, i.e.

$$|\underline{\underline{A}}| > 0 \tag{5.1}$$

and

$$\text{tr } \underline{\underline{A}} < 0 \tag{5.2}$$

where $\underline{\underline{A}}$ is the Jacobian matrix whose four elements are the partial derivatives of the right-hand sides of Eqs. J.1 and J.2 with respect to the state variables.

The graphs of the determinant and the trace in Figure J.1 show that a maximum of two zeros exists for each. We call these zeros $m_1$ and $m_2$ for the determinant and $s_1$ and $s_2$ for the trace. We observe that the determinant vanishes at just those values of $\theta$ which are the turning points for $D_a = g(\theta)$ in the investigation of uniqueness and multiplicity in Chapter Four, that is, Eq. J.9 which determines the zeros of the determinant is identical to Eq. F.6 which determines the turning points of $D_a$. Thus on resolving the uniqueness problem we in fact establish

the sign of the determinant. In particular whenever the steady state is unique the determinant is positive; whenever it is not, the determinant is positive for solutions such that $\theta > m_1$ or $\theta < m_2$ and negative for solutions such that $m_2 < \theta < m_1$. The latter must therefore be unstable by the determinant condition and, from Chapter Four, we know that these solutions correspond to the middle steady state for the first s-shaped region of the heat generation function. The uniqueness conditions and hence the conditions guaranteeing that the determinant is positive, are summarized in Table F.1.

The fact that the determinant condition and the slope condition give the same result, i.e. that the middle steady states are unstable, and the fact that they are equivalent and related to the uniqueness problem can be shown as follows. Consider the system of equations

$$dx/dt = f(x,y) \tag{5.3}$$

$$dy/dt = g(x,y) \ . \tag{5.4}$$

These are analogous to Eqs. J.2 and J.1. At steady state the right-hand side of each vanishes. Using the implicit function theorem we can rewrite $g(x,y) = 0$ as $y = h(x)$, whence $f(x,y)$ becomes

$$f(x,h(x)) \equiv F(x) = 0. \tag{5.5}$$

The derivative of F is

$$F' = f_x + f_y h' \tag{5.6}$$

where the derivative of h is

$$h' = dy/dx = - g_x/g_y \ . \tag{5.7}$$

Substituting this into Eq. 5.6 yields

$$F' = f_x - f_y g_x / g_y$$

$$= \frac{f_x g_y - f_y g_x}{g_y} \tag{5.8}$$

whence we obtain

$$F' = \frac{|\underline{A}|}{g_y} \quad . \tag{5.9}$$

Thus the zeros of the determinant of the Jacobian are also the zeros of the slope of $F(x)$ and vice versa, provided that $g_y$ is bounded. We can interpret $F'$ if we rewrite the steady state equation, Eq. 5.5, using the heat removal function and the heat generation function, viz.,

$$Q_R = Q_G \tag{5.10}$$

where $F = Q_G - Q_R = 0$. This is the same as Eq. 4.4. Now we can observe that $F' = 0$ is the same as

$$Q_R' = Q_G' \tag{5.11}$$

where the derivatives are with respect to $\theta$. Thus the zeros of the determinant, $m_1$ and $m_2$, are the points where the heat removal function is tangent to the heat generation function, cf. Figure 5.1. If the determinant is negative, i.e. $m_1 < \theta < m_2$, then $Q_R' < Q_G'$ (because $g_y$ is negative from Eq. J.1) whereas if the determinant is positive, i.e. $\theta > m_1$ or $\theta < m_2$, then $Q_R' > Q_G'$. We conclude that the determinant condition is equivalent to the slope condition. Now the slope condition is closely related to uniqueness. If the slope condition is satisfied or not satisfied everywhere then there can be at most one solution and hence uniqueness. Thus if the determinant is of one sign, i.e. whenever $m_1$ and $m_2$ are nonreal, we have uniqueness and hence the system can have but one steady state. When $m_1$ and $m_2$ are real and hence $|\underline{A}|$ changes sign, then the slope condition is not satisfied everywhere, therefore multiple solutions are possible and any steady state such that $m_2 < \theta < m_1$ is unstable.

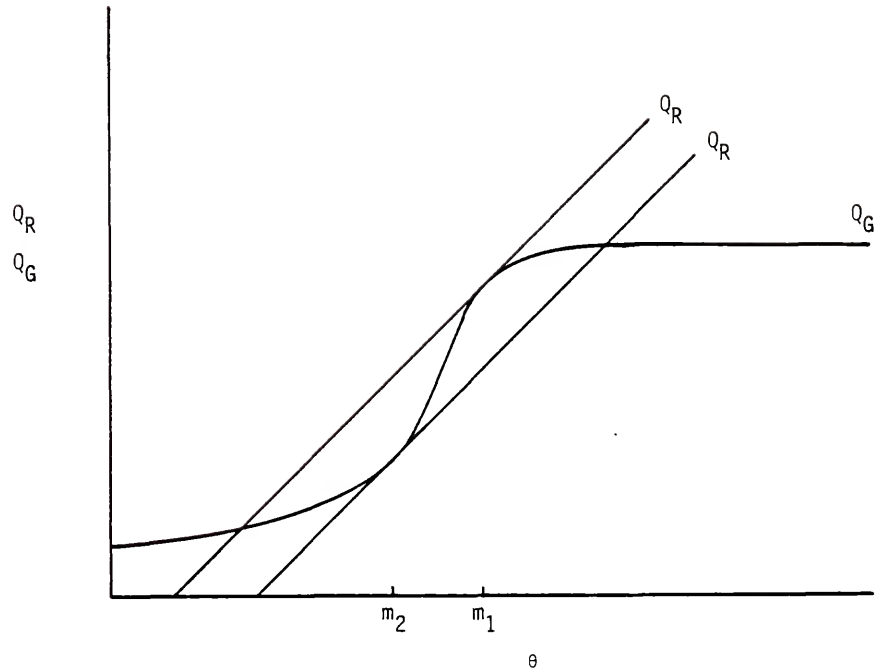


Figure 5.1. The relationship of the zeros of the determinant, $m_1$ and $m_2$, to the heat removal and generation curves.

The values of $m_1$, $m_2$, $s_1$ and $s_2$ are the roots of Equations J.9 and J.10. Inasmuch as the maximum number of roots for each is two, we might estimate their values by approximating $e^{-\eta\theta}$ using its MacLauren series and then neglecting all terms of order greater than two. This gives a quadratic equation for the roots which should be a reasonable approximation if $\eta$ is small or, more precisely, if $(\eta m_1)$ is small. We estimate $m_1$ and $m_2$, the zeros of the determinant, in Appendix F. We estimate $s_1$ and $s_2$, the zeros of the trace, in Appendix J. There we write

$$\text{tr } \underline{\underline{A}} = - \frac{\gamma a_1}{\{ B_R \beta \, e^{-\eta\theta} - (1 + H)\theta \}} (\theta - s_1) (\theta - s_2) \qquad (5.12)$$

where the coefficient for the quadratic term is always negative. The second stability condition is satisfied when the trace is negative, that is, when $s_1$ and $s_2$ are nonreal, or when $s_1$ and $s_2$ are real and $\theta > s_1$ or $\theta < s_2$ (where $s_1 \geq s_2$). The steady state is unstable whenever $s_2 < \theta < s_1$. The first and second conditions for stability are summarized in Table 5.1.

In Table 5.1 the first condition on the determinant and the first two conditions on the trace can be evaluated independently of $D_a$ and $\theta$ and they determine when the roots $m_1$, $m_2$, $s_1$ and $s_2$ are nonreal. Thus these conditions guarantee that the stability conditions are satisfied for all possible values of the steady state. These conditions are in terms of the parameters other than $D_a$ and depend on the evaluation of functions defined elsewhere via the equations cited in the table. Thus these functions define regions in parameter space where the stability conditions are always satisfied, cf. Figures 5.2, 5.3 and 5.4. The first figure shows a region guaranteeing uniqueness and a positive determinant. Because $\eta/\gamma$ is usually much less than one, its complement, the region where multiplicity is possible and where interesting phenomena

TABLE 5.1
STABILITY CONDITIONS FOR AN UNENHANCED GAS-LIQUID CSTR
WITH B IN EXCESS AND $\theta_c = 0$

| Stability Condition | | | Functions Defined In Equation Cited |
|---|---|---|---|
| $\lvert\underline{\underline{A}}\rvert > 0$ | iff | 1. $\frac{\eta}{\gamma} \geq \left(\frac{\eta}{\gamma}\right)_2$ | F.19 |
| | | or | |
| | | 2. $\theta > m_1$ or $\theta < m_2$ | F.16 |
| | | otherwise unstable. | |
| $\text{tr}\,\underline{\underline{A}} < 0$ | iff | 1. $(B_R\beta)_2 < B_R\beta < (B_R\beta)_1$ | J.15 |
| | | or | |
| | | 2. $\eta > \eta_3$ or $\eta > \eta_4$ | J.14 |
| | | or | |
| | | 3. $\theta > s_1$ or $\theta < s_2$ | J.12 |
| | | otherwise unstable. | |

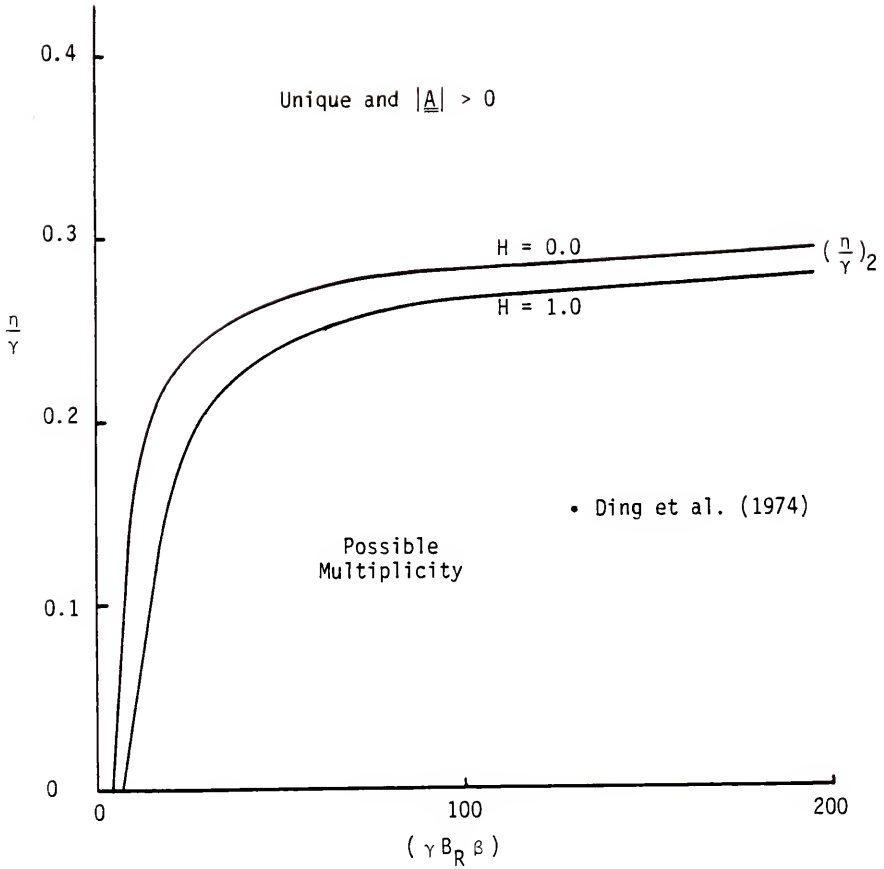


Figure 5.2. Region where uniqueness is guaranteed and the first stability condition is satisfied.

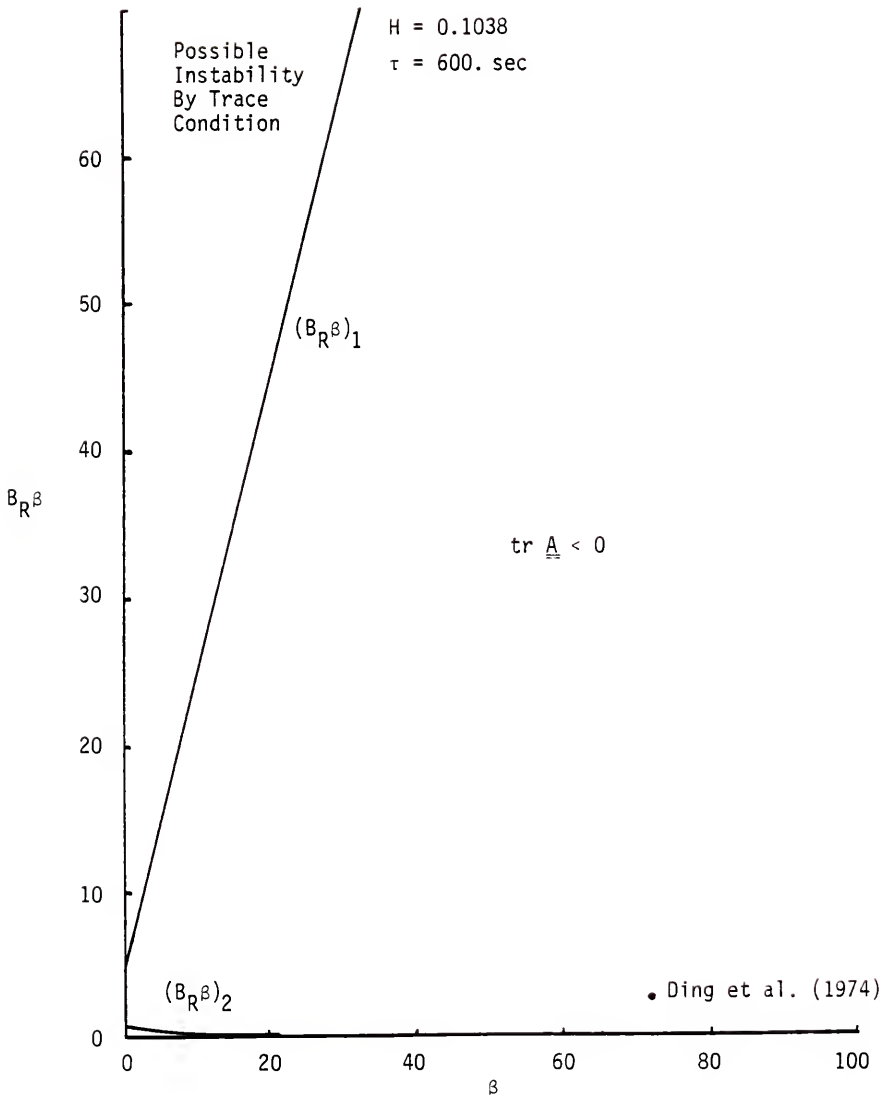


Figure 5.3. Region where the second stability condition is guaranteed: $B_R\beta$ versus β.

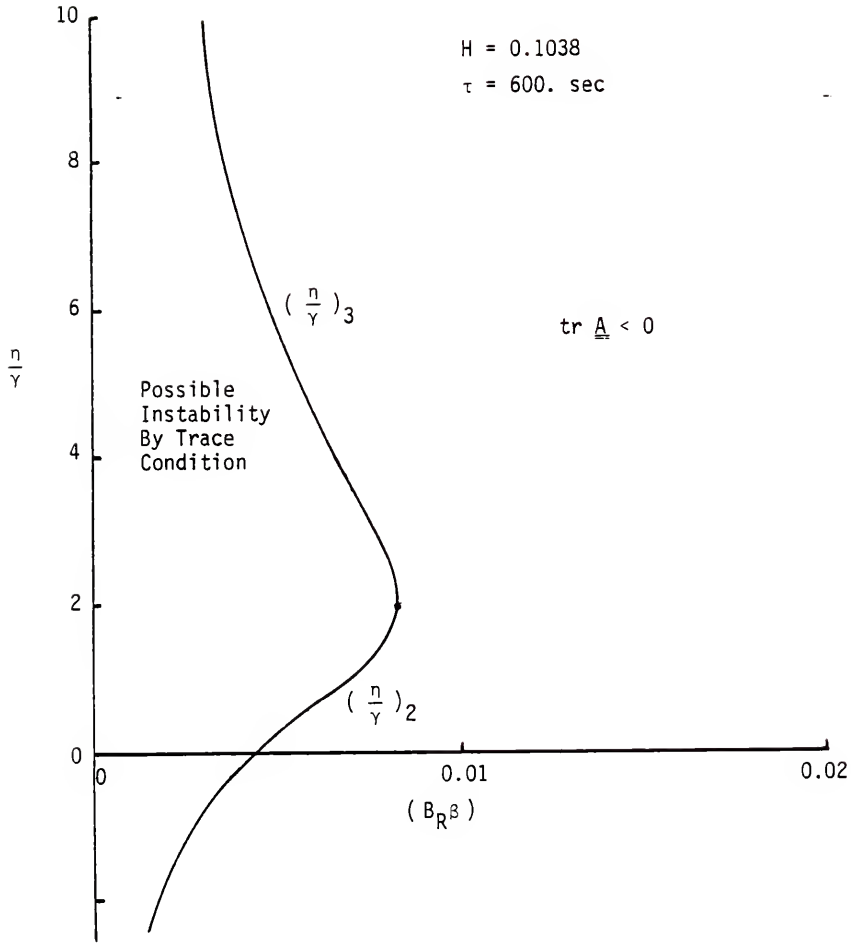


Figure 5.4. Region where the second stability condition is guaranteed: $n/\gamma$ versus $B_R\beta$.
(Data of Ding et al. (1974) is off the graph in the tr $\underline{\underline{A}} < 0$ region.)

might be anticipated, is a large part of the physically allowable region of the plane. In Figures 5.3 and 5.4 regions where the trace is always negative are shown. Thus to investigate the stability of a particular system we must use Figure 5.2 and either Figure 5.3 or Figure 5.4. For example the system studied by Ding et al. (1974), whose results are in the unenhanced mass transfer regime, is shown on Figures 5.2 and 5.3. From Figure 5.2 we see that multiple steady states are possible for this system and Figure 5.3 shows that the second stability condition is always satisfied. Thus the only unstable steady states are those that fail the determinant or slope condition, i.e. the middle steady state, which corresponds with the results found by Ding et al. (1974).

In Table 5.1 the second determinant condition and the third trace condition depend on the values of $m_1$, $m_2$, $s_1$, and $s_2$ which can be established independently of $D_a$ and therefore of $\theta$. If either or both of these conditions must be investigated because the preceding conditions are not satisfied (hence two or all of the above roots are real), then what happens depends on the ordering of the values of $m_1$, $m_2$, $s_1$, and $s_2$. In particular each of the ways that these values can be ordered identifies a performance class for the system and this scheme for classifying the stability and the multiplicity of the critical points is exhaustive.

We calculate the values of the roots via Eqs. F.16 and J.12, or if these approximations are not appropriate, via Eqs. F.6 and J.10. It then follows that the values of $D_a$ found by substituting $\theta = m_1$, $m_2$, $s_1$, and $s_2$ into $D_a = g(\theta)$, Eq. F.3, define the interesting ranges of $D_a$. For example two classes of interest are shown in Figure 5.5 a and b. In each figure there are regions of unique, unstable critical points:

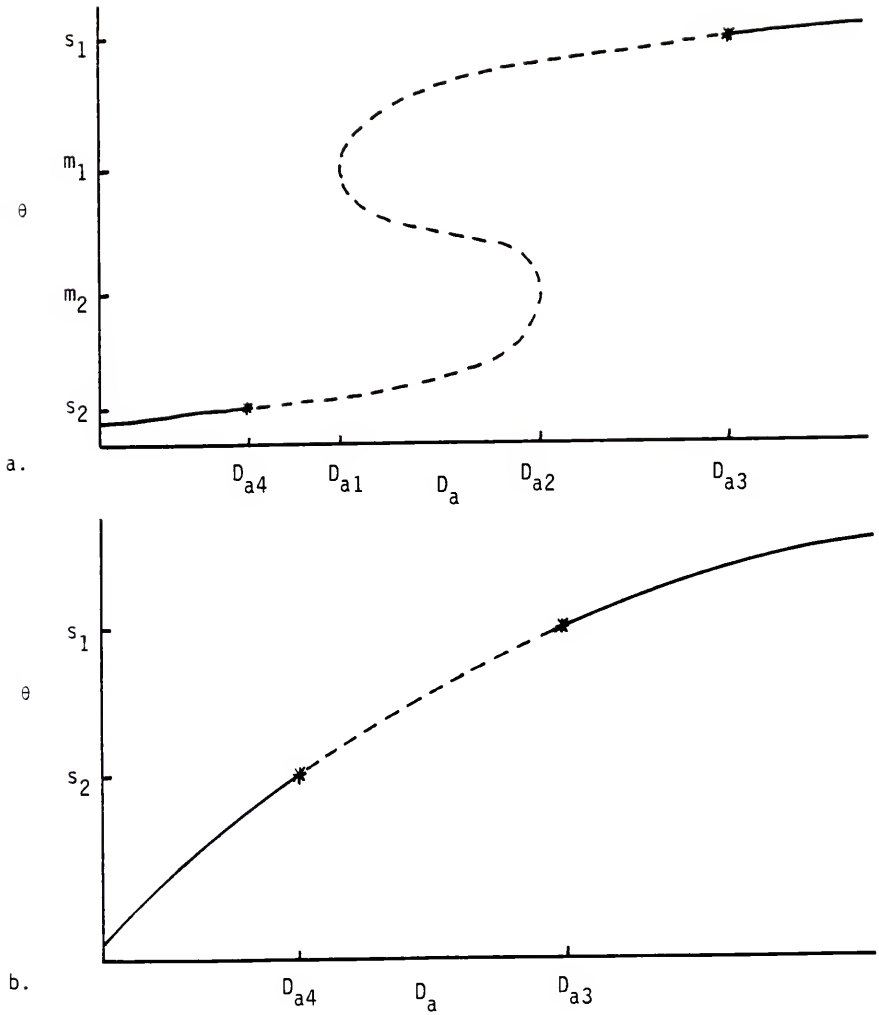


Figure 5.5. Steady state temperature versus Damkohler number.
a. $s_2 < m_2 < m_1 < s_1$ b. $s_2 < s_1$, $m_1$ and $m_2$ are not real

- - - - unstable critical points
——— stable critical points
* bifurcation point

$D_a \in (D_{a4}, D_{a1}) \cup (D_{a2}, D_{a3})$ in Figure 5.5a and $D_a \in (D_{a4}, D_{a3})$ in Figure 5.5b. It is in such regions that we expect to find the natural oscillations that we described in the introduction. In particular the points where the trace vanishes ($\theta = s_1$ or $s_2$, the *'s in Figure 5.5) are centers from which small oscillations bifurcate. If the bifurcation is backward at $D_{a4}$ or forward at $D_{a3}$ then the unique stable solutions shown for $D_a < D_{a4}$ or $D_a > D_{a3}$ are surrounded by small unstable limit cycles. But as shown by Poore (1973) this implies that large stable limit cycles may exist which enclose the unstable periodic solution and the stable state. This is precisely the type of oscillation that we seek and because we have identified the location, proving existence should be possible although it will require numerical solutions of the dynamic equations near the bifurcation points.

All of the foregoing is only for part of the full model but because the determinant must be positive in regions of uniqueness and inasmuch as the determinant condition is equivalent to the slope condition, we may say more generally that the regions of interest for oscillations are the physical absorption, mass transfer controlled, and instantaneous reaction operating regions. But the first and the last of these do not fit our physical picture of an oscillation depending on the interplay of absorption and reaction. Thus the mass transfer controlled operating region is the most likely place to look for natural oscillations. And the foregoing results are pertinent to this region.

We observe that even if we succeed in establishing the existence of an oscillation using a part of the model, the full model must be used to establish quantitative information such as its period, amplitude, etc. Also oscillations that exist under conditions where three

or five steady states exist, may encircle more than one steady state. If so the possibilities are three or five, see Minorsky (1962) and Poore (1973), and in the latter case the orbit samples all regions of the model.

The search for natural oscillations will thus involve determining if the roots $s_1$ and $s_2$ can lie in the mass transfer controlled region. If so, a study of the topology of the functions that determine the sign of the determinant and the trace will be necessary. Finding the oscillations might then require numerical solutions of the dynamic equations near the bifurcation points $s_1$ and $s_2$. This is the basis for our future work.

# CHAPTER SIX
# CONCLUSIONS

Because two-phase reacting systems are quite complex in general, the results shown here are for the specific class of gas-liquid CSTR's where one reactant enters in each phase but reaction occurs only in the liquid phase, and where the gas is supplied in excess and the concentration of the liquid-phase reactant is much greater than that of the dissolved gas. With these assumptions the model is similar to that for a liquid-phase CSTR except that the feed rate of the gaseous reactant is a function of the reactor temperature, i.e. the rate of absorption depends on the solubility of the gas in the liquid and hence is a function of the liquid temperature. Thus the requirements for the natural oscillations outlined in the introduction are met.

Six characteristic times appear in the model equations; two arise in the absorption model and four in the reactor model. These times scale the individual processes and thereby allow us to identify different regions of reactor behavior. The reactor can be viewed as if it were composed of series and parallel processes. First the gas is absorbed into the reacting liquid then it is removed via two mechanisms: bulk reaction and flow. Thus two controlling regimes exist: reaction and flow control, and mass transfer control. Initially at low temperatures reaction is slow and mass transfer easily supplies more solute than can be removed by the flow. This is the reaction and flow control regime. At the lowest temperatures in this regime the solute concentration is essentially the equilibrium concentration of

the gas; we call this the physical absorption region. At higher temperatures the reaction becomes important and it opens another pathway for the removal of the solute; we call this the fast bulk reaction region. The rate of removal via this pathway is unbounded, so ultimately the solute disappears faster than it can be supplied and we enter the mass transfer controlled regime. Here all the solute in the bulk has reacted but the reaction is not fast enough to effect the concentration gradient at the interface and hence the mass transfer coefficient, i.e. $\phi = 1$. This is the unenhanced mass transfer controlled region. At higher temperatures the reaction rate becomes fast enough to increase the mass transfer coefficient and thereby enhance the rate of absorption, i.e. $\phi > 1$; this is called the enhanced mass transfer region. Ultimately the reaction becomes instantaneous near the interface and the concentration of the liquid-phase reactant becomes limiting. This puts an upper bound on the rate of mass transfer and we call this the instantaneous reaction region.

Thus five separate operating regions exist for this class of reactor, cf. Figure 4.4. This figure also shows that the maximum number of steady states is five with at most one solution in each region. If we construct an approximate model which corresponds to one of these operating regions then we know that this model can only give information on the one steady state found in this region and can give no information on multiplicity. This is an important conclusion because several approximate models are reported in the literature that are appropriate to the enhanced mass transfer region only, see Huang and Varma (1981a) and Raghuram and Shah (1977). Their results on multiplicity are meaningless because the above region can have but one physically significant solution.

For this reason their stability analysis is moot, and it is also unnecessary because the slope condition says that the solution in this region is always unstable when multiple solutions exist.

The steady state predictions agree with the experimental results for the chlorination of decane as given by Ding et al. (1974), cf. Figure 4.11. The model predicts that three steady states exist and that enhancement of the mass transfer is not important. It also shows that an isola exists for this system but there is insufficient data to confirm this.

The model predicts three types of multiplicity when the holding time is varied: s-shaped, mushroom and isola, cf. Figures 4.12, 4.13 and 4.14. Each can exist with a maximum of five steady states so we can have a combination of some of the above. For example a double s-shaped pattern or an isola with an s-shaped region is possible as seen in the above figures. But only one mushroom or isola appears to be possible.

Conditions for uniqueness and multiplicity are found via two techniques. The slope condition yields the two inequalities 4.12 and 4.13 which divide the parameter space into three regions. When both conditions are satisfied, uniqueness is guaranteed; when only one condition is satisfied then multiple solutions are possible with a maximum of three steady states; and when neither inequality is satisfied then up to five steady states are possible. These inequalities can be simplified to give weaker but less complicated results, e.g. if $\eta \geq \gamma$, i.e. $H_S \geq E$, then uniqueness is guaranteed. This condition insures that the heat generation function has a nonpositive slope everywhere hence

only one intersection with the heat removal function is possible, cf. Figure 4.4.

A stronger uniqueness condition is found using an idea due to Poore (1973). The adaptation of this idea yields the regions of uniqueness and multiplicity for all parameter space but it can only be applied to our model when mass transfer is unenhanced. This approximation to the model, i.e. $\phi = 1$, $f_i = 0$ and $\theta_i = \theta$, encompasses one of the two s-shaped regions for the heat generation curve. Thus for an unenhanced reactor uniqueness is guaranteed when inequality F.19 is satisfied or, if it is not, when $D_a < D_{a1}$ or $D_a > D_{a2}$ where $D_{a1}$ and $D_{a2}$ are defined by Eqs. 4.18 and 4.19. Two steady states exist when $D_a$ equals $D_{a1}$ or $D_{a2}$ and three steady states exist when $D_{a1} < D_a < D_{a2}$. These results also lead to two simpler uniqueness conditions, viz.,

$$\gamma B_R \beta \leq 4(1 + H)$$

and

$$\eta/\gamma \geq 0.293 \ .$$

All these conditions are summarized in Table F.1. Inasmuch as they assume unenhanced absorption and are thereby limited to the first s-shaped region of the heat generation curve, the multiplicity regions found are only a subset of the multiplicity regions which arise from the full model equations. These regions have been identified for the system studied by Ding et al. (1974) and are shown in Figure 4.15.

A method for determining when an isola or mushroom exists has been developed and is based on the characteristic shapes of these multiplicity patterns. For a single-phase CSTR the region of isola behavior can be found by calculating the zeros of a fifth degree polynomial, Eq. H.21. This is a great improvement over the solution of the three nonlinear

equations proposed by Hlavacek and Van Rompay (1981). Our technique gives the simple result that isolas and mushrooms can not exist for an adiabatic single-phase CSTR. We believe this is the first time this result has been proven although numerical and experimental observations have led to its hypothesis, see Hlavacek et al. (1970). In addition for $\theta_c = 0$ the above results simplify considerably to Eqs. 4.25 and 4.26.

For the gas-liquid CSTR the results are more complicated and only allow a few general conclusions. If the liquid reactant is in excess then isolas and mushrooms can not exist for an adiabatic reactor or for a reactor with unenhanced absorption. Because of this limited insight into the gas-liquid reactor, we have developed a second method for predicting the birth and death of an isola and this may prove useful in the future.

The stability of the steady states is deduced via the slope condition and via the corresponding linear approximation. The former shows that whenever multiple solutions exist the steady states in the fast bulk reaction region and in the enhanced mass transfer region are unstable. For a reactor with unenhanced absorption the concentration of the liquid-phase reactant is approximately its feed value and the linear stability analysis then gives two conditions for stability, viz., $|\underline{\underline{A}}| > 0$ and $\text{tr } \underline{\underline{A}} < 0$ where $\underline{\underline{A}}$ is the Jacobian matrix. The determinant condition is equivalent to the slope condition and the same as the conditions for uniqueness and mutliplicity which were found via Poore's (1973) technique. A maximum of two zeros exists for both the determinant and the trace with respect to the steady state temperature and these are the solutions to Equations J.9 and J.10 which can be approximated by Eqs. F.16 and J.12. These zeros then determine the regions

of instability. If they are imaginary then the stability conditions are met. If they are real and the steady state temperature lies between the two zeros then the state is unstable. These results are summarized in Table 5.1 and are illustrated in Figures 5.2, 5.3 and 5.4.

The ultimate objective of this study is to prove the existence of natural oscillations as described in the introduction. This has not been accomplished because of the unforeseen need to first develop a model with the proper physics. But the results found here give directions as to where these oscillations can be found. Stable limit cycles must exist wherever a steady state is unique (which implies the determinant is positive) but unstable (which implies the trace is positive), see Poore (1973). Because the determinant must be positive and the determinant condition is equivalent to the slope condition we know that these oscillations can only occur in the physical absorption, mass transfer controlled and instantaneous reaction regions. Inasmuch as the natural oscillations that we seek depend on the interaction of reaction and mass transfer and because reaction is very slow in the first region given above and instantaneous in the last region, we anticipate that natural oscillations will most likely occur in the mass transfer controlled region.

A more subtle case is that where the system exhibits an unique, stable steady state, viz. $|\underline{\underline{A}}| > 0$ and tr $\underline{\underline{A}} < 0$, but where the trace is close to zero. Under certain conditions, depending on what happens in the neighboring case where the trace equals zero, the steady state will be surrounded by a small unstable periodic orbit. But as shown by Poore (1973) a large stable orbit must also exist which encloses the small unstable orbit and the stable steady state. Finding such

oscillations will require numerical solutions of the dynamic equations near the bifurcation points where the trace vanishes.

There are also important general conclusions which can be drawn from this study. We know that multiple solutions are possible only when the heat generation curve exhibits at least one s-shaped region. For our gas-liquid CSTR this curve exhibits exactly two, cf. Figure 4.3, hence we should be able to investigate this system using two submodels, each having a heat generation curve with one s-shaped region, and then combine the results to give the result for the full model. The two submodels would be for a reactor with unenhanced mass transfer, i.e. it would consist of the physical absorption, fast bulk reaction and mass transfer controlled regions, and for a reactor operating in the enhanced mass transfer regime, i.e. it would consist of the mass transfer controlled, enhanced mass transfer and instantaneous reaction regions. In fact this was done when finding the uniqueness regions from the slope condition. This is extremely helpful because it simplifies the heat generation function for each submodel.

In addition in the unenhanced absorption regime, reactant B in excess, i.e. $C_B$ constant at its feed value, should be a good approximation and this implies a two state variable problem: $C_A$ and T. This means that the stability conditions are just the determinant and the trace conditions. For a reactor operating in the enhanced mass transfer regime we know that the concentration of the solute is zero in the bulk, i.e. $C_A = 0$. This then is also a two variable system: $C_B$ and T. Furthermore this removes the obstacle that prevented the use of Poore's (1973) technique on this regime in our study. Our form of the enhancement factor is only piecewise differentiable, but accounting

for the variation in $C_B$ allows us to use the fast reaction form for the enhancement factor, Eq. 3.14, which is not only differentiable but also gives the proper limits for slow and instantaneous reaction (see the discussion on the van Krevelen-Hoftijzer approximation in Sherwood, Pigford and Wilke, 1975). The results from these two submodels should then describe the full model.

## APPENDIX A
## STEADY STATE ANALYSIS FOR A SINGLE-PHASE CSTR

The model for a single-phase CSTR and its steady state behavior have been extensively investigated, see Poore (1973), Uppal et al. (1974) and Uppal et al. (1976). We summarize the analysis and some important results. The steady state model is given by the following mass and energy balances:

$$0 = q\,(C_f - C) - V\,k_1\,C \tag{A.1}$$

$$0 = q\,\rho\,C_p\,(T_f - T) - U\,S_c\,(T - T_c) + H_R\,V\,k_1\,C\,. \tag{A.2}$$

Because we are interested in the behavior of the reactor with respect to the holding time, $\tau$, we make the above dimensionless except that the dependence of $\tau$ is left explicit. Solving Eq. A.1 for C and substituting in Eq. A.2 obtains

$$(1 + H_1\,\tau)\,\theta - H_1\,\tau\,\theta_c = B\left(\frac{\tau\,k_1}{1 + \tau\,k_1}\right) \tag{A.3}$$

where $H_1$ is a heat transfer coefficient and B is the dimensionless heat of reaction. The energy balance, Eq. A.3, is written in the classical form; the rate of heat removal equals the rate of heat generation. If these two functions are plotted versus temperature then the intersection points determine the steady states. The left side of Eq. A.3 is the heat removal function and is linear in the temperature, $\theta$. The right side is the heat generation function and it has the form of an s-shaped function with respect to $\theta$. Thus it is the shape of the heat generation function that determines the multiplicity of the reactor, as is seen in Figure A.1.

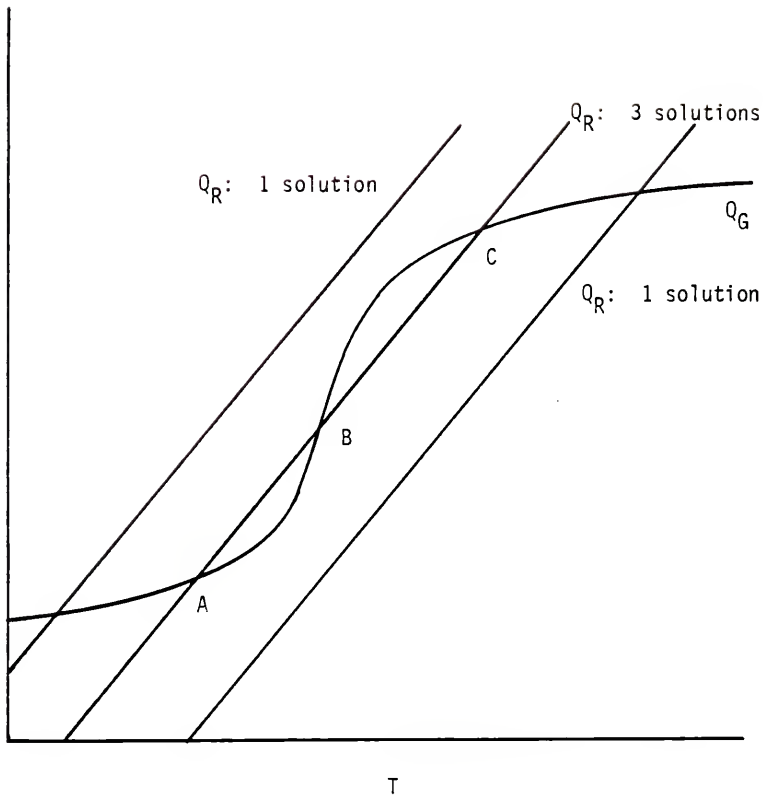


Figure A.1. Heat generation and heat removal functions versus temperature for a single-phase CSTR.

Up to three steady states are possible but at most two are stable. This can be determined from the slope condition: if the slope of the heat generation function is greater than the slope of the heat removal function at a steady state then that state is unstable. This can be understood by considering steady state B in Figure A.1. If the steady state temperature is perturbed to a higher value, then the heat generated is greater than the heat removed, hence the temperature continues to increase. This continues until steady state C is reached. Similarly if the temperature at B is perturbed downward then the steady state moves to A. Thus the slope condition is a sufficient condition for instability and its converse can be shown to be the first of two conditions for stability.

If multiple solutions exist then every other one must satisfy the slope condition and be unstable, cf. Figure A.1. Thus if the slope condition never holds then the reactor has a unique steady state. That is, uniqueness is guaranteed if the slope of the heat removal function is always greater than the slope of the heat generation function at a steady state, viz.,

$$(1 + H_1 \tau) > \frac{B \gamma}{(1 + \theta)^2} \frac{\tau k_1}{(1 + \tau k_1)^2} . \qquad (A.4)$$

The steady state temperature can be removed from the above if the solution of Eq. A.3 is known. Otherwise Eq. A.3 and a bound for $\theta$ can be used to get a weakened form of Eq. A.4. An upper bound for $\theta$ is found when the rate of reaction goes to infinity and a lower bound is found when the rate goes to zero, viz.,

$$\left( \frac{H_1 \tau}{1 + H_1 \tau} \right) \theta_c \equiv \theta_{\ell b} \leq \theta \leq \theta_{ub} \equiv \left( \frac{H_1 \tau}{1 + H_1 \tau} \right) \theta_c + \frac{B}{(1 + H_1 \tau)} .$$

Using this and Eq. A.3 in the above condition yields the uniqueness condition:

$$(1 + H_1 \tau) > \frac{\gamma B}{\left(1 + \left(\frac{H_1 \tau}{1 + H_1 \tau}\right)\theta_c\right)^2} . \qquad (A.5)$$

For an adiabatic reactor this reduces to the particularly simple form that if

$$1 > \gamma B \qquad (A.6)$$

then the reactor has a unique steady state.

The single-phase CSTR exhibits several multiplicity patterns with respect to the holding time, as seen in Figure A.2. The most common is s-shaped multiplicity. Here there is one ignition point from the low temperature steady state to the high temperature steady state and one extinction point from the high to the low temperature steady state. A multiplicity pattern with two ignition points and two extinction points is called a mushroom. The third pattern is an isola which is characterized by two extinction points and no ignition points. Thus if such a reactor is operating at a low temperature steady state, no variation in the holding time will cause a shift to a high temperature steady state. Hence the high temperature branch may not be found experimentally in such a reactor unless the reactor is started at a high temperature in the multiplicity region. Whereas the maximum number of steady states is determined by the heat generation function, these unusual multiplicity patterns seem to be associated with the heat removal function in that mushrooms and isolas have never been experimentally observed for an adiabatic reactor where the heat removal curve is a fixed straight line. Thus these phenomena must depend on the variation of the heat removal

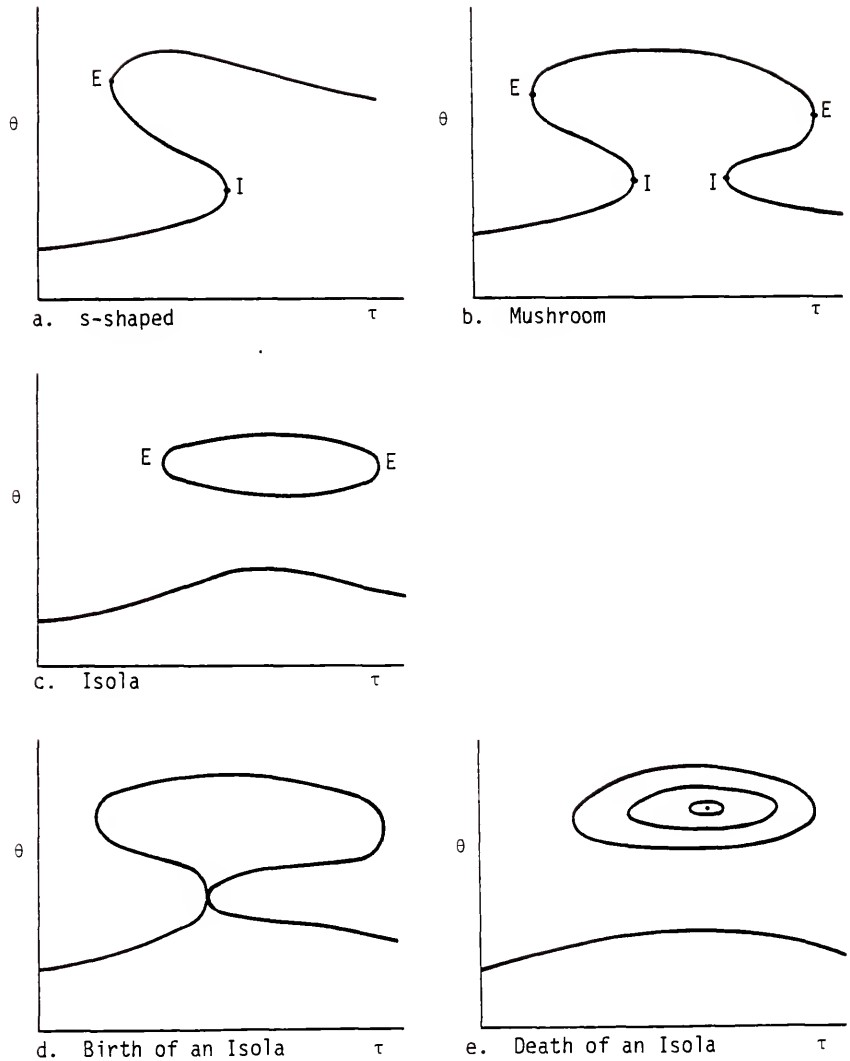


Figure A.2. Multiplicity patterns for a single-phase CSTR.

I = Ignition point, E = Extinction point

function with the holding time, viz.,

$$(1 + H_1 \tau)\, \theta - H_1 \tau\, \theta_c \ .$$

More will be said about these multiplicity patterns in Appendix H.

This brief discussion is intended only to introduce the reader to certain standard ideas and to establish a continuity in going from one-phase to two-phase systems. It foreshadows certain two-phase results and suggests certain lines of investigation. It is not thorough or detailed. In our investigation of two-phase systems we did discover new single-phase results; they are recorded in Appendix H.

## APPENDIX B
## MANN AND MOYES' INTERFACIAL TEMPERATURE RISE: GENERAL RESULT

The general expression for the temperature rise, not given in Mann and Moyes (1977), but using their technique will be derived. For $\alpha >> D$ the film theory equation for diffusion and reaction is independent of the heat equation[1] and becomes

$$D \frac{d^2 C_A}{dz^2} = k_1(T_i) C_A$$

where

at $z = 0$ $\qquad C_A = C_{Ai}(T_i)$

at $z = \delta$ $\qquad C_A = 0$ .

It follows that

$$C_A = C_{Ai} \left[ \cosh \sqrt{k_1/D}\ z - \frac{\sinh \sqrt{k_1/D}\ z}{\tanh \sqrt{k_1/D}\ \delta} \right] \qquad (B.1)$$

where

$$\delta = D/k_L^\circ \ .$$

The macroscopic energy balance over the film is

$$h_L^\circ (T_i - T) = H_S \left( -D \frac{dC_A}{dz} \bigg|_0 \right) + H_R \left[ -D \frac{dC_A}{dz} \bigg|_0 + D \frac{dC_A}{dz} \bigg|_\delta \right]$$

where the heat transfer coefficient for the film theory is[2]

---

[1] An interesting and short research project would be to prove this conjecture by a formal perturbation expansion (it would be singular) and thereby derive estimates of $D/\alpha$ such that the conjecture is true.

[2] Mann and Moyes give the wrong expression for $h_L^\circ$, i.e. they use $k$ instead of $\alpha$. Also this result, Eq. B.2, is a penetration theory result; the corresponding film theory result is $k_L^\circ \alpha / D$. Thus they

$$h_L^\circ = k_L^\circ \sqrt{\alpha/D} \quad . \tag{B.2}$$

Substituting the result for $C_A$ into the energy balance obtains the equation for the temperature rise:

$$(T_i - T) = \sqrt{D/\alpha} \left[ \frac{H_S}{\rho C_p} + \frac{H_R}{\rho C_p} \left( 1 - \frac{1}{\cosh \sqrt{M}} \right) \right] \frac{\sqrt{M}\, C_{Ai}}{\tanh \sqrt{M}} \tag{B.3}$$

where

$$M = k_1 D \,/\, (k_L^\circ)^2 \quad .$$

Using the isothermal film theory predictions for the enhancement factor and the fraction absorbed that reacts in the film, we can identify factors in the above that make its meaning clear. Thus for B in excess the enhancement factor is

$$\phi = \sqrt{M} \,/\, \tanh \sqrt{M}$$

and the fraction that reacts is

$$f_i = \frac{-D \left.\frac{dC_A}{dz}\right|_0 + D \left.\frac{dC_A}{dz}\right|_\delta}{-D \left.\frac{dC_A}{dz}\right|_0}$$

$$= 1 - \frac{1}{\cosh \sqrt{M}}$$

whence

$$T_i - T = \sqrt{\frac{D}{\alpha}} \left[ \frac{H_S}{\rho C_p} + \frac{H_R}{\rho C_p} f_i \right] \phi C_{Ai} \quad . \tag{B.4}$$

Here we find that the temperature rise is the product of three terms: the rate of absorption, $\phi k_L^\circ C_{Ai}$, the heat released, and the inverse of

---

mixed theories in order to obtain an accurate result. In addition it is incorrect to use $h_L^\circ$ because the heat transfer coefficient will be enhanced by heat sources just like the mass transfer coefficient is enhanced by mass sources.

the heat transfer coefficient, $\sqrt{\alpha/D}\ \rho C_p k_L^\circ$. Inasmuch as $f_i$ and $\phi$ (through $k_1$) and $C_{Ai}$ are functions of $T_i$, this is an implicit equation for $T_i$.

This result is obtained for the liquid reactant in excess. So for small concentrations of the liquid reactant or very fast reactions the above gives too large a temperature rise, viz.,

$$\lim_{k_1 \to \infty \text{ or } M \to \infty} (T_i - T) = \lim_{M \to \infty} \sqrt{\frac{D}{\alpha}} \left[\frac{H_S + H_R}{\rho C_p}\right] \sqrt{M}\ C_{Ai}$$

which goes to infinity. This can be corrected for B not in excess or for instantaneous reaction by using the corresponding enhancement factor, see Appendix C.

Thus Eq. B.4 is the general result found via the film theory. Mann and Moyes (1977) report only the slow and fast reaction limits of this. In Appendix D we will derive a similar expression for $T_i$ but without any of the annoying assumptions needed with the film theory, e.g. two different films (one for mass transfer and one for heat transfer) with different thicknesses which are necessary for the relationship between $h_L^\circ$ and $k_L^\circ$, Eq. B.2. Our result agrees with Eq. B.4 when B is in excess.

## APPENDIX C
## PREDICTION OF THE MASS TRANSFER ENHANCEMENT CAUSED BY THE REACTION OF THE DISSOLVED SOLUTE

From the description of the gas-liquid contacting given in Chapter Three a penetration calculation becomes necessary to describe the interfacial region. The details of this calculation are recorded in what follows. In the region $0 < z < \infty$ and $t > 0$ the concentrations of the dissolved solute A and the liquid reactant B satisfy

$$\frac{\partial C_A}{\partial t} = D_A \frac{\partial^2 C_A}{\partial z^2} - k\, C_B\, C_A$$

$$\frac{\partial C_B}{\partial t} = D_B \frac{\partial^2 C_B}{\partial z^2} - k\, C_B\, C_A \qquad \text{(C.1)}$$

whereas on the boundary we impose

$$\text{at } t = 0 \qquad C_A = C_{A\ell} \qquad C_B = C_{B\ell}$$

$$\text{at } z = 0 \qquad C_A = C_{Ai}(T_i) \qquad \frac{\partial C_B}{\partial z} = 0$$

$$\text{as } z \to \infty \qquad \frac{\partial C_A}{\partial t} = -k\, C_B\, C_A \qquad C_B = C_{B\ell} \quad .$$

The solution is simple for two limiting cases: reactant B in excess and instantaneous reaction. We build our model on these two results.

For B in excess the concentration of B is relatively constant, thus we take it to be absolutely constant, albeit not necessarily at the feed value. With this the above reduces to one linear differential equation with psuedo-first order reaction which can be solved using the method of the Laplace transformation. Eq. C.1 now takes the form

$$\frac{\partial C_A}{\partial t} = D_A \frac{\partial^2 C_A}{\partial z^2} - k_1 C_A \quad , \quad C_B = C_{B\ell} \tag{C.2}$$

whence its Laplace transformation is

$$sL(C_A) - C_{A\ell} = D_A \frac{d^2 L(C_A)}{dz^2} - k_1 L(C_A) \quad .$$

with the boundary condition given as

$$L(C_A)\Big|_{z=0} = \frac{C_{Ai}}{s} \quad .$$

It follows that

$$L(C_A) = \left(\frac{C_{Ai}}{s} - \frac{C_{A\ell}}{s + k_1}\right) \exp\left(-\sqrt{\frac{s + k_1}{D_A}}\, z\right) + \frac{C_{A\ell}}{s + k_1} \quad . \tag{C.3}$$

The boundary condition at infinity is satisfied via the above, viz.,

as $z \to \infty$ $\qquad L(C_A) = C_{A\ell} / (s + k_1)$

$$sL(C_A) - C_{A\ell} = L(-k_1 C_A)$$

$$L\left(\frac{\partial C_A}{\partial t}\right) = L(-k_1 C_A)$$

$$\frac{\partial C_A}{\partial t} = -k_1 C_A \quad .$$

We can invert $L(C_A)$ using the following:

$$L^{-1}\left(e^{-z\sqrt{s/D_A}}\right) = \frac{z}{2\sqrt{\pi D_A t^3}}\, e^{-z^2/4D_A t}$$

whence

$$L^{-1}\left(\frac{1}{s} e^{-z\sqrt{s/D_A}}\right) = \operatorname{erfc}\left(\frac{z}{2\sqrt{D_A t}}\right)$$

inasmuch as

$$\frac{z}{2\sqrt{\pi D_A t^3}}\ e^{-z^2/4D_A t} = \frac{\partial}{\partial t}\ \text{erfc}\ \frac{z}{2\sqrt{D_A t}}\ .$$

These results together with the shift theorem and the convolution theorem lead to

$$C_A(z,t) = e^{-k_1 t}\left[\ C_{A\ell} + (C_{Ai} - C_{A\ell})\ \text{erfc}\ \frac{z}{2\sqrt{D_A t}}\ \right] + k_1\, C_{Ai} \int_0^t e^{-k_1 t'}\ \text{erfc}\ \frac{z}{2\sqrt{D_A t'}}\ dt' \qquad (C.4)$$

or

$$C_A(z,t) = e^{-k_1 t}\ C_1(z,t) + k_1 \int_0^t e^{-k_1 t'}\ C_2(z,t')\ dt'$$

where $C_1$ and $C_2$ are solutions of the diffusion equation which satisfy

$$C_1(z,0) = C_{A\ell} \qquad C_2(z,0) = 0$$
$$C_1(0,t) = C_{Ai} \qquad C_2(0,t) = C_{Ai}$$
$$C_1(\infty,t) = C_{A\ell} \qquad C_2(\infty,t) = 0\ .$$

To calculate the mass transfer coefficient or the enhancement factor the flux at the interface must be averaged over all possible exposure times and equated to the mass transfer coefficient times the overall concentration gradient. Assuming random renewal and an average exposure time $\tau_i$ yields

$$\phi\ k_L^\circ\ (C_{Ai} - C_{A\ell}) = \int_0^\infty \frac{1}{\tau_i} e^{-t/\tau_i}\ \left(\ -\ D_A \frac{\partial C_A}{\partial z}\bigg|_{z=0}\ \right)\ dt\ .$$

Interchanging the order of integration and differentiation and using the definition of the Laplace transformation obtains

$$\phi\ k_L^\circ\ (C_{Ai} - C_{A\ell}) = -\ D_A \frac{\partial}{\partial z}\left[\ \frac{1}{\tau_i}\int_0^\infty\ e^{-t/\tau_i}\ C_A\ dt\ \right]_{z=0}$$

$$= -\frac{D_A}{\tau_i} \frac{\partial}{\partial z} L(C_A)\Big|_{z=0,\ s=1/\tau_i}$$

$$= \sqrt{\frac{D_A}{\tau_i}(1 + \tau_i k_1)} \left( C_{Ai} - \frac{C_{A\ell}}{(1 + \tau_i k_1)} \right) .$$

Therefore we find

$$\phi \equiv \frac{k_L}{k_L^\circ} = \sqrt{1 + \tau_i k_1} \ \frac{\left( C_{Ai} - C_{A\ell}/(1 + \tau_i k_1) \right)}{(C_{Ai} - C_o)} \qquad (C.5)$$

where

$$k_L\Big|_{k_1=0} = k_L^\circ = \sqrt{D_A/\tau_i} \ .$$

Thus if $C_{A\ell}$ is zero then

$$\phi = \sqrt{1 + \tau_i k_1} = \sqrt{1 + \tau_i/\tau_{Ri}} \ . \qquad (C.6)$$

Because $C_{A\ell}$ is zero whenever $\phi$ is not one (see the time scale argument in Chapter Three) Eq. C.6 is our desired result. We also observe that when the reaction near the interface is slow so that $\tau_i/\tau_{Ri}$ (i.e. $\tau_i k_1$) is much less than one, both Eqs. C.5 and C.6 reduce $\phi = 1$ as expected.

The fraction of A absorbed that reacts near the interface, $f_i$, is the ratio of the rate of reaction near the interface to the rate of absorption. The average rate of reaction is the total rate in an element of fluid with exposure time t, averaged over all possible exposure times:

$$\frac{1}{\tau_i} \int_0^\infty e^{-t/\tau_i} \left[ \int_0^\infty k_1 \, C_A \, dz \ (Va) \right] dt$$

Interchanging the order of integration, identifying the Laplace transformation and integrating over z yields

$$V \phi \, k_L^\circ \, a \, C_{Ai} \left( \frac{\tau_i k_1}{1 + \tau_i k_1} \right)$$

for $C_{A\ell}$ equal to zero. The rate of absorption is

$$V \phi k_L^\circ a C_{Ai}$$

whence the fraction $f_i$ is

$$f_i = \left( \frac{\tau_i k_1}{1 + \tau_i k_1} \right) \qquad (C.7)$$

where $k_1 = kC_B$ is evaluated at the interfacial temperature $T_i$. The form of $f_i$ is identical to the fraction that reacts in a single-phase CSTR except that $\tau_i$ replaces the reactor holding time. Thus Eqs. C.6 and C.7 establish $\phi$ and $f_i$ for B in excess.

The second limiting case which gives a simple result is that of instantaneous reaction. Here A and B react so rapidly that they can not coexist in the liquid together. A reaction front starts at the gas-liquid interface upon contact of the two phases and moves into the liquid, cf. Figure C.1. To the left of the front B vanishes; to the right A vanishes; at the front itself both vanish. Thus A diffuses without reacting from the interface to the moving front, similarly B diffuses from the bulk. At the front the ratio of the two fluxes is equal to the stoichiometric ratio for the reaction. Thus we have

$$\frac{\partial C_A}{\partial t} = D_A \frac{\partial^2 C_A}{\partial z^2} \qquad 0 < z < \lambda \sqrt{t}$$

$$\frac{\partial C_B}{\partial t} = D_B \frac{\partial^2 C_B}{\partial z^2} \qquad \lambda \sqrt{t} < z < \infty$$

where

at $t = 0$ $\quad C_A = 0 \quad C_B = C_{B\ell}$

at $z = 0$ $\quad C_A = C_{Ai}$

at $z = \lambda \sqrt{t}$ $\quad C_A = 0 \quad C_B = 0$

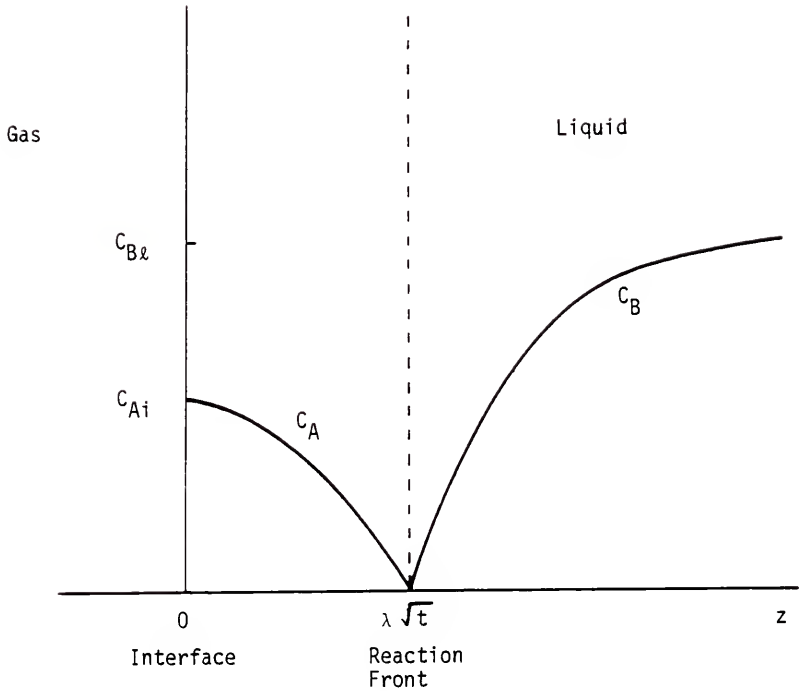


Figure C.1. Concentration profiles near the interface for instantaneous reaction.

as $z \to \infty$ $\qquad C_B = C_{B\ell}$

which yields

$$C_A = C_{Ai}\left(1 - \frac{\mathrm{erf}(\, z/\sqrt{4D_A t}\,)}{\mathrm{erf}(\, \lambda/\sqrt{4D_A}\,)}\right)$$

$$C_B = \frac{C_{B\ell}}{(1 - \mathrm{erf}(\lambda/\sqrt{4D_B}))}\left[\mathrm{erf}(z/\sqrt{4D_B t}) - \mathrm{erf}(\lambda/\sqrt{4D_B})\right].$$

For the reaction

$$A + \nu B \to \text{Products}$$

$\lambda$ can be found by equating the fluxes at the reaction front, viz.,

$$-\nu D_A \left.\frac{\partial C_A}{\partial z}\right|_{\lambda\sqrt{t}} = D_B \left.\frac{\partial C_B}{\partial z}\right|_{\lambda\sqrt{t}}$$

whence we conclude

$$\frac{C_{B\ell}}{\nu C_i}\sqrt{\frac{D_B}{D_A}}\ \mathrm{erf}(\lambda/\sqrt{4D_A})\ e^{\lambda^2/4D_A} = (1 - \mathrm{erf}(\lambda/\sqrt{4D_B}))\ e^{\lambda^2/4D_B}$$

and this establishes the value of $\lambda$. Ordinarily liquid phase diffusivities are very similar, so assuming

$$D_A = D_B = D$$

obtains

$$\mathrm{erf}(\lambda\ /\ \sqrt{4D}\ ) = 1\ /\ (1 + C_{B\ell}\ /\ \nu C_{Ai}) \quad . \tag{C.8}$$

The rate of absorption is equal to the flux of A at the interface, averaged over all exposure times:

$$\phi\ k_L^\circ\ C_{Ai} = \int_0^\infty \frac{1}{\tau_i} e^{-t/\tau_i}\ \left(-D\frac{\partial C_A}{\partial z}\right)\Big|_{z=0} dt$$

$$= \frac{1}{\tau_i}\sqrt{\frac{D}{\pi}}\ \frac{C_{Ai}}{\mathrm{erf}(\lambda/\sqrt{4D}\,)} \int_0^\infty \frac{e^{-t/\tau_i}}{\sqrt{t}}\, dt$$

$$= k_L^\circ \left(1 + C_{B\ell} / \nu C_{Ai}\right) C_{Ai}$$

where $k_L^\circ = \sqrt{D/\tau_i}$ ; whence it follows that

$$\phi = \left(1 + C_{B\ell} / \nu C_{Ai}\right) \equiv \phi_I \quad . \tag{C.9}$$

Because the rate of reaction is a maximum here, Eq. C.9 gives the maximum enhancement. We can use this result, Eq. C.9, and the previous result for noninstantaneous reaction, Eq. C.6, to obtain a criterion for the onset of instantaneous reaction. That is whenever $\phi$ from Eq. C.6 is greater than $\phi_I$ the reaction is instantaneous:

$$\sqrt{1 + \tau_i / \tau_{Ri}} > 1 + C_{B\ell} / \nu C_{Ai} \quad .$$

For enhancement $\tau_i/\tau_{Ri}$ must be much greater than one and $C_{B\ell}/\nu C_{Ai}$ is almost always much greater than one for a gas-liquid system. To a good approximation then the criterion for instantaneous reaction is

$$\frac{\tau_i}{\tau_{Ri}} > \left(\frac{C_{B\ell}}{\nu C_{Ai}}\right)^2 \quad . \tag{C.10}$$

For instantaneous reaction all the absorbed gas reacts near the interface, hence $f_i$ equals one.

Now the enhancement factor is known for two limiting cases and we must determine how they are connected. The first estimate of $\phi$ breaks down when the concentration of B becomes small near the interface, i.e. of the order of $\nu C_{Ai}$, but the second estimate can not be used unless B vanishes there. In this transition region we must account for the variation in the concentration of B. This can be done using the van Krevelen-Hoftijzer approximation (Sherwood, Pigford and Wilke, 1975) in which the region of validity of the formula for B in excess is expanded by estimating the interfacial concentration of B and then

assuming the concentration of B to be uniform at that value. The interfacial concentration of B is found by equating the rate of diffusion of B toward the interface to the excess rate of absorption of A, i.e. the fraction that reacts. But as Sherwood, Pigford and Wilke show the transition region is small and is not greatly different from the extrapolation of the two limiting cases. Thus in keeping with the desire for a simple model and without sacrificing any essential physics, the enhancement factor will be approximated by extrapolating the two limiting cases to their intersection in the transition region.

The results of the interfacial model can be summarized as:

if $\dfrac{\tau_i}{\tau_{Ri}} < \left(\dfrac{C_{B\ell}}{\nu C_{Ai}}\right)^2$ then $\phi = \sqrt{1 + \tau_i / \tau_{Ri}}$

and $f_i = \dfrac{\tau_i / \tau_{Ri}}{1 + \tau_i / \tau_{Ri}}$

or if $\dfrac{\tau_i}{\tau_{Ri}} > \left(\dfrac{C_{B\ell}}{\nu C_{Ai}}\right)^2$ then $\phi = 1 + C_{B\ell} / \nu C_{Ai}$

and $f_i = 1$ .

## APPENDIX D
## INTERFACIAL TEMPERATURE RISE

The interfacial temperature rise is caused by the heat released on absorption of the gas and by the heat released on reaction of the dissolved solute as it diffuses into the liquid. To estimate the magnitude of the temperature rise the energy balance

$$\rho C_p \frac{\partial T}{\partial t} = k \frac{\partial^2 T}{\partial z^2} + H_R \, k \, C_B \, C_A \qquad (D.1)$$

with the initial and boundary conditions

at $t = 0$ $\quad T = T_\ell$

at $z = 0$ $\quad T = T_i$

as $z \to \infty$ $\quad T = T_\ell$

must be solved simultaneously with the corresponding mass balances. This can be done simply for two cases, that of no reaction and that of instantaneous reaction. For the intermediate case, i.e. that corresponding to the B in excess calculations in Appendix C, we can use a reasonable assumption to deduce an approximate temperature rise which bridges the two cases above. In addition the no reaction case will show how the effect of the heat of absorption can be added to the heat of reaction results.

For no reaction the diffusion equations are satisfied by

$$C_A = C_{Ai} + (C_{A\ell} - C_{Ai}) \, \mathrm{erf}\left( z / \sqrt{4Dt} \right) \qquad (D.2)$$

$$T = T_i + (T_\ell - T_i) \, \mathrm{erf}\left( z / \sqrt{4\alpha t} \right) \qquad (D.3)$$

where $C_{Ai}$ and $T_i$ are related through Henry's law, viz.,

$$C_{Ai} = \frac{P_A}{H_o} \exp\left( \frac{H_S}{RT_i} \right) \qquad (D.4)$$

The temperature rise is obtained by equating the heat released on absorption to the energy flux into the liquid at the interface:

$$- D \frac{\partial C_A}{\partial z} \Big|_{z=0} H_S = -k \frac{\partial T}{\partial z} \Big|_{z=0}$$

whence

$$T_i - T_\ell = \frac{H_S}{\rho C_p} \sqrt{\frac{D}{\alpha}} \, (C_{Ai} - C_{A\ell}) \quad . \qquad (D.5)$$

For instantaneous reaction all the reaction takes place at the reaction plane, on each side of which the temperature is described by the diffusion equation. If the interface is assumed to be an adiabatic plane, which is a reasonable approximation for a gas-liquid interface, then the temperature on the interfacial side of the reaction plane is a constant, $T_i$, for all z and t (Figure D.1). That is, since there is no energy flux through the interface, the heat generated at the moving reaction front just heats the liquid behind it to a constant temperature. On the bulk side of the reaction plane the heat generated there is conducted from the plane at $T_i$ to the bulk at $T_\ell$:

$$\frac{\partial T}{\partial t} = \alpha \frac{\partial^2 T}{\partial z^2}$$

where

at $t = 0$ $\qquad T = T_\ell$

at $z = \lambda \sqrt{t}$ $\qquad T = T_i$

as $z \to \infty$ $\qquad T = T_\ell$ .

Thus it follows that

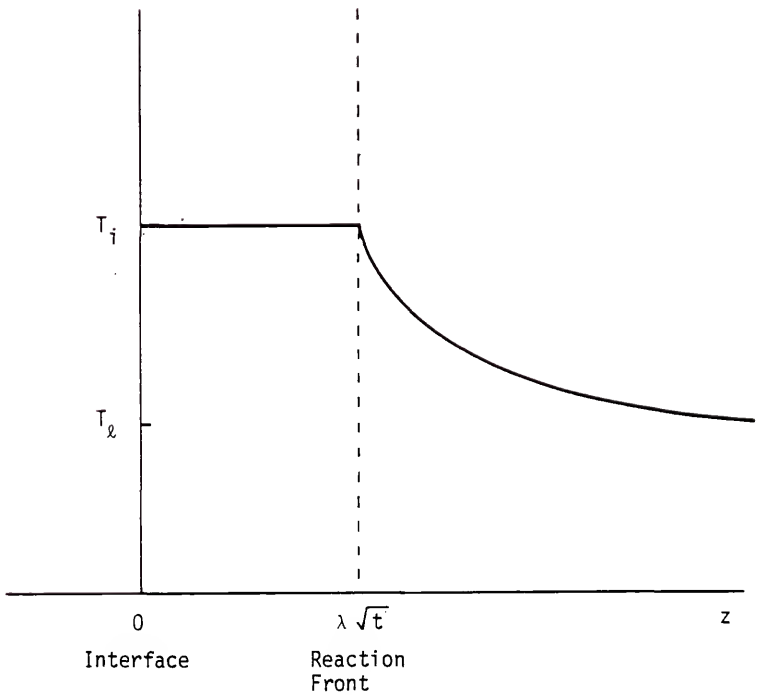


Figure D.1. Temperature profile near the interface for instantaneous reaction.

$$T = T_\ell + \frac{(T_i - T_\ell)}{(1 - \mathrm{erf}(\lambda/\sqrt{4\alpha}))}(1 - \mathrm{erf}(z/\sqrt{4\alpha t})) \quad . \tag{D.6}$$

The interfacial temperature can be found by equating the heat generated by reaction at the plane to the flux of energy into the bulk:

$$-H_R D \frac{\partial C_A}{\partial z}\bigg|_{z=\lambda\sqrt{t}} = -k \frac{\partial T}{\partial z}\bigg|_{z=\lambda\sqrt{t}} .$$

Using the results from Appendix C obtains

$$\frac{H_R}{\sqrt{D}} D\, C_{Ai} \frac{e^{-\lambda^2/4D}}{\mathrm{erf}(\lambda/\sqrt{4D})} = \frac{k}{\sqrt{\alpha}} \frac{(T_i - T_\ell)\, e^{-\lambda^2/4\alpha}}{(1 - \mathrm{erf}(\lambda/\sqrt{4\alpha}))} \quad . \tag{D.7}$$

The position of the reaction plane and hence $\lambda$ are found by equating the mass fluxes at the plane, see Appendix C:

$$-\nu D_A \frac{\partial C_A}{\partial z}\bigg|_{z=\lambda\sqrt{t}} = D_B \frac{\partial C_B}{\partial z}\bigg|_{z=\lambda\sqrt{t}}$$

and if $D_A = D_B = D$ this yields

$$\mathrm{erf}(\lambda/\sqrt{4D}) = \frac{1}{1 + C_B/\nu C_{Ai}} = \frac{1}{\phi_I} \quad . \tag{D.8}$$

Substituting Eq. D.8 into Eq. D.7 gives

$$(T_i - T_\ell) = \frac{H_R}{\rho C_p}\sqrt{\frac{D}{\alpha}}\, \phi_I\, C_{Ai}\, (1 - \mathrm{erf}\,\frac{\lambda}{\sqrt{4\alpha}})\, e^{\frac{-\lambda^2}{4}(\frac{1}{D} - \frac{1}{\alpha})} . \tag{D.9}$$

where $C_{Ai}$ and $T_i$ are related via Henry's law.

To find $T_i$ the last two equations must be solved simultaneously. Their solution can be simplified by making two reasonable approximations:

for most liquids $\alpha >> D$,

whence $(\frac{1}{D} - \frac{1}{\alpha}) \cong \frac{1}{D}$ ;

for most gas-liquid systems $C_B/\nu C_{Ai} >> 1$,

whence $\text{erf}( \lambda/\sqrt{4D} ) << 1/2$ and $\lambda/\sqrt{4D} << 1/2$ .

It follows that

$$\lambda/\sqrt{4\alpha} = ( \lambda/\sqrt{4D} ) \sqrt{D/\alpha} << 1/2 \sqrt{D/\alpha} << 1 .$$

This implies

$$\text{erf}( \lambda/\sqrt{4\alpha} ) << 1$$

and

$$1 > e^{-\lambda^2/4D} >> e^{-1/4} = 0.779 .$$

Because $1/2$ is a weak upper bound for $\lambda/\sqrt{4D}$, we take $e^{-\lambda^2/4D} = 1$.

Therefore Eq. D.9 becomes

$$(T_i - T_\ell) = \frac{H_R}{\rho C_p} \sqrt{\frac{D}{\alpha}} \phi_I C_{Ai} \qquad (D.10)$$

which is implicit in $T_i$ through $\phi_I$ and $C_{Ai}$.

The predicted temperature rise here is much greater than that for no reaction because the heat of reaction is usually much greater than the heat of solution and the rate of absorption is much greater with reaction, i.e. $\phi_I C_{Ai} > (C_{Ai} - C_{A\ell})$. For example the data of Ding et al. (1974) gives the values for the heat of reaction and heat of solution to be 25000 and 4500 calories per mole. Also Eq. D.10 gives the maximum temperature rise inasmuch as all the absorbed gas reacts near the interface.

When reaction near the interface is important but not fast enough to be instantaneous and B is in excess, an approximate temperature rise can be obtained. Whenever the thermal diffusivity is much greater than the molecular diffusivity, $\alpha >> D$, it is reasonable to say that the diffusion and reaction processes take place at the constant temperature

$T_i$ and that the corresponding heat of reaction is released at the interface. Thus we may use the results in Appendix C and the heat transfer problem becomes

$$\frac{\partial T}{\partial t} = \alpha \frac{\partial^2 T}{\partial z^2}$$

where

at $t = 0$ $\quad T = T_\ell$

at $z = 0$ $\quad T = T_i$

as $z \to \infty$ $\quad T = T_\ell$ .

Then $T_i$ can be found via an energy balance at the interface equating the heat generated by reaction and absorption to the energy flux into the liquid.

The heat generated is found from the rate of absorption and the overall rate of reaction given in Appendix C. It is most easily expressed in its averaged form which for surface-renewal theory is

$$(H_S + H_R f_i) \phi k_L^\circ C_{Ai} . \qquad (D.11)$$

The average energy flux for surface-renewal theory[1] is

$$\int_0^\infty -k \frac{\partial T}{\partial z}\bigg|_{z=0} \frac{1}{\tau_i} e^{-t/\tau_i} \, dt .$$

Interchanging the order of integration and differentiation expresses the above in terms of the Laplace transformation of T, see Appendix C, viz.,

$$-\frac{k}{\tau_i} \frac{\partial}{\partial z} L(T) \bigg|_{z=0,\ s=1/\tau_i} .$$

[1] It is not necessary to use the averaged values here. Equating the instantaneous generation to the instantaneous energy flux then averaging with the surface-renewal theory gives the same result. However using the averaged values illustrates the physics more clearly due to the simpler form of the results, see Appendix C. It is not necessary to average the earlier results, Eqs. D.5 and D.10, inasmuch as they are independent of the exposure time.

From the differential equation the Laplace transformation is

$$L(T) = \frac{1}{s}(T_i - T_\ell)\exp(-\sqrt{s/\alpha}\ z) + T_\ell/s$$

whence the flux becomes

$$\rho C_p \sqrt{\alpha/\tau_i}\ (T_i - T_\ell)\ . \qquad (D.12)$$

Equating this expression to the expression for the generated, D.11, and noting that

$\tau_i = D / k_L^{\circ 2}$, obtains

$$(T_i - T_\ell) = \left(\frac{H_S}{\rho C_p} + \frac{H_R}{\rho C_p} f_i\right)\sqrt{\frac{D}{\alpha}}\ \phi\ C_{Ai}\ . \qquad (D.13)$$

This approximation is very similar to the two previous limiting solutions. In each the temperature rise is equal to the rate of absorption, $\phi\ k_L^\circ\ C_{Ai}$, times the heat released divided by a term which describes the rate of conduction of heat into the bulk, $k^\circ_L\sqrt{\alpha/D}$ . In this last term the factor $\sqrt{\alpha/D}$ converts a mass transfer coefficient into a heat transfer coefficient. The above result also has the proper limits for fast and slow reaction, i.e. the previous results, viz.,

$$\lim_{k\to 0}(T_i - T_\ell) = \frac{H_S}{\rho CP}\sqrt{\frac{D}{\alpha}}\,C_{Ai}$$

$$\lim_{k\to\infty}(T_i - T_\ell) = \frac{(H_S + H_R)}{\rho C_p}\sqrt{\frac{D}{\alpha}}\,\phi_I\ C_{Ai}\ .$$

In the above derivations it was not necessary to assume that two fictitious films exist, one for mass transfer and one for heat transfer, see Mann and Moyes' (1977) result in Appendix B. Thus the results are more consistent with our interfacial model and hence more understandable. Eq. D.13 is the result that is used in our reactor model. Its accuracy

has not been examined because of the lack of available data for interfacial temperature rises. The reported temperature rises have all been found via indirect measurements and sometimes the results are filtered through another model, see Beenackers (1978), Verma and Delancy (1975), and Mann and Moyes (1977). But using the data from Ding et al. (1974) the temperature rise can vary from 3°C to 92°C, using Eqs. D.5 and D.10. This is in the range that has been estimated for other systems.

## APPENDIX E
## THE SLOPE CONDITION FOR A GAS-LIQUID CSTR

The slope condition is a necessary condition for stability and can be understood by examining the graph of the heat removal function and the heat generation function versus temperature, cf. Figures 2.1 and 4.4. The slope condition states:

> If the slope of the heat removal function at a steady state is less than the slope of the heat generation function then the steady state is unstable.

The graph of these functions shows that the lowest temperature steady state can not satisfy this condition and that for multiple solutions this condition must hold for every other steady state. Thus if it holds for one steady state then multiple steady states must exist. Conversely if it does not hold anywhere then the steady state must be unique. Hence the converse of the above is an uniqueness condition which we can use to determine regions of uniqueness, i.e. if the slope of the heat removal function is always greater than the slope of the heat generation function then the steady state is unique.

Because we have an understanding of our reactor we know that there are only two operating regions where the slope of the heat generation function is positive, hence only there can the uniqueness condition be violated. These regions are the fast bulk reaction region and the enhanced mass transfer region. This simplifies the investigation of the uniqueness condition because we do not need to consider the right-hand side of Eq. 4.4 in full generality, only the two limiting forms

for these regions given in Table 4.3. But it also transforms the uniqueness condition into two conditions, one for each of the s-shaped regions seen in Figure 4.4. Thus for uniqueness everywhere, both must be true. We will derive each of these after deducing some preliminary results.

In what follows we need bounds on the steady state temperature $\theta$. An upper bound can be found by assuming that all of the gas A that absorbs also reacts, so Eq. 4.4 gives

$$(1 + H)\ \theta - H\ \theta_c = (B_S + B_R)\ \beta\ \phi\ x_i \qquad (E.1)$$

where $\beta = \tau/\tau_M$. To remove the temperature dependence from the right side we use the maximum of $\phi x_i$, viz.,

$$\phi\ x_i \leq \phi_I\ x_i = x_i + x_B/S \leq 1/S$$

where the last inequality is an approximation which is made because $x_i << x_B/S$ and $x_B \leq 1$. Thus an upper bound for the temperature is

$$(1 + H)\ \theta_{ub} - H\ \theta_c = (B_S + B_R)\ (\beta/S)$$

or

$$\theta_{ub} = \left(\frac{H}{1 + H}\right)\ \theta_c + \frac{(B_S + B_R)}{(1 + H)}\ \frac{\beta}{S} \quad . \qquad (E.2)$$

For the fast bulk reaction region we can get a stronger result because $\phi = 1$, viz.,

$$\theta_{ub} = \left(\frac{H}{1 + H}\right)\ \theta_c + \frac{(B_S + B_R)}{(1 + H)}\ \beta \quad . \qquad (E.3)$$

A lower bound for the temperature is found when there is no reaction. Here Eq. 4.4 becomes

$$(1 + H)\ \theta - H\ \theta_c = B_S\ \beta\ x_i \quad . \qquad (E.4)$$

Again in order to remove the temperature dependence on the right side we use the minimum of $x_i$, viz.,

$$x_i \geq x_i\ (\theta_{ub}) \geq x_i\ (\theta \to \infty) = e^{-\eta} > 0$$

which is fair because the solubility decreases with temperature. Thus the lower bound is

$$\theta_{\ell b} = \left( \frac{H}{1 + H} \right) \theta_c + \frac{B_S \beta e^{-\eta}}{(1 + H)} \quad . \tag{E.5}$$

The slope of the heat removal function is, cf. Eq. 4.4,

$$Q_1 = (1 + H) \tag{E.6}$$

where $H = \tau/\tau_H$. The heat generation function in the fast bulk reaction region is

$$(B_S + B_R)\, x_i \frac{\tau}{\tau_R} = (B_S + B_R)\, D_a\, e^{(\gamma-\eta)\theta/(1+\theta)} \tag{E.7}$$

where we have used the fact that $\theta_i = \theta$ in this region. The heat generation function in the enhanced mass transfer region is

$$(B_S + B_R)\, x_i \frac{\tau}{\tau_M} \sqrt{\frac{\tau_i}{\tau_{Ri}}} = (B_S + B_R)\beta \sqrt{D_{ai}}\, e^{\frac{1}{2}(\gamma-2\eta)\theta_i/(1+\theta_i)}. \tag{E.8}$$

In what follows we assume that the concentration of B which appears in Eqs. E.7 and E.8 via the Damkohler numbers is a constant with respect to temperature.

From Eq. E.7 the slope of the heat generation function in the fast bulk reaction region is

$$Q_2 = (B_S + B_R)\, D_a \frac{(\gamma - \eta)}{(1 + \theta)^2} e^{(\gamma-\eta)\theta/(1+\theta)} \quad .$$

But for the uniqueness condition we need $Q_2$ evaluated at the steady state temperature so the above can be simplified by substituting the steady state equation, Eq. 4.4, for this region obtaining

$$Q_2 = \frac{(\gamma - \eta)}{(1 + \theta)^2} \{ (1 + H)\, \theta - H\, \theta_c \} \quad .$$

Thus our first uniqueness condition is $Q_1 > Q_2$ or

$$(1 + H) > \frac{(\gamma - \eta)}{(1 + \theta)^2} \{ (1 + H)\, \theta - H\, \theta_c \} \tag{E.9}$$

for all possible steady state temperatures. This is not a very useful

result inasmuch as it contains the steady state temperature. We can remove this temperature using the bounds on $\theta$ but at the expense of obtaining a weaker condition which still guarantees uniqueness but its converse does not guarantee multiplicity. Substituting $\theta_{ub}$ from Eq. E.3 into the numerator and $\theta_{\ell b}$ from Eq. E.5 into the demoninator yields an upper bound for $Q_2$, viz.,

$$Q_2 \leq \frac{(\gamma - \eta)\,(B_S + B_R)\,\beta}{\left\{1 + \left(\frac{H}{1+H}\right)\theta_c + \frac{B_S\,\beta\,e^{-\eta}}{(1+H)}\right\}^2} \quad . \tag{E.10}$$

Thus uniqueness is guaranteed for the first s-shaped region if

$$(1 + H) > \frac{(\gamma - \eta)\,(B_S + B_R)\,\beta}{\left\{1 + \left(\frac{H}{1+H}\right)\theta_c + \frac{B_S\,\beta\,e^{-\eta}}{(1+H)}\right\}^2} \tag{E.11}$$

where we have used $Q_1$ and $Q_2$ from Eq. E.6 and E.10. Thus if $\eta \geq \gamma$, i.e. $H_S \geq E$, uniqueness is guaranteed. This is the result anticipated in Chapter Four, Eq. 4.11. More generally Eq. E.11 is stronger than the corresponding results of previous authors, Eqs. 2.1 and 2.2, and is capable of dividing the seven-dimensional parameter space into an uniqueness region and a region of possible multiplicity (for a reactor without enhancement).

The slope of the heat generation function in the enhanced mass transfer region is more difficult to calculate because it depends on the interfacial temperature, $\theta_i$. Thus we need to know how $\theta_i$ varies with $\theta$. From Table 3.2 the equation for $\theta_i$ in the enhanced mass transfer region is

$$\theta_i = \theta + (B_S + B_R)\sqrt{\frac{D}{\alpha}}\sqrt{D_{ai}}\;e^{\frac{1}{2}(\gamma-2\eta)\theta_i/(1+\theta_i)} \quad .$$

Differentiating the above with respect to $\theta$ and solving the resulting

algebraic equation for $d\theta_i/d\theta$ obtains

$$\frac{d\theta_i}{d\theta} = \frac{1}{1 - \{ (B_S + B_R) \sqrt{\frac{D}{\alpha}} \sqrt{D_{ai}} \frac{1}{2} \frac{(\gamma - 2\eta)}{(1 + \theta_i)^2} e^{\frac{1}{2}(\gamma-2\eta)\theta_i/(1+\theta_i)} \}}$$

$$\equiv \frac{1}{1 - W} \quad . \tag{E.12}$$

It appears possible that W may be equal to or greater than one for large $\gamma$ and hence that the derivative may become infinite. This suggests that multiple solutions are possible for the interfacial temperature and that when $d\theta_i/d\theta$ becomes infinite we are at an ignition point. This possibility needs to be investigated and should be a future research topic. The slope of Eq. E.8 is then

$$Q_2 = \beta \sqrt{\frac{\alpha}{D}} \frac{W}{1 - W}$$

where W is the quantity in brackets in Eq. E.12. Substituting the steady state equation for this region, Eq. 4.4, gives

$$Q_2 = \beta \sqrt{\frac{\alpha}{D}} \frac{W_2}{1 - W_2} \tag{E.13}$$

where

$$W_2 = \frac{1}{\beta} \sqrt{\frac{D}{\alpha}} \frac{1}{2} \frac{(\gamma - 2\eta)}{(1 + \theta_i)^2} \{ (1 + H) \theta - H \theta_c \} . \tag{E.14}$$

Thus the uniqueness condition for the second s-shaped region (i.e. enhanced mass transfer) is

$$(1 + H) > \beta \sqrt{\frac{\alpha}{D}} \frac{W_2}{1 - W_2} \tag{E.15}$$

for all possible steady state temperatures. As before this is not very useful due to the temperature dependence of $W_2$. We remove this dependence using the bounds on $\theta$ and derive a more practical, but weaker, condition. If $2\eta \geq \gamma$ (i.e. $2H_S \geq E$) then $Q_2 \leq 0$ and uniqueness is

guaranteed. Otherwise $Q_2$ is positive and $(1 - W_2) > 0$. Then $Q_2$ is maximum when $W_2$ is a maximum and this occurs when $\theta$ in the numerator of Eq. E.14 is replaced by $\theta_{ub}$ from Eq. E.2 and $\theta_i$ in the denominator is replaced by its minimum $\theta_{\ell b}$ from Eq. E.5. Thus we have

$$W_2 \leq W_3 = \sqrt{\frac{D}{\alpha}}\ \frac{1}{2S}\ \frac{(\gamma - 2\eta)\ (B_S + B_R)}{\left\{ 1 + \left( \frac{H}{1 + H} \right) \theta_c + \frac{B_S\ \beta\ e^{-\eta}}{(1 + H)} \right\}^2} \tag{E.16}$$

and

$$Q_2 \leq \beta \sqrt{\frac{\alpha}{D}}\ \frac{W_3}{1 - W_3}\ . \tag{E.17}$$

The uniqueness condition for the second s-shaped curve then becomes

$$(1 + H) > \beta \sqrt{\frac{\alpha}{D}}\ \frac{W_3}{1 - W_3}\ . \tag{E.18}$$

This result divides the nine-dimensional parameter space into regions of uniqueness and possible multiplicity.

Together the results, Eq. E.11 and Eq. E.18, divide the parameter space into three regions: an uniqueness region, a region of up to three steady states, and a region of up to five steady states. The intersection of the uniqueness region for each condition yields the uniqueness region for the gas-liquid reactor. The intersection of the multiplicity region for each condition gives a region with the possibility of five steady states. The remaining regions are the intersection of the uniqueness region of one condition with the multiplicity region of the other. Hence these regions have the possibility of three steady states.

To illustrate this we simplify the conditions given by Eqs. E.11 and E.18 by assuming that $d\theta_i/d\theta = 1$ and that $\theta_c \leq 0$. Then the first condition, Eq. E.11, can be simplified, viz.,

$$(1 + H) > (\gamma - \eta)\ (B_S + B_R)\ \beta\ . \tag{E.19}$$

The second condition, Eq. E.18, becomes

$$(1 + H) > \beta \sqrt{\alpha/D}\ W$$

or

$$(1 + H) > 1/2S\ (\gamma - 2\eta)\ (B_S + B_R)\ \beta\ . \tag{E.20}$$

But inasmuch as $(\gamma - \eta) > (\gamma - 2\eta)$ we can write the last inequality as

$$2S(1 + H) > (\gamma - \eta)\ (B_S + B_R)\ \beta\ . \tag{E.21}$$

Because S is much less than one, Eq. E.19 is satisfied whenever Eq. E.21 is satisfied. Thus Eq. E.21 is an uniqueness condition for the reactor. In Figure E.1 the conditions given by Eqs. E.19 and E.21 are shown on a graph of $(\gamma - \eta)/(1 + H)$ versus $\beta(B_S + B_R)$. In region A, Eq. E.21 is satisfied so this is an uniqueness region. In region B only Eq. E.19 holds thus three steady states are possible due to enhanced mass transfer. Up to five steady states are possible in region C where neither condition is satisfied.

Each of the conditions, Eqs. E.11 and E.18, also yields a very simple condition for $\eta$ and $\gamma$, viz.,

$$\eta \geq \gamma \quad \text{and} \quad 2\eta \geq \gamma\ .$$

Thus uniqueness is guaranteed for the gas-liquid reactor if

$$\eta \geq \gamma$$

or

$$H_S \geq E\ . \tag{E.22}$$

That is, the condition $2\eta \geq \gamma$ is sufficient to guarantee uniqueness only for the second s-shaped region. This is the result obtained by Raghuram and Shah (1977), Eq. 2.2, using a reactor model which is only applicable to the enhanced mass transfer region.

In summary we have two strong conditions, Eq. E.9 and Eq. E.15. If both are satisfied for all possible values of the steady state temperature

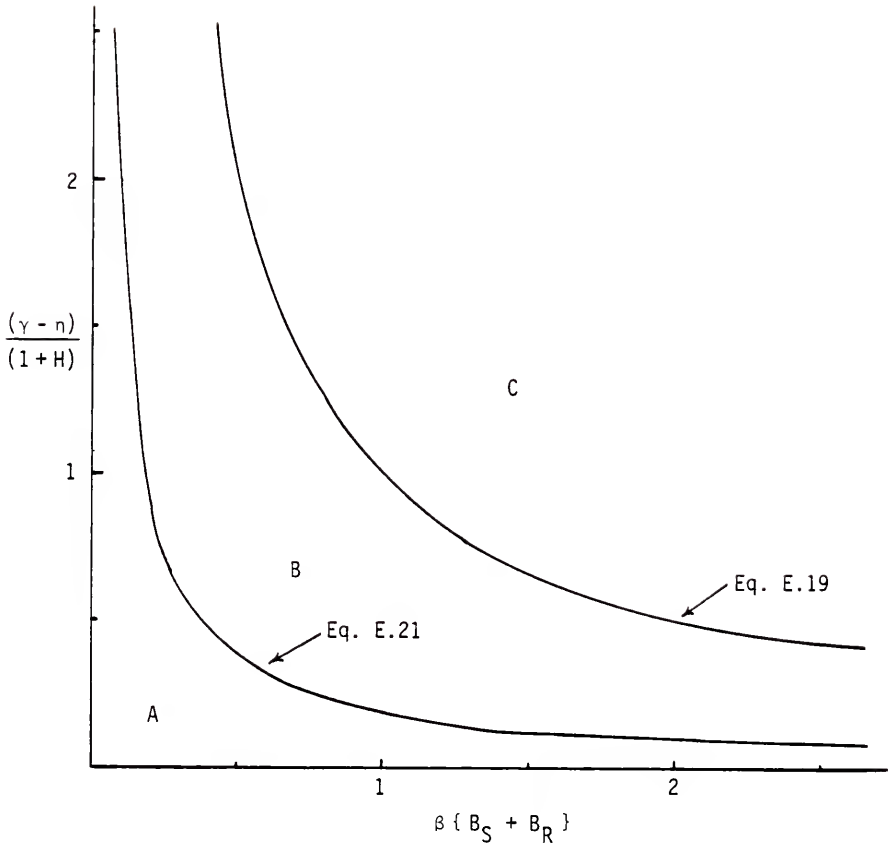


Figure E.1. An uniqueness condition for a gas-liquid CSTR; S = 0.1.

A. uniqueness
B. up to three steady states
C. up to five steady states

in the corresponding region then multiple solutions exist; three solutions exist if only one fails and five if both fail. Stated this way, these conditions require the solution to the steady state temperature equation, hence more practical but weaker conditions are found and are given by Eq. E.11 and Eq. E.18. These depend only on the reactor parameters not the steady state temperature. If both are satisfied, uniqueness is guaranteed. But if one or both fail, multiple solutions are possible but not guaranteed.

## APPENDIX F
## THE APPLICATION OF POORE'S METHOD FOR DETERMINING MULTIPLICITY TO A GAS-LIQUID CSTR

Poore (1973) introduces a nice way of viewing the uniqueness/ multiplicity question in his investigation of the single-phase CSTR. In our two-phase CSTR we can not write the steady state equation in the form he writes his if we try to do the problem in its full generality. But we can apply his idea to the first s-shaped region, i.e. the first three operating regions of our model. Here we know that the maximum number of steady states is three, a result that we will rediscover, which is the result for a single-phase CSTR that allows Poore to obtain explicit results from this analysis. For the first s-shaped region $\phi$ equals one, $f_i$ equals zero and $\theta_i$ equals $\theta$. If we also assume that the concentration of B is a constant at its feed value and that the heat of solution is negligible compared to the heat of reaction, the steady state equations, Eqs. 4.2 and 4.4, become

$$x_A = \frac{\beta\, e^{-n\theta/(1+\theta)}}{\{\, 1 + \beta + D_a\, e^{\gamma\theta/(1+\theta)} \,\}} \tag{F.1}$$

and

$$\{\, (1 + H)\theta - H\theta_c \,\} = \frac{D_a\, B_R\, \beta\, e^{(\gamma-n)\theta/(1+\theta)}}{\{\, 1 + \beta + D_a\, e^{\gamma\theta/(1+\theta)} \,\}} \tag{F.2}$$

where the dimensionless parameters H, $\beta$, and $D_a$ have been used in lieu of the characteristic times. Like Poore we make the approximation

$$e^{\sigma\theta/(1+\theta)} = e^{\sigma\theta} \ .$$

This is the so-called Frank-Kamenetskii approximation and is reasonable whenever $\theta$ is small as compared to one, see Appendix G. This approximation simplifies the temperature dependence of the rate constant and is surprisingly useful in the investigation of reacting systems where functions such as $\tau k/(1+\tau k)$ arise. Such functions can be approximated, using the Frank-Kamenetskii approximation to k, accurately over a range of $\theta$ wider than that suggested above, see Appendix G.

It is instrumental to rewrite Eq. F.2 so that $D_a$, the Damkohler number, can be thought of as a function of the steady state temperature, viz.,

$$D_a = \frac{\{ (1 + H)\theta - H\theta_c \} (1 + \beta) e^{-\gamma\theta}}{\{ B_R \beta e^{-\eta\theta} - \{ (1 + H)\theta - H\theta_c \} \}} \equiv g(\theta) . \qquad (F.3)$$

Thus for each value of $D_a$ the solutions to $D_a = g(\theta)$ are the corresponding steady state temperatures. The steady state temperatures are bounded, see Appendix E and Eqs. E.1 and E.5,

$$\left( \frac{H}{1 + H} \right)\theta_c \equiv \theta_{\ell b} \leq \theta \leq \theta_{ub} \equiv \left( \frac{H}{1 + H} \right)\theta_c + \frac{B_R \beta e^{-\eta\theta_{ub}}}{(1 + H)} \qquad (F.4)$$

and on the interval $(\theta_{\ell b} , \theta_{ub})$, $g(\theta)$ is positive and varies from zero to infinity. Thus if g is strictly monotonic then for each positive value of the Damkohler number there exists an unique solution of Eq. F.3 and therefore from Eqs. F.1 and F.2 an unique steady state, cf. Figure F.1. If g is not monotone it must have an even number, n, of turning points, i.e. zeros of the derivative, and there must be values of the Damkohler number such that more than one solution of Eq. F.3 exists, the maximum number being (n+1), cf. Figure F.1.

This is how Poore (1973) tells us to look at the problem. Arrange the steady state equations such that a certain parameter, here $D_a$, is

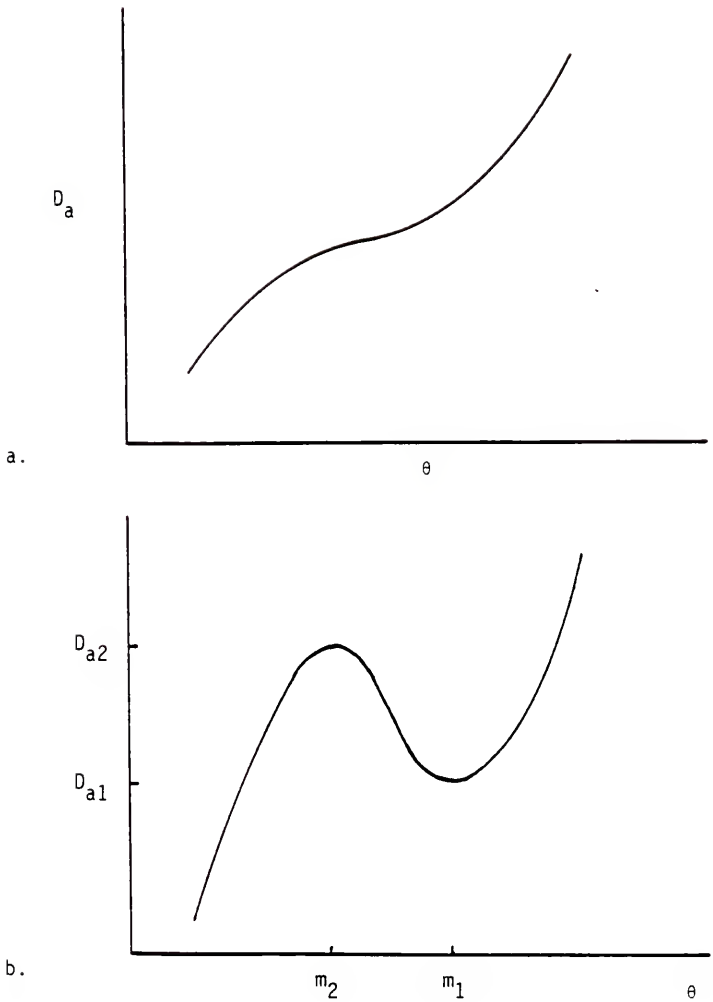


Figure F.1. $D_a = g(\theta)$ versus $\theta$.

a. Uniqueness b. Multiplicity

explicitly a function of one state variable, here $\theta$, with the other parameters being held constant. Then the variation of this function answers the uniqueness/multiplicity question with respect to the parameter singled out. Assuming the range of the function and the allowable values of the parameter coincide, if the function is strictly monotonic on its domain then exactly one value of the state variable exists for each value of the parameter. Otherwise for certain values of the parameter more than one value of the state variable must exist. This is illustrated in Figure F.1 where the Damkohler number, viz. $g(\theta)$, is shown versus temperature from Eq. F.3 on the domain of g given by Eq. F.4. Because $g(\theta)$ varies from zero to infinity, the function g must have an even number of turning points, i.e. points where $dg/d\theta = 0$. If the value of $D_a$ falls between the values of g at these points, viz. $D_{a1}$ and $D_{a2}$, then multiple solutions to $D_a = g(\theta)$, and hence the reactor equations, exist. It follows that if we can find conditions on the parameters remaining in g which make g monotone then these conditions are uniqueness conditions. Thus we investigate the zeros of the derivative of the function g in Eq. F.3.

Differentiating Eq. F.3 with respect to $\theta$ obtains

$$\frac{dD_a}{d\theta} = \frac{(1 + \beta)\, e^{-\gamma\theta}}{\{ B_R\, \beta\, e^{-\eta\theta} - \{ (1 + H)\theta - H\theta_c \} \}^2} \cdot$$

$$\{ \gamma \{ (1 + H)\theta - H\theta_c \}^2 + B_R\, \beta\, e^{-\eta\theta} \{ (1 + H) - (\gamma - \eta) \cdot$$

$$\{ (1 + H)\theta - H\theta_c \} \} \} . \qquad \text{(F.5)}$$

The turning points of g are the zeros of this or the solutions of

$$\{ (1 + H)\theta - H\theta_c \}^2 + \frac{B_R \beta}{\gamma} e^{-\eta\theta} \{ (1 + H) - (\gamma - \eta) \cdot$$

$$\{ (1 + H)\theta - H\theta_c \} \} = 0 . \qquad \text{(F.6)}$$

If $\eta \geq \gamma$ then no solutions exist on the domain of g, Eq. F.4, and g is monotone there. Thus the first uniqueness condition is

$$\eta \geq \gamma \quad \text{or} \quad H_S \geq E \ . \tag{F.7}$$

If $\gamma > \eta$ we observe that $dD_a/d\theta > 0$ for all $\theta > \theta_{ub}$ and $\theta < \theta_{\ell b}$. Thus the real solutions of Eq. F.6 lie in the domain of g: $\theta \in (\theta_{\ell b}, \theta_{ub})$.

We can show that Eq. F.6 has at most two solutions by rewriting the equation and graphing the result. If we let

$$\psi \equiv (1 + H)\theta - H\theta_c$$

where

$$0 \leq \psi \leq B_R\beta$$

then Eq. F.6 can be rewritten as

$$L(\psi) \equiv \psi^2 \, e^{\psi\eta/(1+H)} = -\left( \frac{B_R\beta}{\gamma} e^{-\eta H\theta_c/(1+H)} \right) \cdot$$

$$\{ (1 + H) - (\gamma - \eta)\psi \} \equiv R(\psi) \ . \tag{F.8}$$

The left-hand side L is an increasing function of $\psi$ and the right-hand side R is a straight line with a negative intercept and a positive slope (because for $\eta \geq \gamma$ we already know that uniqueness is guaranteed and hence that Eq. F.8 has no solutions), cf. Figure F.2. From the figure we can see that at most two intersections are possible and hence two critical points for $D_a = g(\theta)$.

We can also derive an uniqueness condition using Eq. F.8 and Figure F.2. When R and L have no points of intersection for $\psi > 0$ then Eq. F.8 has no solution, hence g is monotone and uniqueness is guaranteed. There is only one value of $\psi$ such that L and R are tangent (this will be shown) and if $R < L$ at this point then there can be no intersection, and if $R > L$ at this point then there are two solutions. The tangent point, $\psi_t$, is the solution of a quadratic equation obtained by

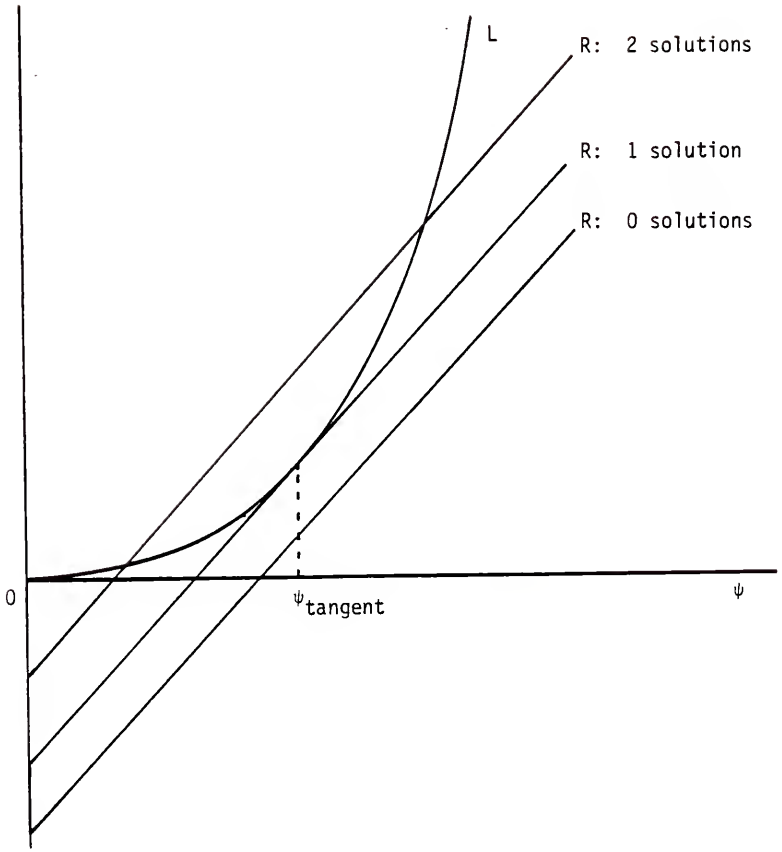


Figure F.2. The left and right sides of Equation F.8.

substituting Eq. F.8 into L' = R' and is given by

$$\psi_t = \frac{-(\gamma - 2\eta) + \sqrt{\gamma^2 + 4\eta\gamma - 4\eta^2}}{2\eta\ (\gamma - \eta)/(1 + H)} \tag{F.9}$$

where the second solution to the quadratic equation is always negative and hence outside our domain. Thus if

$$R(\psi_t) < L(\psi_t) \tag{F.10}$$

then uniqueness is guaranteed for all values of $D_a$. This is a strong condition because it is independent of the steady state solution but it is complicated. Simpler, but weaker, results can be obtained from this. For example, L is always positive so if $R \leq 0$ at an upper bound for $\psi$ then uniqueness is guaranteed. Because $\psi \leq B_R\beta$ we have the uniqueness condition given by

$$B_R\beta(\gamma - \eta) \leq (1 + H)\ . \tag{F.11}$$

To characterize the remaining region of parameter space, i.e. when Eq. F.10 is not satisfied, we must find the zeros of the derivative of $D_a = g(\theta)$. If we call these points $m_1$ and $m_2$ and define

$$D_{a1} = g(m_1) \quad \text{and} \quad D_{a2} = g(m_2) \tag{F.12}$$

then we have uniqueness when $D_a > D_{a2}$ or $D_a < D_{a1}$, two steady states when $D_a$ equals $D_{a1}$ or $D_{a2}$, and three steady states when $D_{a1} < D_a < D_{a2}$, cf. Figure F.1b. Thus when the roots $m_1$ and $m_2$ are found from Eq. F.6, the uniqueness/multiplicity question is answered.

Because we can not solve Eq. F.6 explicitly for $m_1$ and $m_2$, we approximate the exponential for the solubility with a Taylor series, viz.,

$$e^{-\eta\theta} = 1 - \eta\theta + \frac{1}{2}(\eta\theta)^2 - \ldots\ ,$$

substitute this into Eq. F.6 and neglect all terms of order $\theta^3$ and higher. This yields a quadratic equation for the critical points, viz.,

$$\theta^2 \{ (1 + H)(1 + H + B_R\beta\eta) - \frac{1}{2}\frac{B_R\beta\eta^2}{\gamma} \{ (1 + H) - H\theta_c(\gamma - \eta) \} \}$$

$$-\theta \{ B_R\beta(1 + H) + H\theta_c \{ 2(1 + H) + (\gamma - \eta)\frac{B_R\beta\eta}{\gamma} \} \}$$

$$+ (1 + H)\frac{B_R\beta}{\gamma} + H\theta_c \{ H\theta_c + (\gamma - \eta)\frac{B_R\beta}{\gamma} \}$$

$$= 0 . \qquad \text{(F.13)}$$

This will give a reasonable approximation to the roots whenever $\eta\theta << 1$. In fact, even if $\eta$ is large the above may be accurate because as $\eta$ increases, $\theta$ decreases as we can see from the bounds on $\theta$, cf. Eq. F.4. In particular for $\theta_c = 0$ the upper bound for $\theta$ satisfies

$$\theta_{ub} = \frac{B_R\beta}{(1 + H)} e^{-\eta\theta_{ub}}$$

whence as $\eta$ increases, $\theta_{ub}$ decreases which suggests that our approximation might yield useful results. If it does not we must solve Eq. F.6 for the values of $m_1$ and $m_2$.

The roots of Eq. F.13 are

$$m_1, m_2 = \frac{-b_o \pm \sqrt{b_o^2 - 4a_oc_o}}{2a_o} \qquad \text{(F.14)}$$

where $a_o$, $b_o$ and $c_o$ are the coefficients in Eq. F.13, written as

$$a_o\theta^2 + b_o\theta + c_o = 0 .$$

$D_a$ is monotone if and only if $m_1$ and $m_2$ are not real, hence the uniqueness condition for all $D_a$ is

$$b_o^2 < 4a_oc_o \qquad \text{(F.15)}$$

This is a condition on the remaining parameters only and corresponds to the condition, Eq. F.10, for the full equation for $m_1$ and $m_2$. Otherwise if $m_1$ and $m_2$ are real, we have the conditions, cf. Figure F.1:

1. if $D_{a1} < D_a < D_{a2}$
   then three steady states exist

where $D_{a1}$ and $D_{a2}$ are given by Eq. F.12,

2. if $D_a = D_{a1}$ or $D_a = D_{a2}$
   then two steady states exist,

3. if $D_a > D_{a2}$ or $D_a < D_{a1}$
   then uniqueness is guaranteed.

Thus for any assigned values of the parameters $\gamma$, $n$, $B_R$, $\beta$, H and $\theta_c$, we find $a_o$, $b_o$ and $c_o$ and decide first if $m_1$ and $m_2$ are real. If not, we have uniqueness for all $D_a$. Otherwise we calculate $D_{a1}$ and $D_{a2}$ from Eq. F.12 and these define the uniqueness/multiplicity possibilities in terms of $D_a$.

For example, if $\theta_c = 0$, i.e. $T_c = T_f$, then Eq. F.14 becomes

$$m_1, m_2 = \left(\frac{1}{\gamma}\right) \frac{\left[1 \pm \sqrt{2\left(\frac{n}{\gamma}\right)^2 - 4\left(\frac{n}{\gamma}\right) - \frac{4(1+H)}{\gamma B_R \beta} + 1}\right]}{\left[-\left(\frac{n}{\gamma}\right)^2 + 2\left(\frac{n}{\gamma}\right) + \frac{2(1+H)}{\gamma B_R \beta}\right]} \qquad (F.16)$$

whence $m_1$ and $m_2$ are not real if

$$\left(\frac{n}{\gamma}\right)_2 \leq \left(\frac{n}{\gamma}\right) \leq \left(\frac{n}{\gamma}\right)_1 \qquad (F.17)$$

where

$$\left(\frac{n}{\gamma}\right)_{1,2} \equiv 1 \pm \sqrt{\frac{1}{2} + \frac{2(1+H)}{\gamma B_R \beta}} \quad . \qquad (F.18)$$

Eq. F.17 is then an uniqueness condition. Because $(n/\gamma)_1 \geq 1$ and we already know that $(n/\gamma) \geq 1$ is sufficient for uniqueness from Eq. F.7, we conclude that uniqueness is guaranteed for all $D_a$ if and only if

$$\left(\frac{n}{\gamma}\right) \geq \left(\frac{n}{\gamma}\right)_2 \equiv 1 - \sqrt{\frac{1}{2} + \frac{2(1+H)}{\gamma B_R \beta}} \quad . \qquad (F.19)$$

Conversely, whenever the above is not true, multiple solutions must exist for $D_a$ in the closed interval $(D_{a1}, D_{a2})$, but outside this interval we have uniqueness. This accounts for all of the parameter space.

Two simple conclusions can be drawn from Eq. F.19. We observe that $(\eta/\gamma)_2$ is negative if $\gamma B_R \beta/(1 + H)$ is less than four and that $(\eta/\gamma)_2$ has a maximum of $1 - \sqrt{1/2} = 0.293$. This yields two simple uniqueness conditions, viz.,

$$\gamma B_R \beta \leq 4(1 + H) \tag{F.20}$$

and

$$\left( \frac{\eta}{\gamma} \right) \geq 0.293 \ . \tag{F.21}$$

We summarize the uniqueness and multiplicity conditions in Table F.1 and conclude with the caveat that these results are for the unenhanced regime with B in excess, i.e. the first s-shaped region of the heat generation function.

The second s-shaped region of the heat generation function, which likewise admits the possibility of up to three solutions, is described by Eq. 4.4 when bulk reaction has gone to completion, viz.,

$$\{ (1 + H)\theta - H\theta_c \} = \beta(B_S + B_R)\phi x_i \ . \tag{F.22}$$

Here $\phi x_i$ gives the characteristic s shape to the heat generation function. To use Poore's (1973) idea here we must rearrange Eq. F.22 so that some parameter is equal to a function of $\theta$ and the remaining parameters. The Damkohler number, $D_a$, is the natural parameter to choose because we can bound $\theta$ independent of $D_a$ and hence $g(\theta_{\ell b})$ and $g(\theta_{ub})$ are independent of $D_a$. This can not be done with H, $\theta_c$, $\beta$, $B_S$ or $B_R$. But here $D_a$ appears in the energy balance only through $\phi$ and $\phi$ becomes independent of $D_a$ in the instantaneous reaction region.

Even if we find a parameter such that we can put Eq. F.22 into Poore's form and bound $\theta$ independent of this parameter, one major problem remains. We must be able to differentiate the enhancement factor but $\phi$ is only piecewise differentiable. An alternative which is

TABLE F.1
UNIQUENESS AND MULTIPLICITY CONDITIONS FOR A NONADIABATIC, UNENHANCED GAS-LIQUID CSTR WITH B IN EXCESS

Uniqueness Conditions:

1. If $R(\psi_t) < L(\psi_t)$ Eq. F.10

   then uniqueness is guaranteed for all $D_a$,

   where R and L are defined in Eq. F.8

   and $\psi_t$ is defined by Eq. F.9.

   Approximations to this and simplifications which insure the above are:

   a. $b_o^2 < 4a_oc_o$ Eq. F.15

   b. $B_R\beta(\gamma - \eta) \leq (1 + H)$ Eq. F.11

   c. for $\theta_c = 0$, $\left(\frac{\eta}{\gamma}\right) \geq \left(\frac{\eta}{\gamma}\right)_2$ Eq. F.19

   or $\left(\frac{\eta}{\gamma}\right) \geq 0.293$ Eq. F.21

   or $\gamma B_R\beta \leq 4(1 + H)$ Eq. F.20

2. Otherwise, if Eq. F.10 is not satisfied, uniqueness is guaranteed if

   a. $D_a > D_{a2} = g(m_2)$

   b. $D_a < D_{a1} = g(m_1)$

   where $m_1$ and $m_2$ are the solutions of Eq. F.6

   and g is given in Eq. F.3.

TABLE F.1--continued

Multiplicity Conditions:

1. If Eq. F.10 is not satisfied and if

   a. $D_a = D_{a1}$ or $D_{a2}$
      then two steady states exist,

   b. $D_{a1} < D_a < D_{a2}$
      then three steady states exist.

differentiable, based on the van Krevelen-Hoftijzer correction, is little better due to its complexity. Thus we can not see how to adopt Poore's idea to the enhanced mass transfer model.

## APPENDIX G
## THE FRANK-KAMENETSKII APPROXIMATION

In chemical kinetics calculations involving the temperature dependence of the rate constant can be simplified by using an approximation discovered by Frank-Kamenetskii, see Frank-Kamenetskii (1969). This approximation and where it is useful will be discussed in this appendix.

The Arrhenius temperature dependence of the rate constant is described by

$$e^{-E/RT} \quad . \tag{G.1}$$

By defining a reference temperature $T_r$, we make the above dimensionless, viz.,

$$e^{-E/RT} = e^{-\gamma/(1+\theta)} \tag{G.2}$$

where

$$\gamma \equiv E/RT_r$$

and

$$\theta \equiv (T - T_r)/T_r \quad .$$

The MacLauren expansion of the above exponent is

$$-\gamma/(1+\theta) = -\gamma\ (1 - \theta + \theta^2 - \theta^3 + \ . \ . \ . \ )$$

which is absolutely convergent for $|\theta| < 1$. Thus for small $\theta$, i.e. $\theta << 1$, we can neglect all but the first two terms and obtain

$$e^{-E/RT} = e^{-\gamma}\ e^{+\gamma\theta} \quad . \tag{G.3}$$

This is the Frank-Kamenetskii approximation and, because it changes the temperature dependence of the rate constant from exponential in 1/T to exponential in T, it greatly simplifies analysis, especially

when derivatives of the rate constant must be found. But the above derivation indicates that the approximation is accurate only for $\theta << 1$, that is, for temperature near the reference temperature. Because of this one might anticipate that its usefulness is limited to systems with little temperature variation and that the choice of the reference temperature is critical. We will investigate this and the effect of the parameter $\gamma$ on the accuracy of the approximation.

First we calculate the error made by replacing the rate constant, k, with its approximation, $k_{FK}$, viz.,

$$E_r \equiv \frac{k - k_{FK}}{k} = 1 - e^{\gamma\theta^2/(1+\theta)} \quad . \tag{G.4}$$

Thus we observe that the approximation overestimates the rate constant, i.e. $k < k_{FK}$, except when $\theta = 0$. But more importantly we see that the error increases with increasing $\gamma$ and $|\theta|$. The fact that the error increases with $\gamma$ is very important because it is often stated that the approximation is most accurate for large $\gamma$, see Frank-Kamenetskii (1969), Uppal et al. (1974) and Huang and Varma (1981a). This false conclusion is obtained by first defining the reduced temperature as $\theta' = \gamma\theta$ whence the approximation becomes

$$e^{-E/RT} = e^{-\gamma}\, e^{\theta'/(1+\theta'/\gamma)}$$

$$\simeq e^{-\gamma}\, e^{\theta'} \quad .$$

It then follows that the approximation is most accurate for $\theta'/\gamma << 1$. Forgetting that $\theta'$ depends on $\gamma$, the false conclusion follows. But of course $\theta' = \gamma\theta$ and hence the inequality $\theta'/\gamma << 1$ is just $\theta << 1$, which is independent of $\gamma$. So as the error analysis shows the approximation is best for small $\gamma$, i.e. for small activation energies.

Using the data reported by Ding et al. (1974) we can calculate the error in using the Frank-Kamenetskii approximation for the rate constant.

The results in Table G.1 show that the error grows rapidly as the temperature deviates from $T_r$ and that the approximation is poor for $\theta > 0.1$.

We can also use this approximation for the exponential dependence of the solubility, viz.,

$$C_{Ai} = \frac{P_A}{H_o} e^{H_S/RT} \simeq \frac{P_A}{H_o} e^{\eta} e^{-\eta\theta}$$

and the resulting error is shown in Table G.1. Because $\eta < \gamma$ for this data, the Frank-Kamenetskii approximation is much better for the solubility than the rate constant, as anticipated by the error analysis.

We might conclude that the Frank-Kamenetskii approximation is of little use. But with a little foresight the results of most reactor analyses can be expressed as functions of k, which are much less sensitive to the approximation than is k itself. For example the heat generation function for a single-phase reactor is $\tau k/(1+\tau k)$ and so we are more interested in the error in approximating this function than in the error in approximating k. Let

$$g(k) = \frac{\tau k}{1 + \tau k}$$

then the error of interest is

$$E_r = \frac{g(k) - g(k_{FK})}{g(k)}$$

$$= 1 - \left( \frac{1 + \tau k}{1 + \tau k_{FK}} \right) \left( \frac{k_{FK}}{k} \right) .$$

For small $\theta$ we know that $k_{FK} \simeq k$ and hence the error goes to zero. For larger $\theta$ the approximation is poor for k but as k increases with $\theta$, $\tau k$ becomes much greater than one and the error goes to zero. Thus we anticipate the error for g should be small for small and large $\theta$, hence

TABLE G.1
ERROR DUE TO THE FRANK-KAMENETSKII APPROXIMATION --
PARAMETERS TAKEN FROM TABLE 4.4 WITH $T_r = T_f = 297°$

| T (°K) | θ | Rate Constant (%) $\frac{k - k_{FK}}{k}$ | Solubility (%) $\frac{C_{Ai} - C_{Ai_{FK}}}{C_{Ai}}$ | Heat Generation (%) $\frac{g - g_{FK}}{g}$ |
|---|---|---|---|---|
| 310 | .033 | 5.4 | 0.84 | 5.2 |
| 325 | .083 | 37. | 4.5 | 34. |
| 350 | .17 | 230 | 17. | 25. |
| 400 | .33 | $10^4$ | 47. | 0.2 |
| 450 | .50 | $10^6$ | 72. | 0.0 |

the approximation may be reasonable for all $\theta$. This is shown in the last column in Table G.1 where the error starts at zero, rises to a maximum of approximately 35 percent, then falls back to zero. Therefore we conclude that for some functions which appear in reactor analysis the Frank-Kamenetskii approximation is quite useful. Moreover we anticipate that the approximation will be useful for any function of k which is bounded for large k.

Inasmuch as we are interested in finding the steady state temperature, and we know from Chapters Three and Four that this temperature satisfies,

$$(1 + H)\theta - H\theta_c = \text{Heat Generation Function}$$

where the righthand side is a function of k and $C_{Ai}$, this last estimate for the error is the most significant to us. For example in a single-phase CSTR the heat generation function is g(k) given above, so the error in calculating $\theta$ using the Frank-Kamenetskii approximation is essentially the error shown. For our gas-liquid reactor the heat generation function depends on two functions of k and $C_{Ai}$: the rate of absorption, Eq. 4.5, and the total fraction of absorbed A that reacts, Eq. 4.6. The latter is bounded for large k so the approximation should be useful for this function. The rate of absorption is s-shaped in each of two regions; thus it is also bounded for large k. In the first region it is bounded when $\tau k >> 1$ as is the fraction that reacts and also the heat generation for a single-phase reactor, hence the error should be similar to that produced for those functions. The second region is the higher temperature region and the error might therefore be larger. But inasmuch as the function is bounded, the absolute error

can not remain large for a significant range of temperature. Also the approximation predicts the correct trends.

## APPENDIX H
## THE EXISTENCE OF MUSHROOMS AND ISOLAS IN A SINGLE-PHASE CSTR

The multiplicity patterns observed in single-phase CSTR's as a function of holding time are shown in Figure H.1. There are three basic types of multiplicity; s-shaped, mushroom and isola. Their existence has been established both experimentally and numerically, but little is known about conditions for their occurrence. Hlavacek et al. (1970) observed that isolas do not occur for $\theta_c \geq 0$ but not until Hlavacek and Van Rompay (1981) were any methods for establishing their existence known. Even then the result is a set of three simultaneous nonlinear equations, the solution of which is nontrivial. In particular explicit conditions written in terms of the parameters which imply existence or nonexistence are not found. But there are distinguishing characteristics for each multiplicity pattern which should be useful in deducing criteria for their existence.

A simple observation of this kind is that the various multiplicity patterns can be distinguished by the corresponding number of ignition and extinction points. An ignition point is a point on the graph of $\theta$ versus $\tau$ where an increase (or decrease) of the holding time (or whatever parameter is being studied) causes the steady state temperature to jump up or ignite to a higher temperature (see Figure H.1a-b, the points labelled I). An extinction point is similar except that the temperature jumps down to a lower value (see Figure H.1a-c, the points labelled E). An s-shaped multiplicity has one of each, mushrooms two of each, and isolas have two extinction points but no ignition point. The

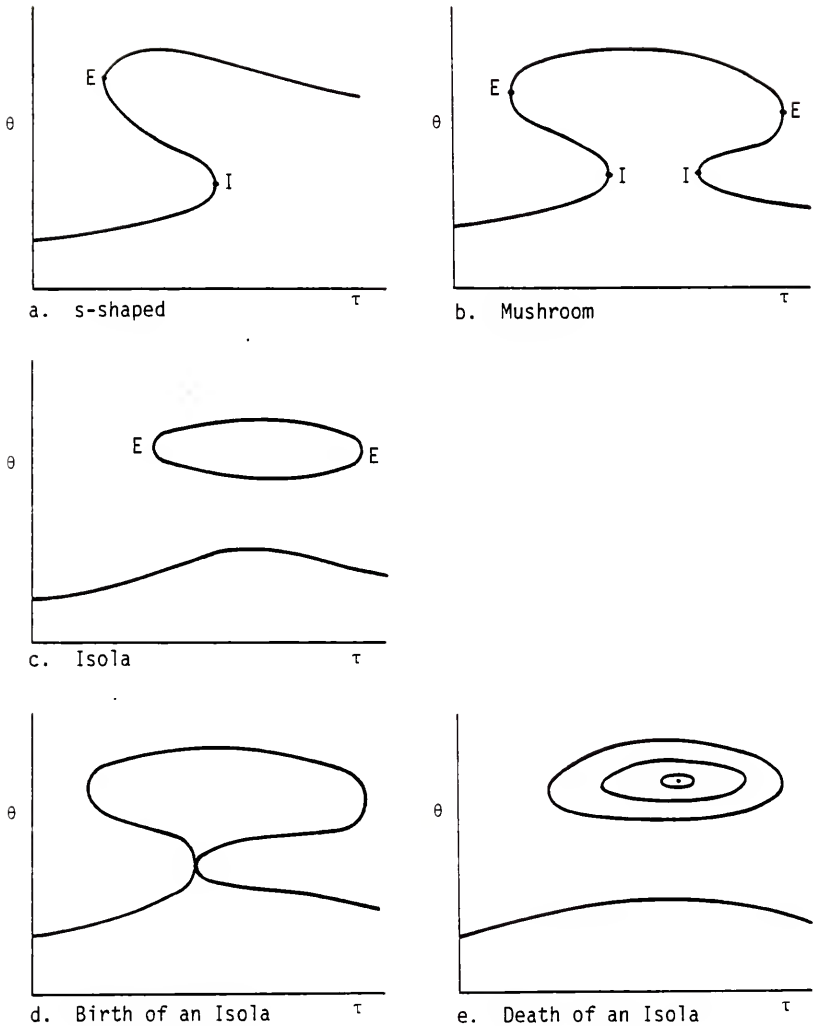


Figure H.1. Multiplicity patterns for a single-phase CSTR.

I = Ignition point, E = Extinction point

patterns also have other distinguishing characteristics. The slope of $\theta$ versus $\tau$ has one zero for an s-shaped pattern or a mushroom and two or three zeros for an isola. The slope becomes infinite twice for an s-shaped pattern or an isola and four times for a mushroom, which is an observation closely related to the number of ignition and extinction points. We can use such observations to identify the regions in parameter space where each behavior pattern is exhibited. Specifically the birth and death of an isola for a single-phase CSTR will be investigated here.

Because an isola can be distinguished by the number of zeros of the slope, $d\theta/d\tau$, this function must be found. The steady state model for a single-phase CSTR is

$$0 = q(C_f - C) - Vk_1C$$

$$0 = q\rho C_p(T_f - T) - US_c(T - T_c) + H_R Vk_1 C \ . \qquad (H.1)$$

Eliminating the concentration and using dimensionless variables where possible, obtains an equation for $\theta$, the steady state temperature, viz.,

$$\psi \equiv \theta + H_1\tau(\theta - \theta_c) + \tau k_f \, e^{\gamma\theta/(1+\theta)} \{ \theta + H_1\tau(\theta - \theta_c) - B \} = 0 \qquad (H.2)$$

where the function is designated $\psi$ and

$$\theta \equiv \frac{T - T_f}{T_f} \qquad \theta_c \equiv \frac{T_c - T_f}{T_f} \qquad k_1 = k_o \, e^{-E/RT}$$

$$B \equiv \frac{H_R \, C_f}{\rho \, C_p \, T_f} \qquad k_f = k_o \, e^{-\gamma} \ (\text{sec}^{-1}) \qquad \gamma \equiv \frac{E}{R \, T_f}$$

$$\tau = \frac{V}{q} \ (\text{sec}) \qquad H_1 = \frac{U \, S_c}{V \, \rho \, C_p} \ (\text{sec}^{-1}) \ .$$

Because the steady state values of $\theta$ corresponding to each value of $\tau$ for fixed values of $H_1$, $k_f$, $\theta_c$, $\gamma$ and B satisfy

$$\psi(\theta,\tau;\ H_1,\ k_f,\ \theta_c,\ \gamma,\ B) = 0$$

we conclude that

$$\frac{d\theta}{d\tau} = -\left(\frac{\partial\psi/\partial\tau}{\partial\psi/\partial\theta}\right) \tag{H.3}$$

where

$$\frac{\partial\psi}{\partial\tau} = H_1(\theta - \theta_c) + k_f\, e^{\gamma\theta/(1+\theta)}\ \{\ \theta + 2H_1\tau(\theta - \theta_c) - B\ \} \tag{H.4}$$

and

$$\frac{\partial\psi}{\partial\theta} = 1 + H_1 + \tau k_f\, e^{\gamma\theta/(1+\theta)}\ \{\ (1 + H_1\tau) + \gamma/(1+\theta)^2\ \{\ \theta + H_1\tau(\theta - \theta_c) - B\ \}\ \}\ . \tag{H.5}$$

Evidently $d\theta/d\tau$ vanishes when either

$$\frac{\partial\psi}{\partial\tau} = 0 \quad \text{or} \quad \frac{\partial\psi}{\partial\theta} \to \infty\ .$$

However $\partial\psi/\partial\theta$ remains finite for physically admissible values of $\theta$ and $\tau$, viz.,

$$\left(\frac{H_1\tau}{1 + H_1\tau}\right)\theta_c < \theta < B \quad \text{and} \quad 0 < \tau < \infty$$

where B is the maximum temperature rise for an adiabatic reactor. It follows therefore, that $d\theta/d\tau$ vanishes if and only if $\partial\psi/\partial\tau$ vanishes and hence that the number of solutions $(\theta,\tau)$ of

$$\psi(\theta,\tau) = 0 \tag{H.2}$$

and

$$\frac{\partial\psi(\theta,\tau)}{\partial\tau} = 0 \tag{H.6}$$

can be used to determine when isolas exist. One solution implies an s or a mushroom whereas three solutions imply an isola, cf. Figure H.1. The transition from one to three solutions and from three to one solution signals the birth and death of the isola, cf. Figure H.1 d and e.

We investigate the number of solutions of Eqs. H.2 and H.6 by eliminating the holding time $\tau$ and examining the resulting equation for $\theta$. We do this because Eq. H.4 is linear in $\tau$ and Eq. H.2 is quadratic, whereas their dependence on $\theta$ is complicated. But even before performing this analysis, the adiabatic result can be obtained. If the heat transfer coefficient vanishes then $H_1 = 0$ and if this is substituted into the slope equation, Eq. H.6, only one solution is possible, $\theta = B$ and $\tau = \infty$. But this is outside the admissible range, thus isolas are not possible in an adiabatic reactor. This agrees with experimental and numerical observations, see Hlavacek et al. (1970).

For a nonadiabatic reactor, viz. $H_1 > 0$, solving the Equations H.2 and H.6 for $\tau$ obtains

$$\tau = \frac{B - \theta}{2H_1(\theta - \theta_c)} - \frac{1}{2k_f e^{\gamma\theta/(1+\theta)}} \tag{H.7}$$

and

$$\tau^2 = \frac{\theta}{H_1(\theta - \theta_c)} \left( \frac{1}{k_f e^{\gamma\theta/(1+\theta)}} \right) . \tag{H.8}$$

As a preliminary step we can eliminate the kinetics which results in a quadratic for $\tau$, viz.,

$$H_1^2\tau^2(\theta - \theta_c)^2 + 2\theta H_1\tau(\theta - \theta_c) - \theta(B - \theta) = 0$$

or if $\chi \equiv H_1\tau(\theta - \theta_c)$ then

$$\chi^2 + 2\theta\chi - \theta(B - \theta) = 0 .$$

Therefore the solution is

$$\chi = -\theta \pm \sqrt{B\theta}$$

or

$$H_1\tau = \begin{cases} (\sqrt{B\theta} - \theta)/(\theta - \theta_c) & \text{if } \theta > \theta_c \\ (\sqrt{B\theta} + \theta)/(\theta - \theta_c) & \text{if } \theta < \theta_c \end{cases} \tag{H.9}$$

whence for each temperature there exists one holding time and we conclude that eliminating $\tau$ does not create or destroy solutions.

Thus we may proceed to eliminate $\tau$ in favor of $\theta$ and deduce an equation for $\theta$ such that $\psi = \partial\psi/\partial\tau = 0$. Eliminating $\tau$ in Eqs. H.7 and H.8 and rearranging obtains a quadratic equation in the group $\Omega$, viz.,

$$\Omega^2 + 2\sqrt{\theta}\,\Omega - (B - \theta) = 0$$

where

$$\Omega \equiv \left( \frac{H_1(\theta - \theta_c)}{k_f\, e^{\gamma\theta/(1+\theta)}} \right)^{\frac{1}{2}} \tag{H.10}$$

whence the solution is

$$\Omega = -\sqrt{\theta} \pm \sqrt{B} \quad .$$

From the Equations H.7 and H.8, it is evident that no solution exists for $\theta \leq \theta_c$ or $\theta \leq 0$ or $\theta \geq B$ (otherwise $\tau$ is negative or not real) and thus that $\Omega$ must be positive, viz.,

$$\Omega = \frac{H_1\tau(\theta - \theta_c)}{\sqrt{\theta}} > 0$$

where the kinetics have been eliminated using Eq. H.8. Thus the only physically admissible value of $\Omega$ is

$$\Omega = \sqrt{B} - \sqrt{\theta}$$

and it follows that

$$\sqrt{\frac{H_1}{k_f}}\,\sqrt{\theta - \theta_c}\; e^{-\frac{1}{2}\gamma\theta/(1+\theta)} = \sqrt{B} - \sqrt{\theta} \quad . \tag{H.11}$$

The number of solutions to this equation will determine the type of multiplicity, three for isola and one for mushroom or s-shaped.

The solutions and the number of them can most easily be seen graphically. Letting $U = \sqrt{\theta}$ (which is real because $\theta > \max(0,\theta_c)$) the equation takes the more easily graphed form

$$L(U) \equiv \sqrt{\frac{H_1}{k_f}}\ \sqrt{U^2 - \theta_c}\ e^{-\frac{1}{2}\gamma U^2/(1+U^2)} = \sqrt{B} - U \equiv R(U) \ . \qquad (H.12)$$

The right side R is linear in U and the left side L is the product of an increasing function $\sqrt{U^2 - \theta_c}$ and a decreasing s-shaped function $e^{-\frac{1}{2}\gamma U^2/(1+U^2)}$ as seen in Figure H.2. The range of interest is $0 < U < \sqrt{B}$ if $\theta_c \leq 0$ or $\theta_c < U < \sqrt{B}$ if $\theta_c > 0$. In Figure H.2, L is shown to be less than R at the ordinate. This is not necessarily true. But if L is greater than R at the ordinate then the maximum number of solutions is two, hence an isola is not possible. That is, if

$$L(U = 0 \ \text{ or } \ \sqrt{\theta_c}) \geq R(U = 0 \ \text{ or } \ \sqrt{\theta_c}) \qquad (H.13)$$

or for $\theta_c \leq 0$ where the lower bound of U is equal to zero, the above becomes

$$H_1(-\theta_c) \geq k_f B \qquad (H.14)$$

and for $\theta_c > 0$ where the lower bound of U is equal to $\sqrt{\theta_c}$, this becomes

$$\theta_c \geq B \ .$$

Equations H.14 and H.15 are sufficient conditions for the absence of an isola. An interpretation of these conditions is: if the cooling water temperature is low enough so that heat is lost faster than it is generated, an isola is not possible; if the cooling water temperature is greater than the maximum temperature for an adiabatic reactor, then an isola is not possible. So in what follows we will only consider L less than R at the ordinate, as shown in the figure.

Either one of three solutions are possible and when we find three, the reactor has an isola. As seen in Figure H.2 there are two instances when L intersects R only twice. We call these critical functions L* and $L_*$. When L is between L* and $L_*$, three solutions exist and hence an isola. So it is these critical functions that define the birth and

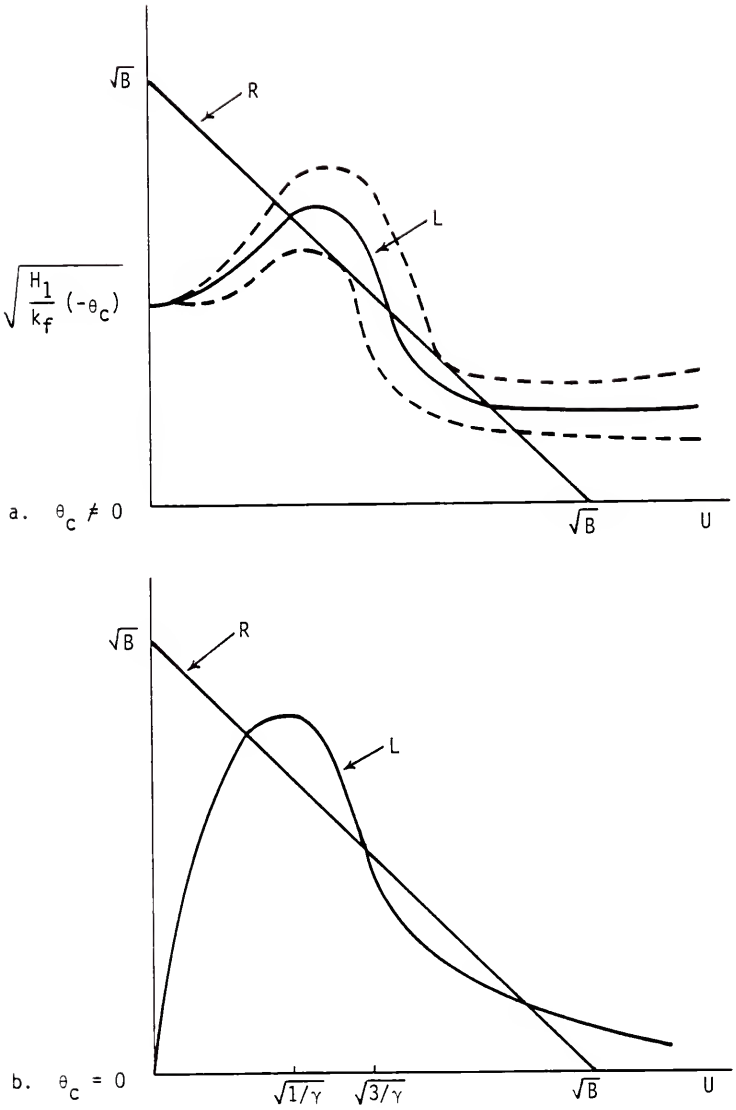


Figure H.2. Number of zeros of $d\theta/d\tau$.

death of an isola. The corresponding critical conditions are that the slope of L equals the slope of R at the point of intersection, viz.,

$$L(U_{cr}) = R(U_{cr}) \tag{H.16}$$

and

$$\frac{dL}{dU}\Big|_{U_{cr}} = \frac{dR}{dU}\Big|_{U_{cr}} . \tag{H.17}$$

Moreover it is simpler to use

$$\left( \frac{1}{L}\frac{dL}{dU} \right)\Big|_{U_{cr}} = \left( \frac{1}{R}\frac{dR}{dU} \right)\Big|_{U_{cr}} \tag{H.18}$$

in place of the second of these. We find

$$\frac{dL}{dU} = \sqrt{\frac{H_1}{k_f}}\, U \sqrt{U^2 - \theta_c}\; e^{-\frac{1}{2}\gamma U^2/(1+U^2)}\; \frac{\{ U^4 - (\gamma-2)U^2 + 1+\gamma\theta_c \}}{(U^2 - \theta_c)\,(1 + U^2)^2} \tag{H.19}$$

and

$$\frac{dR}{dU} = -1 . \tag{H.20}$$

Equation H.18 implies that $U = U_{cr}$ satisfies the fifth degree polynomial equation:

$$f(U) = \sqrt{B}\, U^5 + (\gamma - \theta_c)U^4 - \sqrt{B}\,(\gamma - 2)U^3 - \theta_c(\gamma + 2)U^2 + \sqrt{B}\,(1 + \gamma\theta_c)U - \theta_c = 0 . \tag{H.21}$$

The conditions given by Eqs. H.16 and H.21 establish the boundary (which we call the birth/death locus) of the region where isolas exist in $(H_1, k_f, \theta_c, \gamma, B)$ space. But because f and R are independent of $H_1$ and $k_f$ and because L depends only on the ratio $(H_1/k_f)$ there is a simple way to interpret the results. For preassigned values of $\theta_c$, $\gamma$ and B we find $U_{cr}$ from Eq. H.21 and the corresponding critical values of $(H_1/k_f)$ from Eq. H.16, viz.,

$$\left( \frac{H_1}{k_f} \right)_{cr} = \left\{ \frac{\sqrt{B} - U_{cr}}{\sqrt{U_{cr}^2 - \theta_c}} \right\}^2 e^{\gamma U_{cr}^2/(1+U_{cr}^2)} . \tag{H.22}$$

Therefore given $\theta_c$, $\gamma$ and B we anticipate that Eq. H.21 implies two values of $U_{cr}$ in the physically admissible range and that each of these implies a critical value of $(H_1/k_f)$ from Eq. H.22 such that if $(H_1/k_f)$ lies between the critical values, the system has an isola. Because the polynomial f(U) is fifth degree it has five zeros. But the two solutions of physical interest must be real and lie in the range

$$0 < U < \sqrt{B} \qquad \text{if } \theta_c \leq 0$$

or

$$\sqrt{\theta_c} < U < \sqrt{B} \qquad \text{if } \theta_c > 0$$

(see Figure H.2). That is for $U > \sqrt{B}$, L is positive and R negative, therefore no intersection exists, and from the Equations H.7 and H.8 we know that $\theta > 0$ and $\theta > \theta_c$ must be true for a physical solution to exist.

Before going on, we test our results on the example problem of Hlavacek and Van Rompay (1981) where

$$\theta_c = -0.25\ , \qquad \gamma = 20.\ , \qquad B = 0.5 \quad \text{and} \quad k_f = 1.0\ .$$

The physically meaningful zeros of the polynomial f(U), Eq. H.21, are

$$U_a = 0.1057 \quad \text{and} \quad U_b = 0.5237$$

to which correspond the following critical values of $H_1$:

$$H_{1a} = 1.727 \quad \text{and} \quad H_{1b} = 4.751\ .$$

For $H_1 = H_{1a}$ we have the birth of an isola, cf. Figure H.1d, where the separation point is located at

$$\theta_a = 0.01117 \quad \text{and} \quad \tau_a = 0.1409$$

obtained via Eq. H.9. Whereas for $H_1 = H_{1b}$ we have the death of an isola or a point isola, cf. Figure H.1e, located at

$$\theta_b = 0.2742 \quad \text{and} \quad \tau_b = 0.0385\ .$$

If $H_{1a} < H_1 < H_{1b}$ then the $\theta$ versus $\tau$ graph must exhibit an isola.

These are precisely the values found by Hlavacek and Van Rompay but at considerably less expense than solving the three simultaneous nonlinear equations which they derived.

What we have achieved thus far is to greatly simplify the calculation of the critical values of $H_1$. But our results also can be used to generate explicit conditions for the existence of isolas. First, we have already shown that isolas can not exist for an adiabatic CSTR, i.e. for $H_1 = 0$. For a nonadiabatic reactor the results are simplest if the cooling fluid temperature is the same as the feed temperature, i.e. if $\theta_c = 0$. For illustrative purposes we set $\theta_c = 0$ and, in the first instance, make the Frank-Kamenetskii approximation, viz.,

$$e^{\gamma\theta/(1+\theta)} \simeq e^{\gamma\theta}$$

(which is accurate for $\theta$ much less than 1, see Appendix G) so that the function L(U) is more easily graphed and understood, cf. Figure H.2b. Here we have

$$L(U) = \sqrt{\frac{H_1}{k_f}}\ U\ e^{-\frac{1}{2}\gamma U^2} = \sqrt{B} - U = R(U) \qquad (H.23)$$

whence Eq. H.18 implies the third degree polynomial equation[1]

$$f(U) = U^3 - \sqrt{B}\ U^2 + \sqrt{B}/\gamma = 0\ . \qquad (H.24)$$

This is a great simplification over the earlier fifth degree polynomial equation and it leads easily to important conclusions. First Descarte's Rule of Sign tells us that one zero of f(U) must be real and negative. Second we see that

[1]Using the Frank-Kamenetskii approximation and not setting $\theta_c = 0$ gives a fourth degree polynomial equation; setting $\theta_c = 0$ but not using the Frank-Kamenetskii approximation also gives a fourth degree polynomial equation; but neither is helpful.

$$f(0) = f(\sqrt{B}) = \sqrt{B}/\gamma$$

and that $f'(U)$ vanishes at $U = 0$ and $U = 2/3\sqrt{B}$, cf. Figure H.3. Thus if the remaining two zeros of $f(U)$ are real they are in the physically admissible range. Third we see that f has a relative minimum at $U = 2/3\sqrt{B}$ and hence critical values of U exist if and only if $f(2/3\sqrt{B}) \leq 0$. This implies that an isola may exist if and only if $B\gamma \geq 27/4$. That is, isolas exist if and only if

$$B\gamma \geq 27/4 \tag{H.25}$$

and

$$(H_1/k_f)_a \leq (H_1/k_f) \leq (H_1/k_f)_b \tag{H.26}$$

where $(H_1/k_f)_a$ and $(H_1/k_f)_b$ are the critical values of $(H_1/k_f)$ corresponding to the real positive zeros of $f(U)$, viz., from Eq. H.22

$$\left(\frac{H_1}{k_f}\right)_{a,b} = \left(\frac{\sqrt{B} - U_{cr}}{U_{cr}}\right)^2 e^{\gamma U_{cr}^2} . \tag{H.27}$$

If $B\gamma < 27/4$ then isolas do not exist.

Figure H.2b suggests that another argument can be made directly in terms of L(U) and R(U) themselves. Inasmuch as isolas imply more than one solution of L = R, conditions that imply not more than one solution rule out isolas. In particular if the least slope of L exceeds the slope of R, i.e. -1, then isolas can not exist, cf. Figure H.2b. The least slope of L is realized at its inflection point, $U = \sqrt{3/\gamma}$, and the condition that obtains is that isolas can not exist if

$$H_1/k_f < 1/4e^3 = 5.02 . \tag{H.28}$$

In summary then, isolas can be identified by investigating the zeros of $d\theta/d\tau$. For assigned values of $\theta_c$, $\gamma$ and B we can establish the critical values of $(H_1/k_f)$ (from Eq. H.22) which signal the birth and death of isolas by finding the zeros of a fifth degree polynomial (Eq.

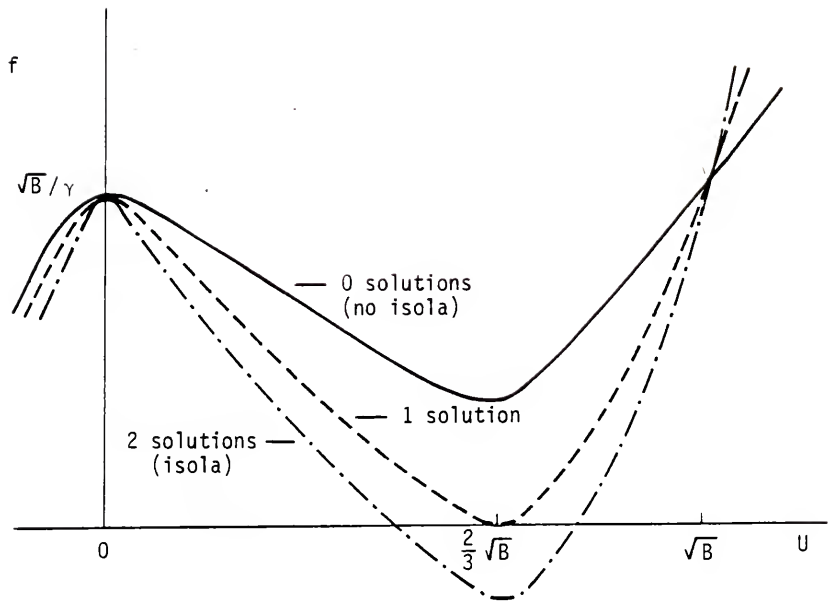


Figure H.3. Zeros of f for $\theta_c = 0$.

$df/dU = 0$ at $U = 0$ and $U = 2/3\sqrt{B}$ .

H.21) that lie in the physically meaningful range. For the special case $\theta_c = 0$, if we make the Frank-Kamenetskii approximation, we can be more explicit and say that

i) isolas exists in some range of $H_1/k_f$, cf. Eqs. H.26 and H.27, if and only if

$$B\gamma \geq 27/4$$

and

ii) isolas can not exist if

$$H_1/k_f < 1/4e^3 = 5.02 \ .$$

Like isolas, mushrooms can be located by their characteristic features. In particular the existence of mushrooms is related to the number of times $d\theta/d\tau$ becomes infinite,[2] where

$$\frac{d\theta}{d\tau} = -\frac{\partial\psi/\partial\tau}{\partial\psi/\partial\theta} \ .$$

But $\partial\psi/\partial\tau$ is finite for all finite $\theta$ and $\tau$. So the problem reduces to finding the number of solutions to

$$\psi = 0$$

and

$$\partial\psi/\partial\theta = 0 \ .$$

The analysis is not simple because neither $\theta$ nor $\tau$ can be eliminated easily, in particular both equations are quadratic in $\tau$. But the equations simplify for the adiabatic case, viz.,

$$\psi = \theta - (B - \theta)\tau k_f \, e^{\gamma\theta/(1+\theta)} = 0 \qquad \text{(H.29)}$$

---

[2]The slope must become infinite four times for a mushroom but this is only a necessary condition. Uppal et al. (1976) found that an isola and an s-shaped pattern are possible together. This combination also gives four infinite slopes. But what is important is that if the slope becomes infinite less than four times, a mushroom can not exist.

$$\frac{\partial \psi}{\partial \theta} = 1 + \tau k_f \, e^{\gamma\theta/(1+\theta)} \left\{ 1 - \frac{\gamma(B - \theta)}{(1 + \theta)^2} \right\} = 0 \, . \qquad \text{(H.30)}$$

Eliminating $\tau$, which also eliminates $k_f e^{\gamma\theta/(1+\theta)}$, gives a quadratic in $\theta$, viz.,

$$(B + \gamma)\theta^2 - B(\gamma - 2)\theta + B = 0 \, . \qquad \text{(H.31)}$$

Thus at most two solutions (i.e. points $(\theta,\tau)$ where $d\theta/d\tau$ becomes infinite) are possible and therefore only s-shaped multiplicity patterns are possible. Hence mushroom multiplicity patterns are not possible for an adiabatic CSTR. This is consistent with experimental and numerical observations. Also from Descarte's Rule of Sign we note that if $\gamma \leq 2$ then no solutions are possible and the steady state is always unique.

## APPENDIX I
## THE EXISTENCE OF MUSHROOMS AND ISOLAS IN A GAS-LIQUID CSTR

As in a single-phase reactor the existence of an isola in a gas-liquid reactor can be deduced from the number of zeros of the slope of the temperature versus the holding time, see Appendix H. But unlike that for the single-phase reactor the heat generation function for the two-phase reactor exhibits two s-shaped regions. The single-phase results suggest therefore that two isolas may exist. One is due to the interaction of the rate of mass transfer and the bulk reaction, the other is due to the enhancement of the mass transfer coefficient via interfacial reaction. Thus more than three zeros for the slope might be anticipated, e.g. two isolas should have five zeros. Because the model is more complicated than that for the single-phase reactor it is necessary to make some approximations if correspondingly useful results are to be attained. If the liquid-phase reactant B is in such excess that its concentration is a constant with respect to the holding time, then the reaction becomes pseudo-first order. This greatly simplifies the analysis. This approximation is reasonable if the holding time is not too large and hence the results obtained will apply only on a limited range of moderately valued holding times.

To calculate $d\theta/d\tau$ we must first eliminate the dissolved gas concentration from the energy balance via substitution of the solute mass balance, see Chapter Three. This yields an equation for $\theta$, the steady state temperature, in terms of $\tau$ and the reactor parameters, viz.,

$$\psi(\theta,\tau;\ \theta_c,\ H_1,\ k_L^\circ,\ a,\ k_1,\ B_R,\ B_S;\ \tau_i,\ S,\ n,\ D/\alpha)$$

$$= \theta + \tau H_1(\theta - \theta_c)$$

$$- \frac{\phi\tau k_L^\circ a x_i\ (1 + \tau k_1)}{\{\ 1 + \tau k_1 + \phi\tau k_L^\circ a\ (1 - f_i)\ \}} \{\ B_S + B_R\ (\ \frac{\tau k_1 + f_i}{1 + \tau k_1}\ )\ \}$$

$$= 0 \qquad \text{(I.1)}$$

where the last set of parameters is implicit in the functions $x_i$, $\phi$, $f_i$ and $\theta_i$, see Chapter Three. $\psi = 0$ implies $\theta$ versus $\tau$ for preassigned values of the parameters and the pertinent slope is

$$\frac{d\theta}{d\tau} = -\ (\ \frac{\partial\psi/\partial\tau}{\partial\psi/\partial\theta}\ )\ .$$

This slope is zero when $\partial\psi/\partial\tau = 0$ because, as in the single-phase reactor, $\partial\psi/\partial\theta$ is never infinite for finite values of $\theta$ and $\tau$, see Appendix H. We calculate the partial derivative and write the corresponding conditions for the slope of the $\theta$ versus $\tau$ curve to be zero, viz.,

$$\psi(\theta,\tau) = 0$$

and

$$\frac{\partial\psi}{\partial\tau} = H_1(\theta - \theta_c) \ - \ \frac{\{\ B_S + B_R\ (\ \frac{\tau k_1 + f_i}{1 + \tau k_1}\ )\ \}}{\{\ 1 + \tau k_1 + \phi\tau k_L^\circ a(1 - f_i)\ \}^2} \cdot$$

$$\{\ \tau k_L^\circ a x_i(1 + \tau k_1) + \phi k_L^\circ a x_i \tau k_1(1 + \tau k_1 + \phi\tau k_L^\circ a(1 - f_i))\ \}$$

$$- \frac{\phi k_L^\circ a x_i \tau k_1 B_R(1 - f_i)}{\{\ 1 + \tau k_1 + \phi\tau k_L^\circ a(1 - f_i)\ \}\ (1 + \tau k_1)}$$

$$= 0\ . \qquad \text{(I.2)}$$

From this the first result is derived: no isola or mushroom is possible for an adiabatic reactor ($H_1 = 0$) with B in excess. That is, the

remaining terms in Eq. I.2 are negative so that $d\theta/d\tau$ does not go to zero anywhere. Unfortunately the complexity of the above precludes further results even at this level of approximation where B is in excess.

However if it is assumed that no enhancement of mass transfer occurs, i.e. that $\phi = 1$ and $f_i = 0$ (so that only one isola is possible), and that the heat of absorption is negligible, i.e. that $B_S = 0$, then the Equations I.1 and I.2 are considerably simpler, viz.,

$$0 = \{\theta + \tau H_1(\theta - \theta_c)\}\{1 + \tau k_1 + \tau k_L^o a\} - \tau k_L^o a x_i \tau k_1 B_R \qquad (I.3)$$

and

$$0 = H_1(\theta - \theta_c)\{1 + \tau k_1 + \tau k_L^o a\}^2 - \tau k_1 B_R k_L^o a x_i (1 + \{1 + \tau k_1 + \tau k_L^o a\}) \; . \qquad (I.4)$$

Eliminating $H_1(\theta - \theta_c)$ yields

$$0 = -\frac{\theta}{\tau}\{1 + \tau k_1 + \tau k_L^o a\}^2 - \tau k_1 B_R k_L^o a x_i \quad . \qquad (I.5)$$

But the right-hand side is strictly negative, thus no mushroom or isola is possible whenever B is in excess and the enhancement and the heat of solution vanish.

This can be understood by examining the graphs of the heat removal and the heat generation functions versus temperature and how they change with $\tau$, cf. Figures 4.3 and 4.4. Under these conditions the heat generation curve exhibits a single s-shaped region, as in a single-phase reactor. A mushroom is formed on the graph of $\theta$ versus $\tau$ when this s-shaped region "passes through" (that is intersects with one, three and then one solution as $\tau$ increases) the straight line for heat removal more than once as $\tau$ is increased and an isola is formed when the s intersects the heat removal line but fails to pass completely through.

These have been found to be possible only when the reactor is nonadiabatic, so that the straight line can also vary with $\tau$. Note that the straight line for the heat removal function for a two-phase or single-phase CSTR is

$$(1 + \tau H_1)\theta - \tau H_1 \theta_c$$

so that the slope with respect to $\theta$ is $(1 + \tau H_1)$ and the intercept is $-\tau H_1 \theta_c$. Thus as $\tau$ is varied both the slope and the intercept of the heat removal line change. It is the variations in the heat removal line and the heat generation curve with changing $\tau$ that cause the unusual multiplicity patterns. But the s-shaped heat generation curve for a two-phase reactor without enhancement behaves differently than the generation curve for a single-phase reactor where isolas and mushrooms are possible. Herein lies the reason for no isolas or mushrooms in such a two-phase reactor. First we will explain how these multiplicity patterns arise in a single-phase CSTR and then we will show that this behavior can not occur in this two-phase system.

In a single-phase reactor the s-shaped region of the heat generation curve, $\tau k_1/(1 + \tau k_1)$, moves to the left (lower temperatures) as the holding time increases, cf. Figure I.1a. Thus for an adiabatic reactor ($H_1 = 0$) where the heat removal function is a straight line with fixed slope and intercept, this region intersects and passes through the line only once, cf. Figure I.1a, causing s-shaped multiplicity on a graph of $\theta$ versus $\tau$, cf. Figure A.2a. But for a nonadiabatic reactor the slope of the heat removal function, $(1 + \tau H_1)$, and its y-intercept, $-\tau H_1 \theta_c$, change on changing $\tau$. Different $\theta$ versus $\tau$ multiplicities arise depending on the relative speeds of the s-shaped region of the heat generation curve and the accelerating slope of the straight line. The s

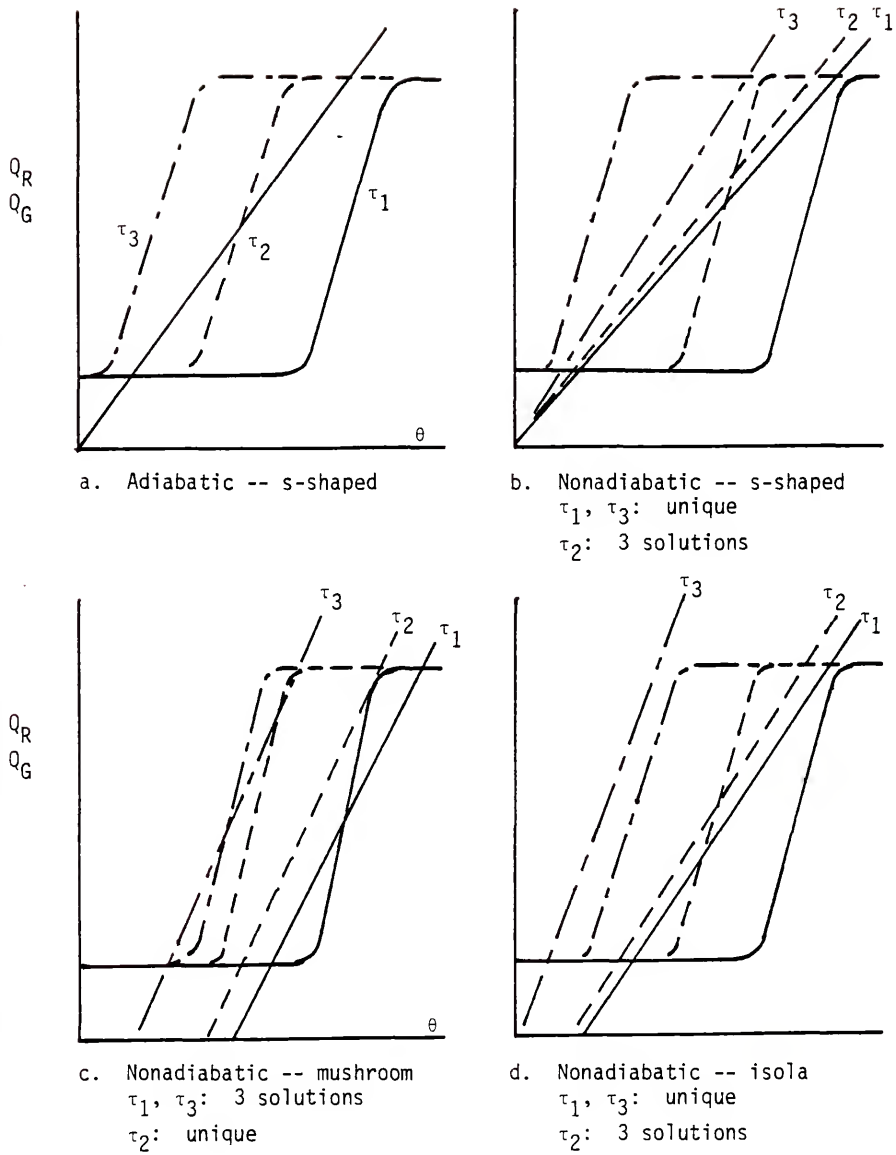


a. Adiabatic -- s-shaped

b. Nonadiabatic -- s-shaped
$\tau_1$, $\tau_3$: unique
$\tau_2$: 3 solutions

c. Nonadiabatic -- mushroom
$\tau_1$, $\tau_3$: 3 solutions
$\tau_2$: unique

d. Nonadiabatic -- isola
$\tau_1$, $\tau_3$: unique
$\tau_2$: 3 solutions

Figure I.1. Formation of multiplicity patterns in a single-phase CSTR.
$\tau_3 > \tau_2 > \tau_1$

may never "catch" the line before its slope is so great that only one intersection is possible hence the steady state is unique for all $\tau$. The s can catch and pass through the line, causing s-shaped multiplicity (Figure I.1b). In some cases the s may pass through the line only to have the slope of the line accelerate so that the line passes through the s-shaped region again (Figure I.1c). This causes two regions of s-shaped multiplicity and the resulting pattern has been labelled a mushroom, cf. Figure A.2b. If the s catches the line but can not pass through completely before the slope accelerates then an isola forms, cf. Figures I.1d and A.2c.

But for the two-phase reactor an additional change in the heat generation function occurs. In the single-phase reactor the s-shaped region of the heat generation function moves to lower temperatures with increasing holding times but retains its shape. For the two-phase case the s changes with holding time. Whereas the temperature for the initial rise in the s decreases with increasing holding times as in the single-phase reactor, the temperature at which the upper plateau is reached is the same for all $\tau$, i.e. the upper plateau is reached when the rate of mass transfer is controlling so $\tau/\tau_M = \tau/\tau_R$ or $kC_B = k_L^o a$, which is independent of $\tau$, cf. Figure I.2. Also the height of this plateau increases in direct proportion to $\tau$, i.e. here in the mass transfer controlled regime the generation function equals $\tau k_L^o a C_{Ai}$. Thus the slope of the straight line can not accelerate through the s because the slope only changes as $(1 + \tau H_1)$ whereas the height of the s increases as $\tau$. For example if the line and curve intersect at three places and the holding time is doubled, then the plateau height doubles but the slope of the straight line does not, $(1+2\tau H_1) < 2(1+\tau H_1)$.

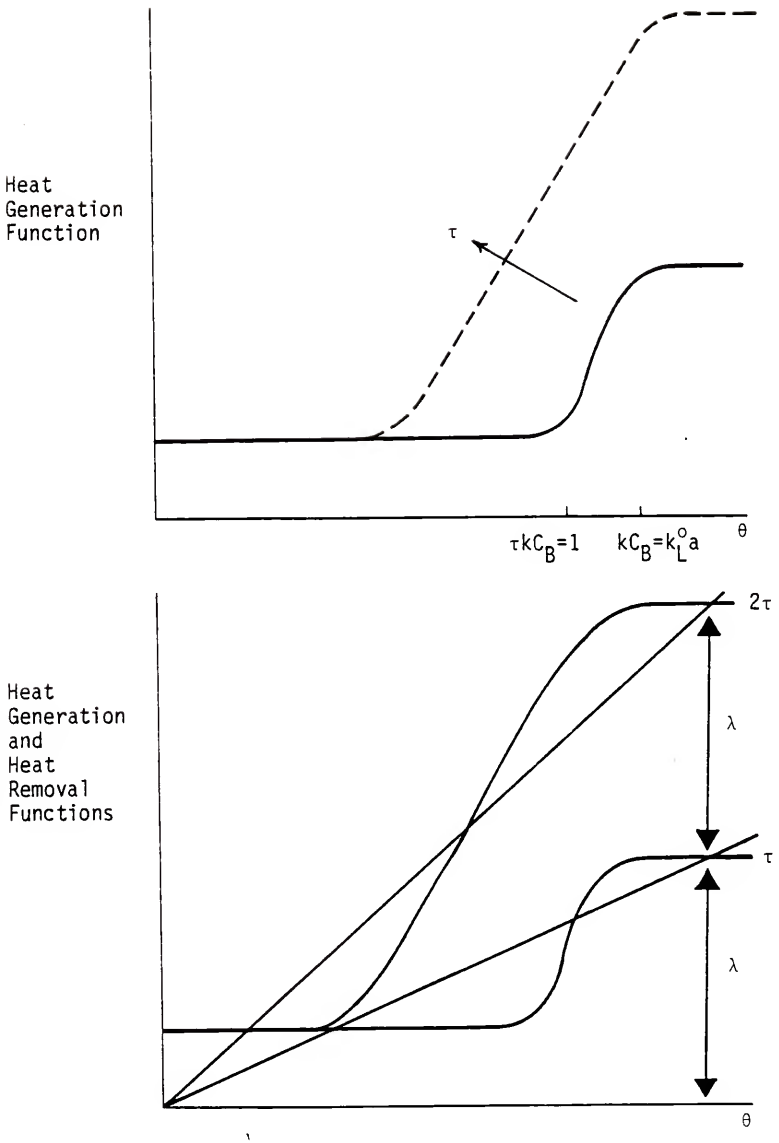


Figure I.2. Steady state analysis for a two-phase CSTR.

So the straight line still intersects the high temperature branch of the s and can not pass above it (Figure I.2b). Thus only s-shaped multiplicity is possible. However this argument does not account for the change in the intercept ($-\tau H_1 \theta_c$) of the straight line for heat removal. If $\theta_c < 0$ the argument might have to include the changing intercepts, but from the isola analysis we guess that $\theta_c$ does not have a significant effect, inasmuch as only s-shaped multiplicity was found to be possible.

If $C_B$ were not constant then the temperature at which the upper plateau is reached would change with holding time because when mass transfer becomes controlling we have

$$kC_B = k_L^o a$$

and

$$C_B = C_{Bf} - \nu C_{Ai} \tau k_L^o a \ .$$

Thus this temperature increases with $\tau$, elongating the s. This should make an isola more likely. In fact if $C_B$ is allowed to vary we can not show that an isola can not exist, moreover we have found isolas numerically. It appears that it is important to allow $C_B$ to vary when performing the multiplicity analysis. But as seen in Chapter Four, $C_B$ is not a simple function of $\tau$ hence the analysis has not been useful.

## APPENDIX J
## STABILITY CONDITIONS FOR AN UNENHANCED GAS-LIQUID CSTR

The first method of Liapunov will be used to investigate the local asymptotic stability of the steady states in the special case of unenhanced mass transfer, i.e. $\phi = 1$, $f_i = 0$ and $\theta_i = \theta$. We also assume that $C_B = C_{Bf}$, $B_S = 0$ and $\theta_c = 0$ whence the equations in Table 3.2 become

$$\frac{dx_A}{dt'} = -x_A\,(1 + D_a\, e^{\gamma\theta}) + \beta(e^{-n\theta} - x_A) \tag{J.1}$$

and

$$\frac{d\theta}{dt'} = -(1 + H)\theta + B_R\, D_a\, x_A\, e^{\gamma\theta} \tag{J.2}$$

where the Frank-Kamenetskii approximation has been used, see Appendix G.

The essence of Liapunov's first method is that conditions which guarantee the local asymptotic stability of a linear system, also guarantee the local asymptotic stability of the corresponding nonlinear system. The necessary and sufficient conditions then for the stability of a steady state in a two-dimensional system are that the determinant and the trace of the Jacobian matrix evaluated at the steady state be positive and negative, respectively, viz.,

$$|\underline{\underline{A}}| > 0 \tag{J.3}$$

and

$$\text{tr}\ \underline{\underline{A}} < 0 \tag{J.4}$$

where $\underline{\underline{A}}$ is the Jacobian matrix of the system. The conditions J.3 and J.4 insure that the real parts of the eigenvalues of $\underline{\underline{A}}$ are negative,

viz.,

$$\lambda_{1,2} = \frac{1}{2} \text{tr } \underline{\underline{A}} \pm \frac{1}{2} \sqrt{(\text{tr } \underline{\underline{A}})^2 - 4|\underline{\underline{A}}|} \quad . \tag{J.5}$$

The Jacobian matrix of the system of Eqs. J.1 and J.2 evaluated at the steady state is

$$\underline{\underline{A}} = \begin{pmatrix} \dfrac{-(1+\beta)\, B_R \beta\, e^{-n\theta}}{\{\, B_R \beta\, e^{-n\theta} - (1+H)\theta \,\}} & \dfrac{-\gamma(1+H)\theta}{B_R} - n\beta e^{-n\theta} \\ \dfrac{(1+\beta)\, B_R\, (1+H)\theta}{\{\, B_R \beta\, e^{-n\theta} - (1+H)\theta \,\}} & (1+H)\,(\gamma\theta - 1) \end{pmatrix} \tag{J.6}$$

where the state variable $x_A$ and the parameter $D_a$ have been eliminated via the steady state versions of Eqs. J.1 and J.2. The determinant and the trace are

$$|\underline{\underline{A}}| = \frac{\gamma(1+\beta)\,(1+H)}{\{\, B_R \beta\, e^{-n\theta} - (1+H)\theta \,\}} \left[ (1+H)\theta^2 - \frac{B_R \beta}{\gamma} e^{-n\theta}\, ((\gamma - n)\theta - 1) \right] \tag{J.7}$$

and

$$\text{tr } \underline{\underline{A}} = \frac{-\gamma}{\{\, B_R \beta\, e^{-n\theta} - (1+H)\theta \,\}} \left[ (1+H)^2 \theta(\theta - 1) - B_R \beta\, e^{-n\theta} ((1+H)\theta - (2 + \beta + H)) \right] \quad . \tag{J.8}$$

Because the denominator in each of the above equations is positive for all admissible values of $\theta$, cf. Eq. F.4, the sign of the right-hand side of each equation is determined by the sign of the last factor in brackets. In particular we observe that if $n \geq \gamma$ then the determinant is always positive.

In determining the sign of the determinant and the trace, the zeros of these factors on the allowable range of $\theta$, their number and their location are important and can be investigated graphically by rewriting the factors, viz.,

$$\theta^2 e^{\eta\theta} = \frac{B_R\beta}{(1 + H)\gamma} ((\gamma - \eta)\theta - 1) \tag{J.9}$$

and

$$\theta(\theta - 1)e^{\eta\theta} = \frac{B_R\beta}{(1 + H)} \left( \theta - \frac{(2 + \beta + H)}{(1 + H)} \right) . \tag{J.10}$$

The left-hand and right-hand sides of the above are shown in Figures J.1 a and b where we see that a maximum of two real solutions is possible for each equation. Thus there are at most two values of $\theta$ such that the determinant vanishes and two values of $\theta$ such that the trace vanishes. This suggests that we can estimate the zeros by expanding the exponent in Eqs. J.9 and J.10 in a Taylor series and then neglecting all terms of order $\theta^3$ and higher in the equations, see Appendix F.

Because Eq. J.9 is identical to Eq. F.6 with $\theta_c = 0$, we conclude that the determinant vanishes for $\theta$ equal to $m_1$ or $m_2$, where $m_1$ and $m_2$ satisfy Eq. F.16 which we used in identifying the regions of uniqueness and multiplicity. Thus we see that whenever the steady state is unique, the determinant is positive, $|\underline{A}| > 0$; whenever it is not, $|\underline{A}| > 0$ for $\theta > m_1$ and $\theta < m_2$ and $|\underline{A}| < 0$ for $m_2 < \theta < m_1$. The steady states such that $m_2 < \theta < m_1$ are unstable, a result which also follows from the slope condition which it turns out is identical to the determinant condition, see Chapter Five.

In summary then the determinant vanishes for $\theta = m_1$ and $m_2$ where $m_1$ and $m_2$ are given by Eq. F.16. Whence the determinant is positive if, see Appendix F,

1. $\frac{\eta}{\gamma} \geq \left( \frac{\eta}{\gamma} \right)_2$ , cf. Eq. F.19;

or if

2. $\theta > m_1$ or $\theta < m_2$ when $\frac{\eta}{\gamma} < \left( \frac{\eta}{\gamma} \right)_2$ .

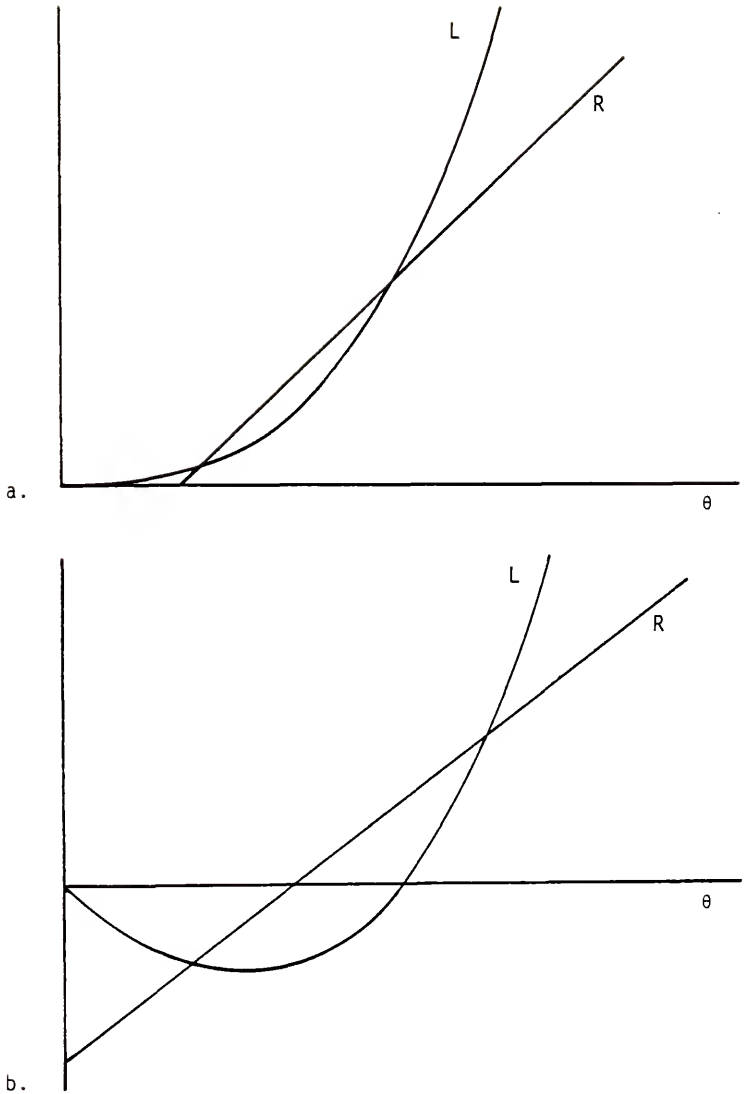


Figure J.1. The left and right sides of Equations J.9 and J.10.

a. Equation J.9 b. Equation J.10

The determinant is negative if

$$\frac{\eta}{\gamma} < \left(\frac{\eta}{\gamma}\right)_2$$

and

$$m_2 < \theta < m_1 \ .$$

The uniqueness conditions and hence the determinant conditions are summarized in Table F.1.

The zeros of the trace can be estimated by approximating the exponential in Eq. J.10, which yields a quadratic equation, viz.,

$$\{ (1 + H)^2 + (1 + H)B_R\beta\eta + \frac{1}{2}(2 + \beta + H)B_R\beta\eta^2 \} \theta^2$$

$$- \{ (1 + H)^2 + (1 + H)B_R\beta + (2 + \beta + H)B_R\beta\eta \} \theta$$

$$+ (2 + \beta + H)B_R\beta = 0 \ . \qquad (J.11)$$

If we define the coefficients in Eq. J.11 to be $a_1$, $b_1$ and $c_1$ and its roots to be $s_1$ and $s_2$, viz.,

$$s_1 , s_2 = \frac{-b_1 \pm \sqrt{b_1^2 - 4a_1c_1}}{2a_1} \ , \qquad (J.12)$$

then the trace is

$$\text{tr } \underline{\underline{A}} = \frac{-\gamma a_1}{\{ B_R\beta \, e^{-\eta\theta} - (1 + H)\theta \}} (\theta - s_1)(\theta - s_2) \ . \qquad (J.13)$$

The trace is negative for all $\theta$ if $s_1$ and $s_2$ are nonreal, i.e. if the discriminant in Eq. J.12 is negative, viz.,

$$0 > b_1^2 - 4a_1c_1 = -(2 + \beta + H)^2(B_R\beta)^2(\eta - \eta_3)(\eta - \eta_4)$$

where

$$\eta_3 , \eta_4 = \frac{-(1 + H)}{(2 + \beta + H)B_R\beta} \{ B_R\beta - (1 + H)$$

$$\mp \sqrt{2(B_R\beta)^2 - 4(2 + \beta + H)B_R\beta + 2(1 + H)^2} \ \} \qquad (J.14)$$

and where $\eta_3$ and $\eta_4$ are nonreal if

$$(B_R\beta)_2 < B_R\beta < (B_R\beta)_1$$

where

$$(B_R\beta)_{1,2} = (2 + \beta + H) \pm \sqrt{(1 + \beta)^2 + 2(1 + \beta)(1 + H)} \quad . \qquad (J.15)$$

If $s_1$ and $s_2$ are real then tr $\underline{\underline{A}} < 0$ if and only if $\theta > s_1$ or $\theta < s_2$.

We can summarize: the trace is negative if

$$(B_R\beta)_2 < B_R\beta < (B_R\beta)_1$$

or if

$$\eta > \eta_3 \quad \text{or} \quad \eta < \eta_4$$

or if

$$\theta > s_1 \quad \text{or} \quad \theta < s_2 \ ;$$

the trace is positive and hence the steady state unstable if

$$\eta_4 < \eta < \eta_3$$

and

$$s_2 < \theta < s_1 \ ;$$

the trace is zero if

$$\theta = s_1 \text{ or } s_2 \ .$$

We now have conditions defining the determinant and trace everywhere. In the regions where $|\underline{\underline{A}}| > 0$ and tr $\underline{\underline{A}} < 0$ the steady states are stable; these are summarized in Table J.1. Thus by calculating $m_1$, $m_2$, $s_1$, and $s_2$ we can determine whether any steady state temperature $\theta$ represents a stable or unstable state. If the determinant is positive and the trace is zero then the eigenvalues, $\lambda_i$, are purely imaginary and oscillations are possible. Also if the steady state is unique (implies $|\underline{\underline{A}}| > 0$) and $s_2 < \theta < s_1$ (implies tr $\underline{\underline{A}} > 0$) oscillations in the form of stable limit cycles must exist.

TABLE J.1
STABILITY CONDITIONS FOR AN UNENHANCED GAS-LIQUID CSTR WITH $\theta_c = 0$

| | | | |
|---|---|---|---|
| $\lvert\underline{\underline{A}}\rvert > 0$ | if | 1. $\frac{\eta}{\gamma} \geq \left(\frac{\eta}{\gamma}\right)_2$ | Eq. F.19 |
| | or | 2. $\theta > m_1$ or $\theta < m_2$ | Eq. F.16 |
| $\mathrm{tr}\,\underline{\underline{A}} < 0$ | if | 1. $(B_R\beta)_2 < B_R\beta < (B_R\beta)_1$ | Eq. J.15 |
| | or | 2. $\eta > \eta_3$ or $\eta < \eta_4$ | Eq. J.14 |
| | or | 3. $\theta > s_1$ or $\theta < s_2$ | Eq. J.12 |

To illustrate the foregoing suppose the parameters $\gamma$, $n$, H, $B_R$ and $\beta$ are such that $m_2 < s_2 < m_1 < s_1$. Then the steady state temperature versus the Damkohler number will look like Figure J.2, where we have defined the following from Eq. F.3:

$$D_{a1} = g(m_1) \qquad D_{a2} = g(m_2)$$

$$D_{a3} = g(s_1) \qquad D_{a4} = g(s_2) \ .$$

For $D_a < D_{a1}$ the system has an unique stable steady state. Three steady states exist for $D_a \in (D_{a1}, D_{a2})$; the low temperature state is stable ($\theta < m_2 < s_2$), the middle state is an unstable saddle point ($m_2 < \theta < m_1$ therefore $|\underline{\underline{A}}| < 0$), and the high temperature state is an unstable spiral or node ($s_2 < \theta < s_1$ therefore tr $\underline{\underline{A}} > 0$). For $D_a \in (D_{a2}, D_{a3})$ the system has an unique but unstable steady state ($s_2 < \theta < s_1$), thus stable limit cycles must exist in this region. An unique stable steady state exists for $D_a > D_{a3}$ ($\theta > s_1 > m_1$). Thus the stability character of all possible steady states is known.

Bifurcation to periodic orbits occurs when the determinant is positive and the trace is zero. Thus $s_1$ and $s_2$ are possible bifurcation points. But for the system shown in Figure J.2, the determinant is negative for $\theta = s_2$ therefore $\theta = s_1$ is the only point where the steady state can bifurcate into a periodic orbit. Because the steady state is unique but unstable for $D_a \in (D_{a2}, D_{a3})$, there must be a stable periodic orbit originating from $\theta = s_1$ for $D_a$ decreasing from $D_{a3}$. This is the type of region we seek for the natural oscillations discussed in the introduction.

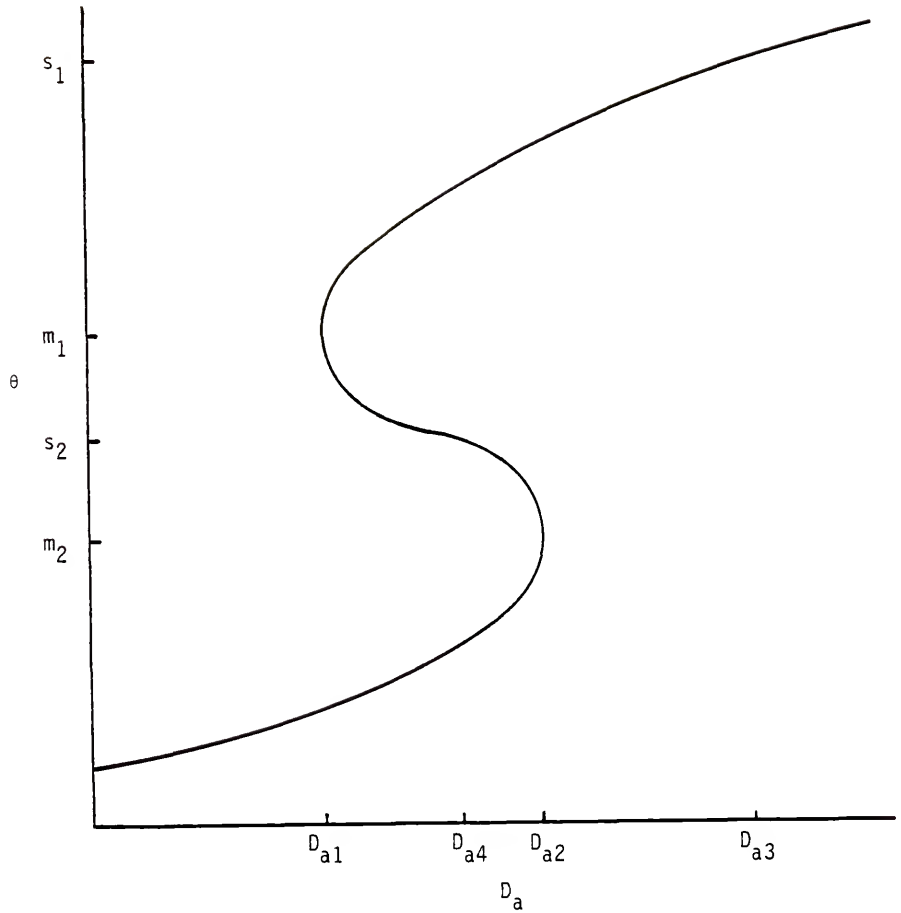


Figure J.2. Steady state temperature versus Damkohler number.

BIBLIOGRAPHY

Astarita, G., Mass Transfer With Chemical Reaction, Elsevier, Amsterdam (1967).

Beenackers, A. A. C. M., "Aromatic Sulfonation in a Cyclone Reactor, a Stirred Cell, and a Cocurrent Tube Reactor," in Chemical Reaction Engineering--Houston, ed. V. W. Weekman, Jr. and D. Luss, ACS Symp. Series, V. 65, 327 (1978).

Chang, H.-C., and J. M. Calo, "Exact Criteria for Uniqueness and Multiplicity of an nth Order Chemical Reaction Via a Catastrophe Theory Approach," Chem. Eng. Sci., 34, 285 (1979).

Charpentier, J. C., "Gas-Liquid Reactors," in Chemical Reaction Engineering Reviews--Houston, ed. D. Luss and V. W. Weekman, Jr., ACS Symp. Series, V. 72, 223 (1978).

Clegg, G. T., and R. Mann, "A Penetration Model For Gas Absorption With First Order Chemical Reaction Accompanied By Large Heat Effects," Chem. Eng. Sci., 24, 321 (1969).

Danckwerts, P. V., "Temperature Effects Accompanying the Absorption of Gases in Liquids," Appl. Sci. Res., A3, 385 (1951).

Danckwerts, P. V., Gas-Liquid Reactions, McGraw-Hill, New York (1970).

Ding, J. S. Y., S. Sharma and D. Luss, "Steady-State Multiplicity and Control of the Chlorination of Liquid n-Decane in an Adiabatic Continuously Stirred Tank Reactor," Ind. Eng. Chem., Fund., 13, 1, 76 (1974).

Frank-Kamenetskii, D., Diffusion And Heat Transfer In Chemical Kinetics, Plenum, New York (1969).

Hancock, M. D., and C. N. Kenney, "Instabilities in Two-Phase Reactors," Chem. React. Eng., Proc. 5th Euro/2nd Int. Symp. on Chem. React. Eng., Amsterdam, B3-47, Elsevier (1972).

Hancock, M. D., and C. N. Kenney, "The Stability and Dynamics of a Gas-Liquid Reactor," Chem. Eng. Sci., 32, 629 (1977).

Hlavacek, V., M. Kubicek, and J. Jelienek, "Modeling of Chemical Reactors--XVII, Stability and Oscillatory Behavior of the CSTR," Chem. Eng. Sci., 25, 1441 (1970).

Hlavacek, V., and P. Van Rompay, "On the Birth and Death of Isolas," Chem. Eng. Sci., 36, 1730 (1981).

Hoffman, L. A., S. Sharma, and D. Luss, "Steady State Multiplicity of Adiabatic Gas-Liquid Reactors: I. The Single Reaction Case," AIChE J., 21, 318 (1975).

Huang, D. T.-J., and A. Varma, "On the Reference Time in the Multiplicity Analysis for CSTRs," Chem. Eng. Sci., 35, 1806 (1980).

Huang, D. T.-J., and A. Varma, "Steady-State and Dynamic Behavior of Fast Gas-Liquid Reactions in Nonadiabatic Continuous Stirred Tank Reactors," Chem. Eng. J., 21, 47 (1981a).

Huang, D. T.-J., and A. Varma, "Steady-State Uniqueness and Multiplicity of Nonadiabatic Gas-Liquid CSTRs," I. and II., AIChE J., 27, 481 (1981b).

Hugo, P., and H.-P. Wirges, "Theoretical and Experimental Study of Self-Sustained Oscillations in a Stirred Tank Reactor," Chem. React. Eng.--Houston, ed. V. W. Weekman, Jr. and D. Luss, ACS Symp. Series, V. 65, 498 (1978).

Leib, T. M., and D. Luss, "Exast Uniqueness and Multiplicity Criteria for an nth Order Reaction in a CSTR," Chem. Eng. Sci., 36, 210 (1981).

Luss, D., and N. R. Amundson, "An Analysis of Chemical Reactor Stability and Control--XIII: Segregated Two Phase Systems," Chem. Eng. Sci., 22, 267 (1967).

Mann, R., and G. T. Clegg, "Gas Absorption With an Unusual Chemical Reaction: The Chlorination of Toluene," Chem. Eng. Sci., 30, 97 (1975).

Mann, R., and H. Moyes, "Exothermic Gas Absorption With Chemical Reaction," AIChE J., 23, 17 (1977).

Minorsky, N., Nonlinear Oscillations, Van Nostrand, Princeton, N.J. (1962).

Poore, A. B., "A Model Equation Arising from Chemical Reactor Theory," Archive For Rat. Mech., 52, 358 (1973).

Raghuram, S., and Y. T. Shah, "Criteria for Unique and Multiple Steady States for a Gas-Liquid Reaction in an Adiabatic CSTR," Chem. Eng. J., 13, 81 (1977).

Raghuram, S., Y. T. Shah, and J. W. Tierney, "Multiple Steady States in a Gas-Liquid Reactor," Chem. Eng. J., 17, 63 (1979).

Schmitz, R. A., and N. R. Amundson, "An Analysis of Chemical Reactor Stability and Control--Va: Two-Phase Systems in Physical Equilibrium--1," Chem. Eng. Sci., 18, 265 (1963a).

Schmitz, R. A., and N. R. Amundson, "An Analysis of Chemical Reactor Stability and Control--Vb: Two-Phase Gas-Liquid and Concentrated Liquid-Liquid Reacting Systems in Physical Equilibrium--2," ibid., 18, 391 (1963b).

Schmitz, R. A., and N. R. Amundson, "An Analysis of Chemical Reactor Stability and Control--VI: Two-Phase Chemical Reacting Systems With Heat and Mass Transfer Resistances," ibid., 18, 415 (1963c).

Schmitz, R. A., and N. R. Amundson, "An Analysis of Chemical Reactor Stability and Control--VII: Two-Phase Chemical Reacting Systems With Fast Reaction," ibid., 18, 447 (1963d).

Shah, Y. T., "Gas-Liquid Interface Temperature Rise in the Case of Temperature-Dependent Physical, Transport and Reaction Properties," Chem. Eng. Sci., 27, 1469 (1972).

Sharma, S., L. A. Hoffman, and D. Luss, "Steady State Multiplicity of Adiabatic Gas-Liquid Reactors: II. The Two Consecutive Reactions Case," AIChE J., 22, 324 (1976).

Sherwood, T. K., R. L. Pigford, and C. R. Wilke, Mass Transfer, McGraw-Hill, New York (1975).

Teramoto, M., T. Nagayasu, T. Matsui, K. Hashimoto, and S. Nagata, "Selectivity of Consecutive Gas-Liquid Reactions," Chem. Eng. Japan, 2, 186 (1969).

Tsotsis, T. T., and R. A. Schmitz, "Exact Uniqueness and Multiplicity Criteria for a Positive-Order Arrhenius Reaction in a Lumped System," Chem. Eng. Sci., 34, 135 (1979).

Uppal, A., W. H. Ray, and A. B. Poore, "On the Dynamic Behavior of Continuous Stirred Tank Reactors," Chem. Eng. Sci., 29, 967 (1974).

Uppal, A., W. H. Ray, and A. B. Poore, "The Classification of the Dynamic Behavior of Continuous Stirred Tank Reactors--Influence of Reactor Residence Time," ibid., 31, 205 (1976).

van Dierendonck, L. L., and J. Nelemans, "Hydrogenation in a Stirred Gas-Liquid Reactor," Chem. React. Eng., Proc. 5th Euro/2nd Int. Symp. on Chem. React. Eng., Amsterdam, Elsevier (1972).

van Krevelen, D. W., and P. J. Hoftijzer, "Kinetics of Gas-Liquid Reactions--General Theory," Rec. Chim. Pays-Bas, 67, 563 (1948).

Verma, S. L., and G. B. Delancey, "Thermal Effects in Gas Absorption," AIChE J., 21, 96 (1975).

## BIOGRAPHICAL SKETCH

Daniel White, Jr., was born on October 16, 1950, the first son of Daniel and Evelyn White. After attending school in rural New Jersey he matriculated at the University of Rochester, graduating in 1973 with a B.S. degree in chemical engineering. He received an M.S. degree in chemical engineering from the University of Florida in 1974. After a brief interlude at the University of Delaware, he returned to the University of Florida in 1977 where, aside from employment in industry due to pecuniary difficulties, he has been working on a Ph.D.

I certify that I have read this study and that in my opinion it conforms to acceptable standards of scholarly presentation and is fully adequate, in scope and quality, as a dissertation for the degree of Doctor of Philosophy.

L. E. Johns, Chairman
Professor of Chemical Engineering

I certify that I have read this study and that in my opinion it conforms to acceptable standards of scholarly presentation and is fully adequate, in scope and quality, as a dissertation for the degree of Doctor of Philosophy.

R. W. Fahien
Professor of Chemical Engineering

I certify that I have read this study and that in my opinion it conforms to acceptable standards of scholarly presentation and is fully adequate, in scope and quality, as a dissertation for the degree of Doctor of Philosophy.

J. P. O'Connell
Professor of Chemical Engineering

I certify that I have read this study and that in my opinion it conforms to acceptable standards of scholarly presentation and is fully adequate, in scope and quality, as a dissertation for the degree of Doctor of Philosophy.

J. F. Mahoney
Associate Professor of Industrial and Systems Engineering

I certify that I have read this study and that in my opinion it conforms to acceptable standards of scholarly presentation and is fully adequate, in scope and quality, as a dissertation for the degree of Doctor of Philosophy.

T. J. Anderson
Assistant Professor of Chemical Engineering

This dissertation was submitted to the Graduate Faculty of the College of Engineering and to the Graduate Council, and was accepted as partial fulfillment of the requirements for the degree of Doctor of Philosophy.

December 1982

Dean, College of Engineering

Dean for Graduate Studies and Research